Dynamical behavior of ultracold atomic gases

Von dem
Fachbereich Physik
der Universität Hannover
und der
Università degli Studi di Trento

zur Erlangung des Grades

Doktor der Naturwissenschaften
- Dr. rer. nat. -

genehmigte

Dissertation

von

Dipl. Phys. Paolo Pedri
geboren am 25. Januar 1974 in Trento (Italien)

2005

Referenten :	Prof. Sandro Stringari
	Prof. Dr. Maciej Lewenstein
Korreferenten :	Prof. Lev Pitaevskii
	Prof. Dr. Wolfgang Ertmer
Tag der Promotion :	17. Dezember 2004

.

To my parents and my sister

Abstract

The experimental achievement of Bose-Einstein condensation (BEC) in 1995 has aroused a large interest among the community of the physics of ultracold atomic gases. Recently new topics have attracted the attention of this very active field of research , in particular we could mention low dimensional systems, atoms in lattices, and classical and Fermi gases. As for the case of BEC, the study of the dynamical aspects of these systems provides a very valuable information. In particular time-of-flight experiments and measurements of collective excitations have been successfully realized providing a clear signature of the BEC and the regime of interaction. Following this line, in this thesis, we want to study some dynamical aspects of these new systems nowadays avaliable due to the remarkable development of the experimental techniques.

In the first chapter we present the state of the art of the field, providing the historical path and the motivation for the work developed in the next chapters.

In the second chapter, we discuss some general concepts in order to introduce the formalism and notation employed throughout the thesis, as well as those topics analyzed in more detail in the further chapters.

In chapter three, we explain some general techniques which are useful to deal with one dimensional systems, and analyze in detail the expansion of a one dimensional Bose gas in a guide, which differs significantly from the expansion of a BEC. In particular we are able to predict the range of parameters for which the self-similarity of the expansion is violated.

Chapter four is devoted to the physics of atoms in a periodic potential. We start, as in the previous chapter, introducing some general concepts and techniques employed further. First we discuss the physics of the superfluid case in a trap, showing that under certain conditions a three dimensional gas exhibits one dimensional properties.

In particular, static properties and the lowest collective excitations differ significantly from those of a BEC. We extend the analysis to the insulating phase showing that correlation properties depend on the on-site one-dimensional regime. These correlations can be measured in current time of flight experiments.

In the fifth chapter we analyze the dynamics of classical and Fermi gases. We show in detail how expansion and collective excitations depend on the interaction regime and the trap anisotropy. In particular, the expansion can be used to distinguish between a normal Fermi gas and a superfluid one.

We summarize in the last chapter the new results presented in this thesis.

Keywords

Bose-Einstein condensation, ultracold gases, dynamical behavior

Sommario

La relizzazione sperimentale della condensazione di Bose-Einsein, avvenuta nel 1995, ha destato un notevole intersse nella comunità della fisica degli atomi ultra freddi. Di recente nuovi sistemi hanno attratto l'attenzione di questo campo molto attivo della ricerca, in particolare possiamo menzionare sistemi a bassa dimensionalità, atomi su reticolo, e gas classici e di Fermi. Come avvenuto nel caso dei condensati di Bose-Einstein, lo studio degli aspetti dinamici di questi sistemi fornisce importanti informazioni. In particolare lo studio dell'espansione e delle eccitazioni collettive sono stati utilizzati con successo per rivelare la BEC e il reggime di interzione. Seguendo questa liena guida, in questa tesi, vogliamo studiare alcuni aspetti dinamici di questi nuovi sistemi oggi disponibili grazie al rapido sviluppo delle tecniche sperimentali.

Nel primo capitolo presentiamo lo stato dell'arte nel settore di ricerca, fornendo un cammino storico e le motivazioni per il lavoro sviluppato nei succeccivi capitoli.

Nel secondo capitolo, discutiamo concetti generali allo scopo di introdurre il formalismo a la notazione utilizzati nella tesi, e gli argomenti analizzatti in dettaglio nei capitoli successivi.

Nel terzo capitolo, esponiamo alcune tecniche generali utili per trattare sistemi unidimensionali, e analizziamo in dettaglio l'espansione di un gas unidimensionale in una guida, il quale differisce significativamente da quella di un condensato. In particolare siamo in grado di predirre la gamma dei parametri per i quali l'espansione non segue un legge di scaling.

Il quarto capitolo è dedicato alla fisica degli atomi in potenziali periodici. Come nel precedente capitolo vengono introdotti alcuni concetti e tecniche generali utilizzate nel seguito. Dapprima trattiamo il caso superfluido mostrando che, in particolari condizioni, un gas tridimensionale esibisce proprietà proprie dei sistemi unidimension-

ali. In particolare le proprità statiche e le più basse eccitazioni collettive differscono significativamente da quelle di un condensato. Nel seguito estendiamo l'analisi alla fase isolante mostrando che le proprietà di correlazione dipendono del reggime del sito unidimensionale. Queste correlzioni possono essere rivelate da attuali esperimeti.

Nel quinto capitolo analizziamo la dinamica dei gas classici e di Fermi. Mostriamo in dettaglio come l'espansione e le eccitazioni collettive dipendono dal regime di interazione e l'anisotropia della trappola. In particolare, l'espansione può essere usata per distinguere il reggime di interazione, normale o superfluido nel caso quantistico, o il reggime collisionale nel caso di un gas classico.

L'ultimo capitolo è dedicato ad un riassunto dei nuovi risultati presentati in questa tesi.

Parole chiave

condensazione di Bose-Einstein, atomi ultrafreddi, comportamento dinamico

Zusammenfassung

Die experimentelle Realisierung der Bose-Einstein-Kondensation (BEK) im Jahre 1995 führte zu einem regen Interesse unter den Physikern, die auf dem Gebiet der ultrakalten Atome arbeiten. In letzter Zeit traten neue Fragen dieses sehr aktiven Gebietes in den Mittelpunkt des Interesses, insbesondere niedrig dimensionale Systeme, Atome in optischen Gittern sowie klassische Gase und Fermi-Gase sind hierbei zu nennen. Im Falle der BEK liefert die Untersuchung der dynamischen Aspekte dieser Systeme sehr wertvolle Informationen. Im speziellen sind „time-of-flight“ Experimente und Messungen von kollektiven Anregungen erfolgreich realisiert worden. Diese widerspiegeln in klarer Form die Bose-Einstein Phase und das Regime der Wechselwirkung. Daher werden wir in dieser Arbeit dieser Linie folgen und einige dynamische Aspekte dieser neuen Systeme untersuchen, die heutzutage dank bemerkenswerter Fortschritte der experimentellen Techniken zugänglich geworden sind.

Im ersten Kapitel erläutern wir den momentanen Kenntnisstand auf diesem Gebiet, indem wir auf die historische Entwicklung eingehen und die Motivation für die weitere Arbeit darlegen.

Im zweiten Kapitel werden einige allgemeine Fragestellungen diskutiert, um den im weiteren Verlauf der Arbeit verwendeten Formalismus und die Notation einzufhren.

Das dritte Kapitel befasst sich mit der Erklärung einiger Techniken, die für die Behandlung eindimensionaler Systeme nützlich sind. Zudem analysieren wir im Detail die Expansion eines Bose-Gases in einem Wellenleiter, welche sich signifikant von der Expansion eines BEK unterscheidet. Im besonderen können wir den Parameterbereich vorhersagen, für den die Selbstähnlichkeit der Ausdehnung des Gases verletzt wird.

Kapitel vier ist der Physik kalter Atome in periodischen Potentialen gewidmet. Wir beginnen, ähnlich wie in den vorangegangenen Kapiteln, mit der Einführung von

generellen Konzepten und Techniken, die im Weiteren benutzt werden. Zunchst diskutieren wir die Physik des suprafluiden Falles in einer Falle, indem wir zeigen, dass unter bestimmten Bedingungen ein dreidimensionales Gas das Verhalten eines eindimensionalen Gases zeigt. Im besonderen unterscheiden sich die statischen Eigenschaften und die kollektiven Anregungen deutlich von denen eines BEK. Wir erweitern die Untersuchung auf die Isolatorphase, indem wir zeigen, dass Korrelationseigenschaften vom eindimensionalen „on-site“ Regime abhängen. Diese Korrelationen können in gegenwärtigen „time-of-flight“Experimenten gemessen werden.

Im vorletzten Kapitel untersuchen wir die Dynamik von klassischen Gase sowie von Fermigasen. Wir zeigen konkret, wie die Expansion und die kollektiven Anregungen vom Wechselwirkungsbereich und der Anisotropie der Falle abhängen. Insbesondere kann diese Expansion zur Unterscheidung eines gewöhnlichen Fermigases von einem suprafluiden Fermigas dienen.

Das letzte Kapitel fasst die neuen Ergebnisse zusammen, die in dieser Arbeit dargelegt werden.

Schlüsselworte

Bose-Einstein Kondensation, ultrakalte Atome, dynamisches Verhalten

Acknowledgment

First of all I would like to thank Sandro Stringari, I was really lucky to meet him, he started to teach me patiently since the time of my laurea degree and further during my PhD, I was always impressed by his physical intuition and even more from a human point of view. Second, but not less important, it is an honor to thank Maciej Lewenstein, he gave me the great opportunity to work in his group and to spend some time in Hannover, for these reasons I am really grateful to him. The third person I want to thank is my friend and colleague Luis Santos for his fundamental help and support. A person of the group of Trento I really want to thank is Lev Pitaevskii, he was always ready to listen to my questions and giving me useful advices.

I thank all the people of the group of Trento and Hannover but in particular I thank Chiara Menotti, a dear person whom I have the luck to work and spend nice time with, my dear German friend Klaus Osterloh, Claudio Osterloni, a person who is able, difficult to believe, to talk more than me, pretty impressive I would say, my Polish friend Jarek Korbic, Giancarlo Corbici, a very nice person, with a very nice wife and at the and the two poor devils which had the bad luck to share the office with me: Zbigniew Idziaszek and Laurent Sanchez-Palencia, thanks for your patience!

A special place of this acknowledgment is just for Filip Flögel, a dear friend who gave me an incredible support. What I have really appreciated is that everything came from his heart, thanks again.

Among the people that I met during these years, and in some case even earlier, there are my dear old and new friends Sonia Bacca, Luca Doria, Ludovico Carbone, Sofia Quaglioni, Gobind Das and Vittorio Barone Adesi. One hundred pages would not be enough to describe how many adventure we had together and make us really good friends for life.

Another special place of this acknowledgment is reserved for the PhD secretary Luisa Rossi Doria for suffering me three long years, the secretary of Hannover Frau Christel Franco and the secretary of the Institute for Theoretical Physics of Stuttgart Frau Ildiko Poljak for her kindness and help.

During my period in Germany I was living in a WG and it could not have been better than what it has been, I am really glad to thank the people I was living with: Kim Florian "The Lazy" Hülser and Marijke Carelsberg. It was simply great!

I thank also my professor of mathematics at high-school Adriano Zatelli, a fundamental person of my life, I think that everything started at that time, he transmitted the passion for the science to me, and for this I will be forever grateful to him.

My main gratitude goes to my parents and my sister and, for this reason, I want to dedicate this thesis to them.

I know that I have forgotten to mention a lot of people but the acknowledgment can not be longer than the thesis.

Paolo Pedri

This thesis is based on the following works

- Mott-insulator phase of coupled 1D atomic gases in a 2D optical lattice

  D.M. Gangardt, P. Pedri, L. Santos, G.V. Shlyapnikov

  cond-mat/0408437

- Collisions and expansion of an ultracold dilute Fermi gas

  B. Jackson, P. Pedri, S. Stringari

  Europhys. Lett. **67**, 524 (2004)

- Dynamics of a classical gas including dissipative and mean field effects

  P. Pedri, D. Guéry-Odelin, S. Stringari

  Phys. Rev. A **68**, 043608 (2003)

- Violation of self-similarity in the expansion of a 1D Bose gas

  P. Pedri, L. Santos, P. Ohberg, S. Stringari

  Phys. Rev. A **68**, 043601 (2003)

- Three-dimensional quasi-Tonks gas in a harmonic trap

  P. Pedri, L. Santos

  Phys. Rev. Lett. **91**, 110401 (2003)

- Expansion of an interacting Fermi gas

  C. Menotti, P. Pedri, S. Stringari

  Phys. Rev. Lett. **89**, 250402 (2002)

The author has also contributed in the following other works

- Creation and mobility of discrete solitons in Bose-Einstein condensates

  V. Ahufinger, A. Sanpera, P. Pedri, L. Santos, and M. Lewenstein

  Phys. Rev. A **69**, 053604 (2004)

- Scissors modes of two-component degenerate gases: Bose-Bose and Bose-Fermi mixtures

  M. Rodrguez, P. Pedri, P. Törmä, and L. Santos

  Phys. Rev. A **69**, 023617 (2004)

Contents

Chapter 1

Introduction

The experimental achievement of Bose-Einstein (BEC) condensation [1–3] has aroused a large interest among the community working in ultracold atomic gases. Recently, other topics have attracted a growing attention in this very active community, and in particular the physics of low dimensional atomic gases, atoms in periodic potentials, and classical and Fermi gases. In this thesis we will analyze some dynamical properties of these novel systems. We will focus our attention on the expansion and the collective excitations, a very useful tool that has been successfully used to reveal the appearance of the Bose-Einstein Condensation [1, 3] and the role of interactions [4–6]. In the next sections we will present the state of the art of this field, providing the motivation and the guiding line for the work presented in the next chapters. The last section contains an overview of the thesis.

1.1 Low dimensional systems

The development of the trapping techniques has allowed for the realization of very anisotropic geometries, where the confinement is so strong in one or two dimensions,

that at low temperatures the transversal motion is "frozen", and does not contribute to the dynamics of the system. In this way two- [7–10] and one-dimensional [7, 11, 12] systems have been accomplished. Low-dimensional gases present significantly different properties compared to the three-dimensional ones. A remarkable example is provided by the existence of quasi-condensation [13–16], whose effects have been recently observed experimentally [17–19].

During the last years, the 1D Bose gases have been the subject of growing interest, in particular the limit of impenetrable bosons [20], which behave to a large extent as a noninteracting Fermi system, acquiring some remarkable properties. The conditions for the experimental realization of strongly correlated 1D gases are rather restrictive [13, 21], since a large radial compression, a sufficiently small density, and eventually a large scattering length are needed. Fortunately, recent experimental developments have opened perspectives in this sense. Especially interesting is the possibility to modify at will the interatomic interactions by means of Feshbach resonances [22, 23], and the capability of loading an atomic gas in an optical lattice [24]. As we discuss below, the large confinement available in optical lattices have been recently employed for the experimental realization of 1D strongly-interacting gases [53–57].

From the theoretical side, the physics of 1D Bose gases was first investigated by Girardeau [20], who considered the limit of impenetrable bosons, also called Tonks-Girardeau (TG) gas, pointing out a non trivial relation with the physics of ideal Fermi gases. This analysis was later extended by Lieb and Liniger [25], who solved analytically the problem for any regime of interactions, using Bethe Ansatz. Yang and Yang [26] extended the analysis including finite temperature effects. It has been developed also a very useful effective theory which take into account only the linear dispersion relation of the spectrum [27,28], being simpler than Bethe-Ansatz. Recently,

the experimental accessibility of trapped gases has encouraged the investigation of the harmonically trapped case. The Bose-Fermi (BF) mapping has been employed to the case of an inhomogeneous gas in the TG limit [29–32]. However, there is unfortunately, to the best of our knowledge, no exact solution for arbitrary interaction strength in the case of trapped gases. The problem of the equilibrium of a trapped gas can be analyzed using a local density approximation and employing the Lieb-Liniger (LL) equation of state locally to evaluate the equilibrium density profiles [33]. A similar formalism has been recently employed to analyze the collective oscillations in the presence of harmonic trapping [34]. Both Refs. [33] and [34] have shown the occurrence of a continuous transition from the mean field (MF) regime to the TG one as the intensity of the interaction is varied. Recently, the stability and phase coherence, and correlation properties of 1D trapped Bose gases have been discussed [35–38]. The local correlation properties have been also analyzed. In particular, it was found that inelastic decay processes, such as three body recombination, are suppressed in the TG regime, and intermediate regimes between MF and TG. This fact opens promising perspectives towards the accomplishment of strongly interacting 1D Bose gases with large number of particles. This analysis have been very recently extended to the case of finite temperatures [39]. Recently the TG gas and intermediate regime have been realized in an optical lattice [40, 53, 54, 57].

The expansion of a one-dimensional Bose gas in a guide was analyzed in Ref. [41], by means of a hydrodynamic approach based on the local LL model. The expansion dynamics was shown to be different for different interaction strengths, and its analysis could be employed to discern between the TG and MF regimes. In particular, the self-similar solution is violated.

In this thesis, we extend the analysis of Ref. [41] by introducing a variational ap-

proach, which permits us to study the asymptotic regime at large expansion times. This method is shown to be in excellent agreement with previous direct numerical simulations, and additionally permits us to recover the results of Refs. [33] and [34]. More importantly, our variational approach allows us to determine the regime of parameters for which the self-similarity of the expansion is violated.

1.2 Lattices

Recent developments in loading atoms in optical lattices [24, 42–46] open fascinating perspectives towards the achievement of strongly-interacting systems in cold atomic gases. In this sense, a remarkable example is provided by the recent observation of the superfluid to Mott-Insulator (MI) transition in cold bosonic gases in optical lattices [24, 47, 48]. Other strongly-interacting systems in cold atomic gases have been recently considered theoretically, as the case of large scattering length [49], rapidly rotating Bose gases [50, 51], and one-dimensional systems, both bosonic [33–35, 38, 41] and fermionic [52]. As commented above, the accomplishment of strongly-interacting 1D gases requires tight transversal trapping, low atom numbers, and possibly the increase of a via Feshbach resonances [13, 21, 33].

In this sense, 2D optical lattices are favorable, since the on-site transverse confinement can be made very strong and for sufficiently small tunneling rates each lattice site behaves as an independent 1D system. As previously discussed, recent experiments on strongly correlated 1D gases have been performed along these lines [53–57].

The experiments on 1D systems in 2D optical lattices motivate the analysis of an interesting physics in a (2D) array of coupled 1D Bose gases. In a 2D lattice the coupling is provided by the inter-site tunneling, and each lattice site is a 1D

tube filled with bosonic atoms. This regime is easily achievable experimentally by lowering the lattice potential, and it represents the bosonic analog of 1D coupled nanostructures [58]. As was first shown by Efetov and Larkin [59], for infinitely long 1D tubes at zero temperature any infinitesimally small tunneling drives the system into the superfluid phase. The gas then enters an interesting cross-dimensional regime, in which it presents 1D properties in a 3D environment [60, 61]. For 1D tubes of finite length L, at sufficiently small tunneling rate the system can undergo a cross-over from such anisotropic 3D superfluid state to the 2D Mott insulator state [61]. Strictly speaking, this 2D MI phase requires a commensurable filling of the tubes, i.e. an integer average number of particles N per tube. Then the system of finite-length tubes at zero temperature is analogous to that of infinite tubes at a finite temperature T, and the critical tunneling t_c for the $T = 0$ cross-over to the MI phase can be obtained from the finite-temperature results of Ref. [59] by making a substitution $1/T \to L$, we will came back to this point in chapter 4.

In this thesis we presented the analysis of correlation properties of this 2D Mott insulator. We show that the momentum distribution is crucially modified by a combined effect of correlations along the 1D tubes and inter-tube hopping. For the case of a weakly interacting gas in the tubes, the phase coherence is maintained well inside the MI phase. This is similar to the situation in 2D and 3D lattices, studied by means of Quantum Monte Carlo calculations [62, 63] and investigated experimentally through the observation of an interference pattern after switching off the confining potential [24]. However, an increase of the interaction between particles in 1D tubes reduces the inter-tube phase coherence and flattens the momentum distribution in the transverse directions. In particular, the interference pattern observed in Ref. [24] should be largely blurred if the 1D tubes are in the TG regime.

In this thesis we also analyze the situation in which the tunneling is sufficiently large to guarantee the superfluid character of the system, but sufficiently weak to assume the 1D character of the local chemical potential. In this regime, which we call the quasi-Tonks regime, we predict that the combination of tunneling and 1D local chemical potential results in important modifications of the 3D ground-state density and excitations.

1.3 Classical and fermionic gases

As commented at the beginning of the introduction, the favored signature of Bose-Einstein condensation in weakly interacting gases is the time-of-flight expansion [1,3]. In this technique, the asymmetric trapping potential is switched off and the evolution of the spatial density is monitored. After long time expansion, the observed inversion of the aspect ratio reflects the anisotropy of the initial confinement. In an ideal Bose-Einstein condensate, this effect is a direct consequence of the Heisenberg uncertainty constraint on the condensate wave function. For an interacting BEC, the inversion is also produced by the anisotropy of the pressure gradients caused by the hydrodynamic forces. The changes in the shape of the expanding gas can be characterized by scaling factors, which provide an easy quantitative tool for the analysis of on-going BEC experiments. The set of equations for those factors have been derived in many papers [64–67], providing excellent agreement with experiments [68, 69] and pointing out the difference with respect to the expansion of a non condensed gas. A similar effect has also been predicted for a Fermi gas in its superfluid phase [70], we will come to this point further. Strong anisotropy has been recently measured in the expansion of a highly degenerate Fermi gas [87] close to a Feshbach resonance. Resonance

scattering can also give rise to anisotropic expansion in the normal phase as proven in the experiments of [72, 73], carried out in a less degenerate regime. Some recent experiments on bosonic atoms above the critical temperature have also reached the collisional regime investigating both the oscillations of the low lying quadrupole mode and the expansion in asymmetric traps [18, 74–76].

So far analytic calculations for the expansion of a classical gas have been limited to either the ballistic or to the hydrodynamic regime [65]. As a consequence in this thesis we want to generalize such calculations to all intermediate collisional regimes. Our approach relies on an approximated solution to this equation by means of a scaling ansatz. This solution is used to investigate two kinds of related problems: the lowest collective oscillation modes and the time-of-flight expansion when the confinement is released.

Concerning the issue of an expanding Fermi cloud, in this thesis we study also the problem of the expansion of an ultracold sample of fermions initially trapped in an anisotropic harmonic trap. We will show that also in the case of fermions the expansion of the gas provides valuable information about the state of the system and the role of interactions. We will consider a gas of atoms interacting with attractive forces. This is a natural requirement for the realization of Cooper-pairs and hence for the achievement of the superfluid phase [77, 78]. Such interactions are naturally present in some fermionic species like ^{6}Li and can otherwise be obtained by changing the scattering length profiting of the presence of a Feshbach resonance.

Anisotropy is not however a unique feature exhibited by superfluids and also in the normal phase one can expect a similar behavior if collisions are sufficiently important [65,79–81]. This effect is expected to be particularly important in the case of Fermi gases interacting with large scattering lengths near a Feshbach resonance [72,73,87]. At

first sight one would expect that the effects of collisions are suppressed at low temperature because of Pauli blocking. This is certainly true if one works close to equilibrium, as happens in the study of small amplitude oscillations [82]. In the problem of the expansion, however, large deformations in momentum space can be produced if one starts from a highly deformed cloud, with the result that collisions become effective even if the gas is initially at zero temperature. This interesting possibility was first pointed out in [83]. In this thesis we calculate explicitly the dynamics of the expansion of a dilute, degenerate normal Fermi gas, taking into account the role of collisions. The main purpose is to provide quantitative predictions for the aspect ratio and the thermal broadening of the density distribution, as a function of the relevant parameters like the ratio of the trap frequencies, the scattering length and the number of atoms.

1.4 Overview of the thesis

In the following we briefly discuss the contents of this thesis.

In the second chapter we present a general technical introduction in order to clarify the notation in the rest of the thesis. We start explaining the difference between a classical and a quantum ideal gas, and describing a simplified way to deal with interacting systems using a pseudopotential. Although Bose-Einstein condensation is not among the topics discussed in this thesis, an explanation about BEC is also given. We have found important to present these concepts for completeness and historical reasons, since the time-of-flight measurements have been largely used in experiments related to BEC. We additionally discuss the role of the dimensionality. We then describe the dynamics of a classical and a normal Fermi gas and we conclude with a brief reminder of BCS theory.

In chapter three we consider in more detail the physics in one dimension, providing an overview of the main techniques used in one dimension. We then explain in detail the dynamics of a one dimensional bosonic gas and how this can be used to reveal information about the regime of interaction of the gas.

In chapter four we introduce some useful techniques to deal with lattices. We discuss in detail a system composed of an array of one dimensional systems. We will start with the superfluid regime describing the static properties and the lowest collective modes of a trapped gas. In this case, the main role is played by the one dimensional chemical potential that differ to the three dimensional one, giving rise to new cross-dimensional phenomena that are not possible to observe in the absence of lattice. We will describe also the correlation properties in the insulating phase and how these can be detected. These remarkable properties depend on the internal interaction-regime of the one-dimensional sites.

In chapter four we present a detailed discussion on the expansion of a classical gas, a normal Fermi gas and a superfluid Fermi gas. We discuss how the collisions, the geometry of the trap and the regime (normal or superfluid) affect the expansion and the lowest collective modes. This is still an active subject of research and new experiment and theoretical results have been presented expecially regarding the BEC-BCS crossover [84–89].

The last chapter is devoted to a summary of the novel results presented in this thesis.

Chapter 2

Dilute gases

This chapter contains a short introduction about the physics of cold dilute atomic gases: bosons, fermions and classical gases. We start from the ideal gas, which is an useful tool to understand many phenomena. Later on we introduce the interaction by means of a pseudopotential [90]. We proceed by describing briefly the concept of Bose-Einstein-Condensation and the role of dimensionality [91, 92]. An additional section is devoted to classical gases and normal Fermi liquids [93, 94]. We conclude with a short description of BCS theory [94]. This chapter should be understood as a reference for the next chapters of this thesis.

2.1 Ideal gas

The many body Hamiltonian of a non interacting system in an external potential reads

$$\hat{H} = \int d^3r \hat{\Psi}^+(\mathbf{r}) \left(-\frac{\hbar^2}{2m}\Delta + V_{\text{ext}}(\mathbf{r}) \right) \hat{\Psi}(\mathbf{r}) \tag{2.1}$$

where $\hat{\Psi}$ and $\hat{\Psi}^+$ are quantized fields. They can commute or anti-commute depending on the bosonic or fermionic nature of the particles considered. m is the mass of the

particle. In typical experiments [1–3] the external potential can be considered, with a very good approximation, as harmonic

$$V_{\text{ext}}(\mathbf{r}) = \frac{m}{2}\sum_j \omega_j^2 x_j^2. \tag{2.2}$$

Let us define the one-body density-matrix as

$$\rho_1(t, \mathbf{r}_1, \mathbf{r}_2) = \langle \hat{\Psi}^+(t, \mathbf{r}_1)\hat{\Psi}(t, \mathbf{r}_2)\rangle \tag{2.3}$$

where $\langle\cdot\rangle$ is an average. It can be also a statistical mixture, one of the most important being the thermal one, for which the average reads

$$\langle \hat{A}\rangle = \frac{tr\left\{\hat{A}\exp[-(\hat{H}-\mu\hat{N})/T]\right\}}{tr\left\{\exp[-(\hat{H}-\mu\hat{N})/T]\right\}} \tag{2.4}$$

where $\hat{A}$ is an operator, tr means trace, $\hat{H}$ is the Hamiltonian, $\hat{N}$ is the number of particles, and μ is the chemical potential. For what follows it is better to use center of mass $\mathbf{r} = (\mathbf{r}_1 + \mathbf{r}_2)/2$ and relative $\mathbf{s} = \mathbf{r}_1 - \mathbf{r}_2$ coordinates. Let us now define the Wigner function,

$$f(t, \mathbf{r}, \mathbf{p}) = \frac{1}{(2\pi)^{(3/2)}}\int d^3 s \rho_1(t, \mathbf{r}, \mathbf{s}) e^{-i\mathbf{s}\cdot\mathbf{p}/\hbar} \tag{2.5}$$

The dynamics of the Wigner function follows the equation [1]:

$$\frac{\partial f}{\partial t} + \frac{\mathbf{p}}{m}\cdot\nabla_{\mathbf{r}} f + \mathbf{F}\cdot\nabla_{\mathbf{p}} f = 0 \tag{2.6}$$

where $\mathbf{F}(\mathbf{r}) = -\nabla_{\mathbf{r}} V_{\text{ext}}(\mathbf{r})$. Eq. (2.6) is called Boltzmann equation[2]. It seems then that there is no much difference between classical and quantum ideal gases. This is

[1] it is possible to generalize it to a rotating frame but one has to be careful with the definition of momentum

[2] The Boltzmann equation contains also the collisional term. In this case, since there is no interaction between the particles the collisional term vanishes.

however not correct. In order to clarify this point let us consider a gas in a three dimensional harmonic potential at equilibrium. In the case of a *classical gas* at finite temperature the Wigner function reads

$$f_0(\mathbf{r},\mathbf{p}) = \exp\left[-\sum_j \left(\frac{p_j^2}{2mT} + \frac{m\omega_j^2 x_j^2}{2T}\right)\right]. \tag{2.7}$$

For a *Bose gas at zero temperature*, where all the particles are in the same quantum state, the Wigner function reads

$$f_0(\mathbf{r},\mathbf{p}) = \exp\left[-\sum_j \left(\frac{p_j^2}{2m\hbar\omega_j} + \frac{m\omega_j x_j^2}{2\hbar}\right)\right]. \tag{2.8}$$

By inspection of the previous formula, we notice that in the classical case the momentum distribution is spherically symmetric, whereas in the quantum case, due to Heisenberg uncertainty principle, an asymmetry is present. This leads to different behavior in the expansion after removal of the trap, since for large time the density reflects the initial momentum distribution (see appendix A.1). As a consequence of this fact, the shape of the density for large time will be spherically symmetric in the case of classical gas, whereas for the Bose gas considered above it is not the case.

Another important point to mention is that the Winger function is real. This follows from the fact that the one-body density matrix can be seen as a kernel of an Hermitian operator, but not positively defined. For example, let us consider the first excited state of the harmonic oscillator and compute the Wigner function

$$f_0(x,p) = \left(\frac{p^2}{m\hbar\omega} + \frac{m\omega x^2}{\hbar} - 1\right)\exp\left[-\left(\frac{p^2}{2m\hbar\omega} + \frac{m\omega x^2}{2\hbar}\right)\right]. \tag{2.9}$$

For small values of the momentum and position, the function assumes negative values and, consequently, cannot be interpreted as a density distribution in the phase-space. Anyway the average of any observable can be computed as in the classical case.

Another difference that is worth to mention concerns the dynamics of the expansion, where Boltzmann equation reads

$$\frac{\partial f}{\partial t} + \frac{\mathbf{p}}{m} \cdot \nabla_{\mathbf{r}} f = 0. \tag{2.10}$$

In the case where interactions are absent, it is easy to solve this equation. We have to substitute $\mathbf{r} \rightarrow \mathbf{r} - \mathbf{p}t/m$. This can be "pictorially" understood as follows: a particle starting at the position $\mathbf{r}$ with momentum $\mathbf{p}$ will have, after a time t, the same momentum but the new position $\mathbf{r} + \mathbf{p}t/m$. Using this method it is possible to calculate easily the dynamics of the expansion. This leads to an anisotropic behavior in the quantum case previously considered, but also to interference phenomena in the case of the expansion from a double well potential. If we calculate the time dependence of the density, we obtain that in the classical case we have just to sum the density of each well. On the contrary, in the quantum case interference phenomena appear.

We have shown how the Boltzmann equation takes into account also quantum phenomena. Let us continue with some static properties of an ideal gas. In order to do this we define the partition function

$$Z(T, \mu, V) = tr \left\{ \exp\left(-\frac{H - \mu N}{T} \right) \right\}, \tag{2.11}$$

where T is the temperature, μ is the chemical potential and V is the volume. For an ideal gas the result is

$$Z = \pm T \sum_j \ln(1 \mp e^{(\mu - \varepsilon_j)/T}), \tag{2.12}$$

where the upper sign refers to bosons and the lower one to fermions. From this formula, and deriving with respect to the chemical potential μ, we obtain the mean occupation number for any single quantum state:

$$n_j = \left[\exp\left(\frac{\varepsilon_j - \mu}{T} \right) \mp 1 \right]^{-1}. \tag{2.13}$$

These distributions are called Bose Einstein (−) and Fermi Dirac (+) statistics. We note that for sufficiently high temperature we retrieve the usual Boltzmann statistics typical of classical gases. The previous formula can be used to calculate the Wigner function of a large sample using local density approximation

$$f(\mathbf{r},\mathbf{p}) = \left[\exp\left(\frac{\varepsilon(\mathbf{p},\mathbf{r})-\mu}{T}\right) \mp 1\right]^{-1}, \tag{2.14}$$

where $\varepsilon(\mathbf{p},\mathbf{r})$ is the classical energy of a single particle in an external potential.

2.2 Interaction between particles

The interacting systems are usually difficult to treat. However for some system the analysis can be simplified. We introduce the interaction between atoms and show how to describe the process at low energy in the case of a short range potential. In what follows we summarize some concepts of scattering theory [95, 96], which allows us to write an effective potential in order to treat the interaction in a simpler way. The interatomic potential can depend on many parameters such the electronic spin and the nuclear spin. Here we restrict our analysis to central potentials.

The Schrödinger equation related to the single particle scattering problem reads

$$\left(-\frac{\hbar^2}{2m_r}\Delta + v(\mathbf{r})\right)\psi(\mathbf{r}) = E\psi(\mathbf{r}), \tag{2.15}$$

where m_r is, in this case, the reduced mass. The solution of this equation, for large distances[3] assumes the form

$$\psi^{\pm}(\mathbf{r}) \sim e^{i\mathbf{k}\cdot\mathbf{r}} + \frac{e^{\pm ikr}}{r} f(\mathbf{k}',\mathbf{k}). \tag{2.16}$$

The scattering amplitude takes the form

$$f(\mathbf{k}',\mathbf{k}) = -\frac{m_r(2\pi)^{3/2}}{2\pi\hbar^2}\int d^3r' e^{-i\mathbf{k}'\cdot\mathbf{r}'} V(\mathbf{r}')\psi^{+}(\mathbf{r}'). \tag{2.17}$$

[3] this means that r must be much larger than the range of the interatomic interaction

The scattering amplitude can be decomposed using spherical harmonics Y_l^m:

$$f(\mathbf{k}', \mathbf{k}) = f(\theta) = \sum_{l=0}^{\infty} (2l+1) \frac{e^{i\delta_l(k)} - 1}{2ik} P_l(\cos\theta), \tag{2.18}$$

where P_l are the Legendre polynomials and δ_l is the scattering phase shift. The knowledge of all the phase shifts allow to build the scattering amplitude. The cross section is related to the scattering amplitude through the following relation

$$\sigma_{tot} = \int |f(\theta)|^2 d\Omega = \frac{4\pi}{k^2} \sum_l (2l+1) \sin^2 \delta_l. \tag{2.19}$$

If we consider scattering between identical particles one has to take into account the statistic of the particles. If we consider bosons or fermions with the same internal state the function of the coordinates must be symmetric or antisymmetric respectively. This means that for identical particles we have to consider even values of l for bosons and odd values of l for fermions. If there is also an internal degree of freedom, the function of the coordinates can be symmetric or antisymmetric depending on the internal state. For example two fermions in a singlet state can have s-wave scattering, but two fermions in a triplet state cannot. Since we are working at very low temperature only the s-wave (l=0) is involved. Comparing the energy related to the thermal wave length and the energy for p-wave $l = 1$, it is possible to calculate the temperature below which the p-wave is suppressed, which is the typical case in experiments.

Let us now define the s-wave scattering length

$$a = \lim_{k \to 0} \frac{\delta_0(k)}{k}. \tag{2.20}$$

This can be though as the radius of a hard sphere. We substitute the real potential by a pseudopotential of the form

$$V_{\text{eff}}(\mathbf{r} - \mathbf{r}') = g\delta^3(\mathbf{r} - \mathbf{r}'), \tag{2.21}$$

where the constant g is chosen in order to give the same low energy properties of the real potential. Using Born approximation the result is

$$g = \frac{4\pi\hbar^2 a}{m}. \tag{2.22}$$

In conclusion we have shown that for low energies the short range interaction can be simplified introducing the concept of scattering length and pseudopotential.

2.3 BEC and role of the dimensionality

In this section, we mention only some important concepts regarding BEC. For a more extended analysis see [91,92]. In order to define what is the BEC let us start from the Bose-Einstein statistics (2.14). Let us consider the case of a three dimensional system of free bosons in a box. The total number of particles is

$$N = \sum_{\mathbf{k}} \left[\exp\left(\frac{\varepsilon_{\mathbf{k}} - \mu}{T} \right) - 1 \right]^{-1}, \tag{2.23}$$

where $\varepsilon_{\mathbf{k}} = \hbar^2 k^2 / 2m$. We keep fixed the number of particles, and hence the chemical potential is an implicit function of the temperature, T, and N. The number of particles with $\mathbf{k} \neq \mathbf{0}$ can be calculated as follows

$$N_T = \sum_{\mathbf{k}\neq\mathbf{0}} \left[\exp\left(\frac{\varepsilon_{\mathbf{k}} - \mu}{T} \right) - 1 \right]^{-1}. \tag{2.24}$$

The r.h.s. of Eq.(2.24) is limited from above. Hence, the contribution of the particles with momentum zero are essential to ensure the correct number of particles. As a consequence, below a certain critical temperature, the state with zero momentum starts to be macroscopically occupied. The critical temperature is

$$T_c = \frac{2\pi\hbar^2}{m} \left(\frac{\rho}{g_{3/2}(1)} \right)^{3/2}, \tag{2.25}$$

with $g_{3/2}(1) = 2.612$. The fraction of condensed particles is

$$\frac{N_0(T)}{N} = 1 - \left(\frac{T}{T_c}\right)^{3/2} \tag{2.26}$$

for $T < T_c$. One can use the same arguments and calculate the critical temperature and condensate fraction in the trapped case. A discussion on this issue can be found in [91, 92]. It is possible to define the BEC through the density matrix. The appearance of an eigenvalue of the same order of the averaged density is a signature of the onset of BEC. In the case of an ideal gas one can diagonalize the one-body density matrix by Fourier transform, and observe the appearance of a $\delta^3(\mathbf{k})$ below the critical temperature defined above. This definition is much more general because it can be used for interacting systems.

The next step is to derive a dynamical equation for an interacting system. The starting point is the dynamical equation for the quantum field

$$i\hbar\frac{\partial\hat{\Psi}(t,\mathbf{r})}{\partial t} = \left(-\frac{\hbar^2}{2m}\Delta + V_{ext}(\mathbf{r}) + g\hat{\Psi}^+(t,\mathbf{r})\hat{\Psi}(t,\mathbf{r})\right)\hat{\Psi}(t,\mathbf{r}). \tag{2.27}$$

The idea now is to substitute the quantum field by a classical field plus fluctuations [97].

$$\hat{\Psi} = \phi + \delta\hat{\Psi}, \tag{2.28}$$

where ϕ is a classical field, an the fluctuation $\delta\hat{\Psi}$ obeys approximately the bosonic commutation relation [98]. Keeping terms linear in the fluctuations we obtain

$$i\hbar\frac{\partial\phi(t,\mathbf{r})}{\partial t} = \left(-\frac{\hbar^2}{2m}\Delta + V_{ext}(\mathbf{r}) + g|\phi(t,\mathbf{r})|^2\right)\phi(t,\mathbf{r}). \tag{2.29}$$

This is the so-called Gross-Pitaevskii equation [99–101]. While for the fluctuations we get

$$i\hbar\frac{\partial\delta\hat{\Psi}(t,\mathbf{r})}{\partial t} = \left(-\frac{\hbar^2}{2m}\Delta + V_{ext}(\mathbf{r}) + 2g|\phi(t,\mathbf{r})|^2\right)\delta\hat{\Psi}(t,\mathbf{r}) + g\phi(t,\mathbf{r})^2\delta\hat{\Psi}^+(t,\mathbf{r}). \tag{2.30}$$

Let us consider the particular case of an homogeneous gas at equilibrium [92, 94, 102]. Assuming an homogeneous solution for the condensate part we obtain

$$\phi = \sqrt{\rho} \qquad \mu = g\rho. \tag{2.31}$$

For the excitation spectrum, after a canonical transformation [102], we obtain

$$\varepsilon(\mathbf{k}) = \left[\frac{\hbar^2 k^2}{2m}\left(\frac{\hbar^2 k^2}{2m} + 2g\rho\right)\right]^{1/2}. \tag{2.32}$$

This spectrum exhibits a linear behavior for small momenta and single particle behavior for large momenta. This is very important for the superfluid properties and the dynamical stability of the condensate.

Now we want to point out the role of the dimensionality in this phase transition. Up to now we have only consider three-dimensional systems. The situation is different in two and one dimension. In two dimensions the BEC is possible just at $T = 0$[4]. In one dimension the BEC is not possible even at zero temperature, due to interactions between particles. It is possible to derive the previous statements from general principles [92, 104]. We return to the issue of one dimensional Bose systems in chapter 3.

2.4 Classical Gases and normal Fermi liquid

The theory of a normal Fermi liquid was proposed by Landau (see for example [93, 94]). The basic idea is a one-to-one continuous mapping between the eigenstates of a non interacting system and an interacting one. For this reason it is crucial that the interactions do not drive any phase transition in the system. In this theory the concept of particle is substituted by that of quasi-particle, that can be seen as a

[4] in presence of a vortex lattice the situation change drastically and the long range order is lost [103]

particle dressed by the interaction with all the rest of the system. The quasiparticle distribution function is a Fermi-Dirac distribution

$$n_{\mathbf{k}} = \left[\exp\left(\frac{\varepsilon_{\mathbf{k}} - \mu}{T}\right) + 1\right]^{-1}. \tag{2.33}$$

The energy of the quasiparticle is defined as a variation of the total energy with respect to the quasi-particle distribution

$$\varepsilon_{\mathbf{k}} = \frac{\delta E}{\delta n_{\mathbf{k}}}. \tag{2.34}$$

The equation describing the dynamics of such a system is a richer version of the Boltzmann equation used for dilute classical gases

$$\frac{\partial f}{\partial t} + \nabla_{\mathbf{p}}\varepsilon_{\mathbf{p}} \cdot \nabla_{\mathbf{r}} f - \nabla_{\mathbf{r}}\varepsilon_{\mathbf{p}} \cdot \nabla_{\mathbf{p}} f = C[f]. \tag{2.35}$$

Since we work in presence of a harmonic external potential, the trap frequency, and in general any typical time related to the macroscopic motion of the system, provides a time scale that must be compared with the average time of collisions between the quasi-particles, τ. According to this comparison, we can distinguish two regimes. If $\omega\tau \ll 1$ the system is in the hydrodynamic regime, where the local equilibrium is ensured by collisions. If the opposite occurs, $\omega\tau \gg 1$, the collisional term can be neglected and the system is in the collisionless regime. Eq. (2.35) predicts the so-called zero sound, which is the propagation of a density fluctuation at zero temperature in collisionless regime. This excitation have a different nature with respect to the normal sound where collisions are crucial.

Let us now comment the collisional term of Eq. (2.35). In general the collisional integral can be written in the following form

$$C[f](t, \mathbf{r}, \mathbf{p}_1) = \int d^3p_2 d^3p_1' d^3p_2' W(\mathbf{p}_1, \mathbf{p}_2 \to \mathbf{p}_1', \mathbf{p}_2') F(f(\mathbf{p}_1), f(\mathbf{p}_2), f(\mathbf{p}_1'), f(\mathbf{p}_2')), \tag{2.36}$$

where the transition probability W includes the momenta and energy conservation, and it must be calculated from a microscopic point of view. The function F depends on the statistics, and for a fermionic system reads

$$F(x_1, x_2, x_1', x_2') = (1 - x_1)(1 - x_2)x_1'x_2' - (1 - x_1')(1 - x_2')x_1x_2. \tag{2.37}$$

This expression contains the Pauli exclusion principle, and hence the transition probability depends on the inital state and the final one. For a classical gas the collisional integral reads

$$F(x_1, x_2, x_1', x_2') = x_1'x_2' - x_1x_2. \tag{2.38}$$

Here we conclude the brief summary concerning the topic of normal Fermi liquid and classical gases. For a detailed description, as already commented at the beginning of this section, we refer to [93, 94].

2.5 Superfluid Fermi gases

In this section we are interested in fermionic gases with attractive interactions. We have seen that at sufficiently low temperature two fermions of the same species do not have s-wave scattering. In this section, we consider a two-component fermionic gas. In these systems atoms of different species interact via 's-wave scattering, and at a certain temperature the surface of the Fermi see in unstable under formation of Cooper pairs, i.e. particles near the Fermi surface with opposite momentum couple with each other giving rise to superfluid phenomena.

In the following, we summarize the basic idea of the BCS theory (for more detail see for example [92, 94]). Here we present just the main useful results for what we

need further in the thesis. The starting point is the BCS Hamiltonian

$$\hat{H} = \sum_{\mathbf{k},s} \varepsilon_{\mathbf{k}} \hat{a}^{+}_{\mathbf{k}s} \hat{a}_{\mathbf{k}s} - g \sum_{\mathbf{k}\mathbf{k}'} \hat{a}^{+}_{\mathbf{k}\uparrow} \hat{a}^{+}_{-\mathbf{k}\downarrow} \hat{a}_{-\mathbf{k}'\downarrow} \hat{a}_{\mathbf{k}'\uparrow}, \tag{2.39}$$

where $\varepsilon_{\mathbf{k}} = \hbar^2 k^2/2m - \mu$. At this point we proceed as in the bosonic case defining a new set of operators:

$$\begin{aligned} \hat{a}_{\mathbf{k}\uparrow} &= u_{\mathbf{p}} \hat{b}_{\mathbf{k}\uparrow} + v_{\mathbf{p}} \hat{b}^{+}_{-\mathbf{k}\downarrow}, \\ \hat{a}_{\mathbf{k}\downarrow} &= u_{\mathbf{p}} \hat{b}_{\mathbf{k}\downarrow} - v_{\mathbf{p}} \hat{b}^{+}_{-\mathbf{k}\uparrow}. \end{aligned} \tag{2.40}$$

In order to preserve the fermionic nature of the new operator, the coefficients $u_{\mathbf{k}}$ and $v_{\mathbf{k}}$ must fulfilled the relation $u^2_{\mathbf{k}} + v^2_{\mathbf{k}} = 1$. These coefficients assume the following form

$$|u_{\mathbf{k}}|^2 = \frac{1}{2}\left(1 + \frac{\varepsilon_{\mathbf{k}}}{\sqrt{\varepsilon^2_{\mathbf{k}} + |\Delta|^2}}\right); \qquad |v_{\mathbf{k}}|^2 = \frac{1}{2}\left(1 - \frac{\varepsilon_{\mathbf{k}}}{\sqrt{\varepsilon^2_{\mathbf{k}} + |\Delta|^2}}\right). \tag{2.41}$$

The value of the gap Δ must be found solving the equation

$$\frac{g}{2} \sum_{\mathbf{k}} \frac{1 - 2n_{\mathbf{k}}}{\sqrt{\Delta + \varepsilon^2_{\mathbf{k}}}} = 1, \tag{2.42}$$

where

$$n_{\mathbf{k}} = \langle \hat{b}^{+}_{\mathbf{k}\uparrow} \hat{b}_{\mathbf{k}\uparrow} \rangle = \langle \hat{b}^{+}_{\mathbf{k}\downarrow} \hat{b}_{\mathbf{k}\downarrow} \rangle \tag{2.43}$$

is the thermal average of the quasi-particles occupation number. Finally, the Hamiltonian reads

$$\hat{H} = \sum_{\mathbf{k}} E_{\mathbf{k}} (\hat{b}^{+}_{\mathbf{k}\uparrow} \hat{b}_{\mathbf{k}\uparrow} + \hat{b}^{+}_{\mathbf{k}\downarrow} \hat{b}_{\mathbf{k}\downarrow}) + \text{const...} \tag{2.44}$$

The energy spectrum acquires the form

$$E_{\mathbf{k}} = \sqrt{\varepsilon_{\mathbf{k}} + \Delta}. \tag{2.45}$$

The gap is

$$\Delta(T = 0) = \tilde{\varepsilon} \exp\left(-\frac{1}{\nu(\mu) g}\right). \tag{2.46}$$

The critical temperature is provided by

$$T_c = 0.57\tilde{\varepsilon} \exp\left(-\frac{1}{\nu(\mu)g}\right), \tag{2.47}$$

where $\nu(\mu)$ is the density of states at the Fermi surface and [105]

$$\tilde{\varepsilon} = \frac{1}{2}\left(\frac{2}{\mathrm{e}}\right)^{7/3} E_F. \tag{2.48}$$

As a consequence of the opening of the gap, below the critical temperature the system acquires superfluid properties flowing without viscosity. No excitation can be created if the system moves slower than the critical velocity $v_c \simeq \Delta/k_F$. In other words the gap shell prevents the formation of particle-hole excitations, but the chemical potential is practically the same as that of a non interacting system since the gap is very small compared to the Fermi energy.

Chapter 3

One dimensional systems

In this chapter we introduce some techniques which are useful to deal with one-dimensional systems. We start our analysis with the fermionization technique, where the idea is to map the system to a free Fermi system [20,106,107]. Then we discuss the exact solution for an homogeneous delta-interacting Bose gas found by Lieb and Liniger [25] using Bethe Ansatz. Although for this model the many-body wave function is available exactly, it is difficult to extract information about the system. For this reason we proceed with the discussion of the bosonization technique [27, 28]. We conclude this chapter with the analysis of the dynamical behavior of an harmonically confined one dimensional gas [34, 41, 108]. In particular, we discuss our results concerning the non-self-similar expansion of 1D Bose gases in a guide.

3.1 Fermionization

The basic idea of fermionization is to map the problem into another one that is exactly solvable. The first example is the XX model, the Hamiltonian reads

$$\hat{H} = -J \sum_{\langle ij \rangle} \left(\hat{S}_i^x \hat{S}_{i+1}^x + \hat{S}_i^y \hat{S}_{i+1}^y \right) = -J \sum_{\langle ij \rangle} [\hat{S}_i^+ \hat{S}_{i+1}^- + \hat{S}_i^- \hat{S}_{i+1}^+], \tag{3.1}$$

where $\hat{S}_j^x$ and $\hat{S}_i^y$ are spin operators at the site i with usual commutation rules, $\langle ij \rangle$ denotes the sum only over nearest neighboring sites. We have defined the ladder operators $\hat{S}_i^{\pm} = \hat{S}_i^x \pm i\hat{S}_i^y$, which *anti-commute* at the same site $\{\hat{S}_i^-, \hat{S}_i^+\} = 1$ but *commute* at different sites $[\hat{S}^-, \hat{S}_i^{\pm}] = 0$. We can reproduce the fermionic commutation rules by means of the so-called Jordan-Wigner transformation [107]. We define a set of spinless fermionic operators $\hat{f}_i$, $\hat{f}_i^+$ for every site i with the usual anti-commutation rules and define

$$S_i^+ = \hat{K}^+(i) f_i^+, \qquad S_i^- = f_i \hat{K}(i), \qquad \hat{K}(i) = \exp\left[i\pi \sum_j^{i-1} \hat{f}_i^+ \hat{f}_i \right]. \tag{3.2}$$

After some algebra we can rewrite the Hamiltonian in the following form

$$\hat{H} = -\frac{J}{2} \sum_i \left(\hat{f}_i^+ \hat{f}_{i+1} + \hat{f}_{i+1}^+ \hat{f}_i \right). \tag{3.3}$$

This is the Hamiltonian corresponding to a free fermionic system. In order to compute correlation functions we have to express the spin operators $\hat{S}_i^{\alpha}$ in terms of these new operators $\hat{f}_i$ and work in this new Hilbert space.

Another example is provided by a bosonic one-dimensional system of impenetrable bosons. The term "Impenetrable" means that the interaction is so strong that the probability to find two particles at the same position vanishes. Let us start with the lattice case, the Hamiltonian reads

$$\hat{H} = -J \sum_{ij} (\hat{b}_i^+ \hat{b}_{i+1} + \hat{b}_{i+1}^+ \hat{b}_i) + \frac{U}{2} \sum_i \hat{b}_i^+ \hat{b}_i^+ \hat{b}_i \hat{b}_i - \mu \sum_i \hat{b}_i^+ \hat{b}_i \quad \text{where } U \to \infty. \tag{3.4}$$

This is equivalent to the constrain $\hat{b}_i^+\hat{b}_i^+ = 0$, meaning that the Hilbert space is reduced to zero or one particle per site and the operators at the same site *anti-commute* instead of *commute*. The usual bosonic commutation relations are preserved at different sites. Applying the same transformation shown above we obtain the Hamiltonian of a free fermionic system

$$\hat{H} = -J\sum_{ij}(\hat{f}_i^+\hat{f}_{i+1} + \hat{f}_{i+1}^+\hat{f}_i) - \mu\sum_i \hat{f}_i^+\hat{f}_i. \tag{3.5}$$

The same problem in the continuous case has been solved by Girardeau [20]. In this case the Hamiltonian reads

$$\hat{H} = \sum_i^N \frac{\hbar^2}{2m}\frac{\partial^2}{\partial x_i^2} + g\sum_{i,j<i}^N \delta(x_i - x_j) \qquad \text{where} \quad g \to \infty. \tag{3.6}$$

Also in this case it exist a mapping between hard core bosons and free fermions. In order to show this, let us write the corresponding Slater determinant. In this case the probability to find two particles in the same point is automatically zero but the wave function is antisymmetric. The fermionic wave function reads

$$\Psi_F(x_1, x_2, \cdots, x_N) = \begin{vmatrix} \phi_1(x_1) & \phi_1(x_2) & \cdots & \phi_1(x_N) \\ \phi_2(x_1) & \phi_2(x_2) & \cdots & \phi_2(x_N) \\ \vdots & \vdots & \ddots & \vdots \\ \phi_N(x_1) & \phi_N(x_2) & \cdots & \phi_N(x_N) \end{vmatrix}. \tag{3.7}$$

This function is an eigenstate of the Hamiltonian (3.6) with the condition that the function is zero when two particles are at the same point. In order to obtain the bosonic wave function we multiply by an antisymmetric function:

$$\Phi_B(x_1, x_2, \cdots, x_N) = A(x_1, x_2, \cdots, x_N)\Phi_F(x_1, x_2, \cdots, x_N), \tag{3.8}$$

where A is a totally antisymmetric function

$$A(x_1, x_2, \cdots, x_N) = \prod_{i,j<i} \frac{x_i - x_j}{|x_i - x_j|}. \tag{3.9}$$

The function A assumes the values ± 1, and hence the function (3.8) is still an eigenstate with the same eigenvalue but now it is totally symmetric. It is important to note that all the properties related to the density are exactly like those of a free fermionic system since $|\Psi_B|^2 = |\Psi_F|^2$, but correlation properties are different, for example the momentum distribution $\tilde{\rho}(p)$ of free fermionic system is a step-function, whereas for a hard core bosons it exhibits a divergency for the momentum $p = 0$, $\tilde{\rho}(p \simeq 0) \propto 1/p^{1/2}$.

With these examples we have shown how to map a system into a free fermionic system. In this way we can in principle calculate all the physical quantities. However, we must say that even if the wavefunction is known, it is not straightforward to compute these quantities, as for example the one-body density matrix [32].

3.2 Lieb Liniger model

This model has the same Hamiltonian (3.6) but the coupling constant has a finite value. In this sense, it is much more general because any regime of interactions is considered. This model is exactly solvable, as shown by Lieb and Liniger (LL) in 1963 [25]. The system is composed by N bosons interacting via a δ potential in a finite one dimensional box with periodic boundary condition, the Hamiltonian reads

$$H = \sum_{i}^{N} \frac{\hbar^2}{2m} \frac{\partial^2}{\partial x_i^2} + g \sum_{i,j<i}^{N} \delta(x_i - x_j), \tag{3.10}$$

where $g = 2\hbar/ma_{1D}$ and a_{1D} is called the one-dimensional scattering length [21]. We come back to this point in Sec. 3.4. The Hamiltonian (3.10) can be diagonalized exactly by means of Bethe Ansatz [109]. In the thermodynamic limit, a bosonic 1D gas at zero temperature with a given linear density ρ, is characterized by an energy per particle:

$$\epsilon(\rho) = \frac{\hbar^2}{2m} \rho^2 e(\gamma(\rho)), \tag{3.11}$$

where $\gamma = 2/n|a_{1\mathrm{D}}|$. The function $e(\gamma)$ fulfills

$$e(\gamma) = \frac{\gamma^3}{\lambda^3(\gamma)} \int_{-1}^{1} \eta\left(x|\gamma\right) x^2 dx, \tag{3.12}$$

where $\eta\left(x|\gamma\right)$ and $\lambda(\gamma)$ are the solutions of the LL system of equations [25]:

$$\eta\left(x|\gamma\right) = \frac{1}{2\pi} + \frac{1}{2\pi} \int_{-1}^{1} \frac{2\lambda(\gamma)}{\lambda^2(\gamma) + (y-x)^2} \eta\left(y|\gamma\right) dy, \tag{3.13}$$

$$\lambda(\gamma) = \gamma \int_{-1}^{1} \eta\left(x|\gamma\right) dx. \tag{3.14}$$

It is worth to mention two particular cases. The first one is when the coupling constant is very large $g \to \infty$, or in other words when $\rho a_{1D} \ll 1$. In that case, the energy per particle assumes the following form

$$\varepsilon(\rho) = \frac{\hbar^2 \pi^2}{6m} \rho^2, \tag{3.15}$$

that it is the expression for a non-interacting homogeneous one dimensional Fermi gas. On the other hand, for small values of the coupling constant $g \to 0$, or equivalently $\rho a_{1D} \gg 1$, the energy per particle reads

$$\varepsilon(\rho) = \frac{1}{2} g \rho. \tag{3.16}$$

For details about the derivation of the previous equations we refer to the literature (see for example [25, 109]).

3.3 Bosonization

The bosonization is a technique that allows to write an effective theory that takes into account just the linear part of the spectrum. It is possible to apply this technique just in one dimension where bosons and fermion are not "different", in the sense that in order to exchange two particle in one dimension they must necessarily interact so it is not possible to separate the concepts of statistic and interaction [27].

Here we summarize the way to derive the effective Hamiltonian and we briefly discuss about conformal symmetry [28, 110]. The quantum field can be written in density an phase representation

$$\hat{\Psi}(x) = e^{i\hat{\theta}(x)}[\hat{\rho}(x)]^{1/2}. \tag{3.17}$$

The density can be written in the following form using Poisson formula

$$\hat{\rho}(x) = \left[\rho_0 - \frac{1}{\pi}\frac{\partial}{\partial x}\hat{\phi}(x)\right]\sum_p e^{i2pi(\pi\rho_0 x - \hat{\phi}(x))}, \tag{3.18}$$

where $\hat{\phi}$ is a field that can be introduced instead of $\hat{\rho}$. Essentially it takes into account the density fluctuations with respect to the equilibrium position of the particles in a lattice. The two fields $\hat{\phi}$ and $\hat{\theta}$ fulfill the following commutation relation

$$\left[\frac{1}{\pi}\hat{\phi}(x), \frac{\partial}{\partial x'}\hat{\theta}(x')\right] = i\delta(x - x'). \tag{3.19}$$

We define the conjugate momentum $\hat{\Pi}$ of the field $\hat{\phi}$ as

$$\pi\hat{\Pi}(x) = \frac{\partial}{\partial x}\hat{\theta}(x). \tag{3.20}$$

At this point we can rewrite the Hamiltonian using these new fields

$$\hat{H} = \frac{\hbar}{2\pi}\int dx \left[\frac{v_s K}{\hbar}(\pi\hat{\Pi}(x))^2 + \frac{v_s}{K}\left(\frac{\partial}{\partial x}\hat{\phi}(x)\right)^2, \right] \tag{3.21}$$

where we have taken into account just quadratic terms. The parameters v_s (sound velocity) and K (Luttinger parameter) totally characterize the low energy properties of any massless one-dimensional system [28]. It is important to note that it is not easy to calculate these two coefficient, but once they are fixed it is possible to determine all the properties of the system.

The action of the system reads

$$S = \frac{\hbar}{2\pi K}\int dx d\tau \left[\frac{1}{v_s}\left(\frac{\partial\hat{\phi}}{\partial\tau}\right)^2 + v_s\left(\frac{\partial\hat{\phi}}{\partial x}\right)^2\right]. \tag{3.22}$$

From this action we can compute the Green function at zero temperature for an infinite system:

$$G(x,\tau) = \frac{\rho_0}{[\rho_0(x^2 + v_s^2\tau^2)]^{1/4K}}. \tag{3.23}$$

Coming back to the action, we see that it is invariant by a class of transformation, for example continuous rotation or scale transformation. The system presents also a conformal symmetry, i.e. invariance under transformations which preserve locally the angles. This is particularity useful for the computation of the correlation functions. For example we can compute the Green function at finite temperature for an infinite system or for a finite system with periodic boundary conditions at zero temperature. In the latter case the results reads

$$G(x,\tau) = n\left[\frac{\pi^2/N^2}{\sinh(\pi\zeta/L)\sinh(\pi\zeta^*/L)}\right]^{1/4K}, \tag{3.24}$$

where $\zeta = v_s\tau + ix$. Therefore, we have shown that it is possible to compute the correlation functions of a finite one-dimensional bosonic gas at zero temperature. For further details we refer to Refs. [28, 110]. This technique is used in chapter 4 to calculate the correlation properties of an array of finite-size bosonic one-dimensional systems.

3.4 Expansion

In this section, we extend the analysis of Ref. [41] on the expansion dynamics of a one-dimensional Bose gas in a guide. It has been shown that the expansion violates under certain conditions the self-similarity typical of BEC [64], and that the problem can be solved by employing the hydrodynamic approach, and the local Lieb-Liniger model. We have developed a variational approach based on a Lagrangian formalism

to study the expansion for any regime of parameters. We have identified the possible physical situations at which self-similarity is violated. The particular properties of the expansion of a gas in the strongly-interacting regime could therefore be employed to discern between mean-field and strongly-interacting regimes. In addition, the asymptotic behavior of the expanded cloud could be employed to discriminate between different initial interaction regimes of the system. Our discussion has been restricted to the analysis of the density properties. In fact the present formalism cannot describe the dynamics of the coherence in the system, i.e. we are limited to the diagonal terms of the corresponding single-particle density matrix. The description of the non diagonal terms lies beyond the scope of this section, and requires other techniques of analysis [35, 38, 111].

3.4.1 Local Lieb-Liniger model

We analyze in the following a dilute gas of N bosons confined in a very elongated harmonic trap with radial and axial frequencies ω_ρ and ω_z ($\omega_\rho \gg \omega_z$). We assume that the transversal confinement is strong enough so that the interaction energy per particle is smaller than the zero-point energy $\hbar\omega_\rho$ of the transversal trap. In this way, the transversal dynamics is effectively "frozen" and the system can be considered as dynamically 1D.

We assume that the interparticle interaction can be approximated by a delta function pseudopotential as discussed in chapter 2. Therefore the Hamiltonian that describes the physics of the 1D gas becomes

$$\hat{H}_{1\mathrm{D}} = \hat{H}^0_{1\mathrm{D}} + \sum_{j=i}^{N} \frac{m\omega_z^2 z_i^2}{2}, \tag{3.25}$$

where

$$\hat{H}^0_{1\mathrm{D}} = -\frac{\hbar^2}{2m}\sum_{j=1}^{N}\frac{\partial^2}{\partial z_j^2} + g_{1\mathrm{D}}\sum_{i=1}^{N-1}\sum_{j=i+1}^{N}\delta\left(z_i - z_j\right) \tag{3.26}$$

is the homogeneous Hamiltonian in absence of the harmonic trap, m is the atomic mass, and $g_{1\mathrm{D}} = -2\hbar^2/ma_{1\mathrm{D}}$. The scattering problem under one-dimensional constraints was analyzed in detail by Olshanii [21], and it is characterized by the one-dimensional scattering length $a_{1\mathrm{D}} = (-a_\rho^2/2a)[1-\mathcal{C}(a/a_\rho)]$, with a the three-dimensional scattering length, $a_\rho = \sqrt{2\hbar/m\omega_\rho}$ the oscillator length in the radial direction, and $\mathcal{C} = 1.4603\ldots$. We assume that at each point x the gas is in local equilibrium, with local energy per particle provided by Eq. (3.11). Then, one can obtain the corresponding hydrodynamic equations for the density and the atomic velocity

$$\frac{\partial}{\partial t}\rho + \frac{\partial}{\partial z}(\rho v) = 0, \tag{3.27}$$

$$m\frac{\partial}{\partial t}v + \frac{\partial}{\partial z}\left(\frac{m}{2}v^2 + \mu_{\mathrm{le}}(\rho) + \frac{1}{2}m\omega_z^2 z^2\right) = 0., \tag{3.28}$$

where

$$\mu_{\mathrm{le}}(\rho) = \left(1 + \rho\frac{\partial}{\partial\rho}\right)\epsilon(\rho) \tag{3.29}$$

is the Gibbs free energy per particle. The system has only one control parameter [13, 33, 34], namely $A = N|a_{1D}|^2/a_z^2$, where $a_z = \sqrt{\hbar/m\omega_z}$ is the harmonic oscillator length in the z direction. The regime $A \gg 1$ corresponds to the MF limit, in which the stationary-state density profile has a parabolic form. On the other hand, the regime $A \ll 1$ corresponds to the TG regime [112], which is characterized by a stationary-state density profile with the form of a square root of a parabola.

3.4.2 Numerical results

In Ref. [41], equations (3.11), (3.13), (3.14), and (3.29) were employed to simulate numerically the expansion of a 1D gas in the framework of the hydrodynamic formalism.

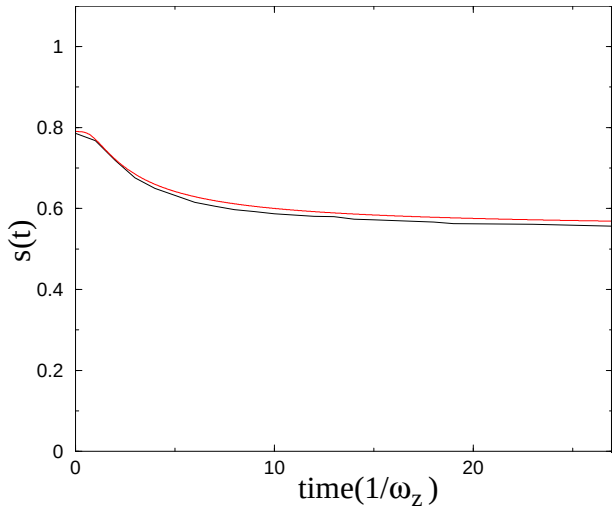

Figure 3.1: *Time evolution of the exponent $s(t)$ for $A = 0.43$, $\omega_\rho = 2\pi \times 20kHz$ and $N = 200$ atoms ($\omega_z = 2\pi \times 1.8Hz$ at $t = 0$). Our variational result (dashed line) shows a very good agreement with the results obtained from the direct resolution of Eqs. (3.27) and (3.28).*

The expansion follows the sudden removal of the axial confinement, while the radial one is kept fixed. In particular, it was observed that during the expansion the density profile is well described by the expression

$$\rho(z,t) = \rho_m(t)\left(1 - \left(\frac{z}{R(t)}\right)^2\right)^{s(t)}, \tag{3.30}$$

where $\rho_m(t)$ provides the appropriate normalization, $R(t)$ is the radius of the cloud, and the exponent $s(t)$ takes the value $s(0) = 1$ for an initial MF gas. The function $s(t)$ decreases monotonically in time, approaching an asymptotic value (see Fig. 3.1). Therefore, contrary to the expansion dynamics for a BEC [64,65,113], the self-similarity of the density profile is violated. At this point we discuss the physics behind this violation of the self-similarity. If the local chemical potential presents a fixed power law dependence on the density, $\mu_{\rm le} \propto \rho^\lambda$, it is easy to show from the hydrody-

namic equations (3.27) and (3.28), that there exists a self-similar solution of the form $\rho = (\rho_0/b)(1-(z/bR)^2)^{1/\lambda}$, where $\ddot{b} = \omega_z^2/b^{\lambda+1}$. For the particular case of the TG gas, the scaling law can be also obtained from the exact BF mapping [41]. However, since μ_{le} is obtained from the LL equations, the dependence of $\mu_{\rm le}$ on ρ is quadratic for a low density and linear for a large one. Therefore, μ_{le} does not fulfill a fixed power law dependence during the expansion, and the self-similarity is violated. In particular, as the expansion proceeds the whole system approaches the low density regime, and consequently the exponent s decreases monotonically. In the next section, we analyze in more detail this effect.

3.4.3 Variational calculation

In this section, we complete our understanding of the expansion of a one-dimensional Bose gas in a guide by means of a variational Ansatz using a Lagrangian formalism. The Lagrangian density for the system is of the form

$$\mathcal{L} = -m\rho\frac{\partial\phi}{\partial t} - \frac{1}{2}m\rho\left(\frac{\partial\phi}{\partial z}\right)^2 - \frac{1}{2}m\omega_z^2 z^2\rho - \varepsilon(\rho)\rho, \tag{3.31}$$

where the velocity field is defined as $v = \partial\phi/\partial z$. The equations of motion are obtained from the functional derivation of the action $\mathcal{A} = \int \mathcal{L}dtdz$: $\delta\mathcal{A}/\delta\phi = 0$ (continuity equation), $\delta\mathcal{A}/\delta\rho = 0$ (which after partial derivation with respect to z provides the Euler equation). From the numerical results we have observed that the density is at any time well described by Eq. (3.30). Therefore, we assume the following Ansatz for the density

$$\rho = \frac{C(s)}{b}\left(1 - \frac{z^2}{R^2b^2}\right)^s, \tag{3.32}$$

where b and s are time dependent variables, R is the initial Thomas-Fermi radius, and $C(s)$ is related to the normalization to the total number of particles. For the ϕ field

we consider the following form:

$$\phi = \frac{1}{2}\alpha z^2 + \frac{1}{4}\beta z^4, \tag{3.33}$$

where α and β are time dependent parameters. We stress at this point, that in the analysis of the self-similar expansion of a BEC [64,65,113], a quadratic ansatz (in z) for the ϕ field provides the exact solution. However, for the problem under consideration, it is necessary to include higher order terms to account for the violation of the self-similarity. We have checked that terms of higher order than z^4 introduces only small corrections, and therefore we reduce to the form of Eq. (3.33).

We are interested in the dynamics of the parameters b and s, related to the size and the shape of the cloud, respectively. Integrating the Lagrangian density in z, $L = \int \mathcal{L} dz$, one finds a Lagrangian for the above mentioned parameters:

$$\begin{aligned} L(\dot{\alpha},\ \alpha, \dot{\beta}, \beta, b, s) = \\ \frac{mNR^2}{2}\Bigg\{ & -\frac{\dot{\alpha} b^2}{2s+3} - \frac{3}{2}\frac{\dot{\beta} b^4}{(2s+5)(2s+3)} \\ & -\frac{\alpha^2 b^2}{2s+3} - 2\frac{\alpha\beta b^4}{(2s+5)(2s+3)} - \\ & -\frac{\beta^2 b^6}{(2s+7)(2s+5)(2s+3)} \\ & -\frac{b^2\omega_z^2}{2s+3}\Bigg\} - \int dz \rho \epsilon(\rho). \end{aligned} \tag{3.34}$$

We perform a gauge transformation[1]

$$L(t, q, \dot{q}) \to L(t, q, \dot{q}) + \frac{d}{dt} g(t, q), \tag{3.35}$$

[1]The Lagrangian (3.34) does not depend on $\dot{b}$ and $\dot{s}$, and consequently one obtains the dynamics only for α and β imposing $\partial L/\partial b = \partial L/\partial s = 0$, and later on from these two conditions one can obtain the dynamics of b and s. The gauge transformation (3.35) turns out to simplify significantly the calculations.

where

$$g(t,q) = \frac{mNR^2}{2}\left\{-\frac{\alpha b^2}{2s+3} - \frac{3}{2}\frac{\beta b^4}{(2s+5)(2s+3)}\right\}. \tag{3.36}$$

The resulting Lagrangian is of the form $L = L(\alpha, \beta, \dot{b}, b, \dot{s}, s)$. Imposing the conservation laws $\partial L/\partial\alpha = \partial L/\partial\beta = 0$, we obtain a Lagrangian depending only on two relevant parameters s and b, of the form $L = K - V$, where

$$\frac{V}{E_{1D}} = \left(\frac{B(b,s)}{f_0(s)} + \frac{A^2b^2}{[\eta_0 f_0(s_0)]^2}\frac{1}{2s+3}\right), \tag{3.37}$$

$$\frac{K}{E_{1D}} = \frac{A^2\left(M_{11}\dot{b}^2 + 2M_{12}\dot{b}\dot{s} + M_{22}\dot{s}^2\right)}{[\eta_0 f_0(s_0)]^2(2s+3)}, \tag{3.38}$$

where $E_{1D} = \hbar^2/2m|a_{1D}|^2$ is the typical energy associated with the interatomic interactions. In Eq. (3.37), we use the function $B(b,s) = \int dy(1-y^2)^s\epsilon(\rho(y))/E_{1D}$, where we integrate over the rescaled axial coordinate $y = z/Rb$. In Eqs. (3.37) and (3.38), we define the dimensionless central density $\eta_0 = \rho_0|a_{1D}|$, where ρ_0 is the initial central density, and the parameter $s_0 = s(t=0)$. We have additionally employed the auxiliary functions $f_n(s) = \int y^n(1-y^2)^s dy$, and the coefficients

$$M_{11} = 1, \tag{3.39}$$

$$M_{12} = \frac{-b}{2s+3} \tag{3.40}$$

$$M_{22} = \frac{b^2(121+186s+96s^2+16s^3)}{4(s+1)(2s+3)^2(2s+5)^2} \tag{3.41}$$

From the Lagrangian L, one obtains the corresponding Euler-Lagrange equations for the parameters b and s. In order to find the initial conditions η_0 and s_0 for the expansion, we have numerically minimized the potential V in the presence of the harmonic trap for different values of A, assuming $b = 1$ (see Fig. 3.2). When $A \gg 1$, s_0 tends to 1, as expected for the MF case. On the contrary, when $A \ll 1$, s_0 tends to 1/2 (TG profile). As expected from Ref. [33], for $A \ll 1$, $\eta_0 \propto A^{1/2}$, whereas for $A \gg 1$, the MF dependence $\eta_0 \propto A^{2/3}$ is recovered.

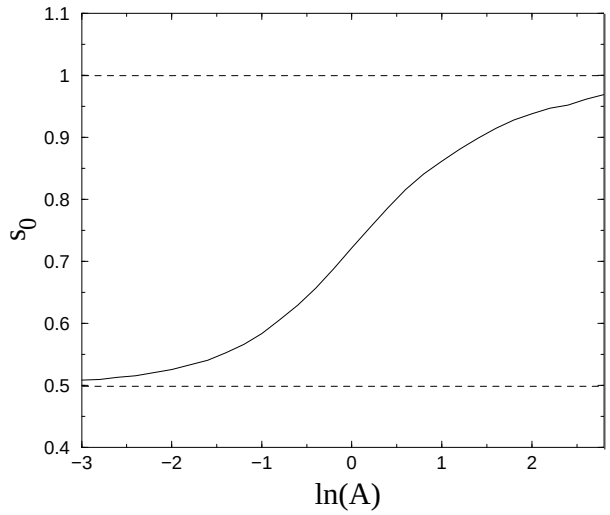

Figure 3.2: *Equilibrium values (at $t = 0$ before opening the trap) of the exponent s, as a function of the parameter A. The dashed lines denote the MF limit, $s_0 = 1$, and the TG one, $s_0 = 1/2$.*

Our variational approach allows to calculate the lowest compressional mode, offering an alternative method as the one discussed in Ref. [34]. Expanding the potential V around the equilibrium solution up to second order in b (see Fig. 3.3), and neglecting for small oscillations the time-dependence of s, we obtain

$$\frac{\omega_m^2}{\omega_z^2} = 1 + \frac{1}{2A^2} \frac{[\eta_0^2 f_0(s_0)]^2}{f_2(s_0)} \left. \frac{\partial^2 B}{\partial b^2} \right|_{b=1} . \tag{3.42}$$

Our results show a continuous transition from the MF value, $\omega_m = \sqrt{3}\omega_z$, to the TG one, $\omega_m = 2\omega_z$, in excellent agreement with the results obtained by means of a sum rule formalism [34].

From the corresponding Euler-Lagrange equations, we have obtained the dynamics of $b(t)$ and $s(t)$. We have checked in all our calculations that the energy and number of particles remain a constant of motion. We have compared the variational results with our simulations based on the exact resolution of the hydrodynamic equations [41],

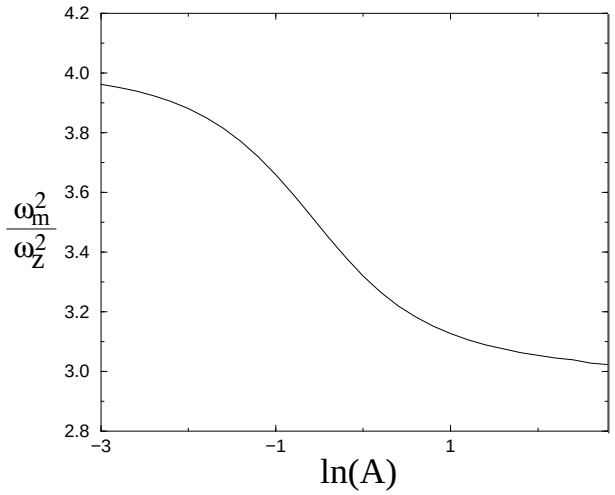

Figure 3.3: *Frequency of the lowest compressional mode as a function of the parameter A.*

obtaining an excellent agreement (see Fig. 3.1).

We have analyzed the asymptotic value, $\dot{b}_\infty$, for different values of A. It is easy to obtain, that for a power law dependence of the local chemical potential $\mu_{\rm le} \propto \rho^\lambda$, the derivative of the scaling parameter asymptotically approaches a value $\dot{b}_\infty = \sqrt{2/\lambda}\omega_z$. Therefore a continuous transition from $\dot{b}_\infty = \omega_z$ (TG) to $\dot{b}_\infty = \sqrt{2}\omega_z$ (MF) is expected. We recover this dependence from our variational calculations (see Fig. 3.4).

We have analyzed the behavior of s during the expansion dynamics for different values of A. In particular, we have defined the asymptotic ratio $\xi = s_\infty/s_0$, with $s_\infty = s(t \to \infty)$ (see Fig. 3.5).

Deeply in the TG regime ($A \ll 1$) or in the MF one ($A \gg 1$), $\xi \simeq 1$, i.e. the expansion is well-described by a self-similar solution. However, for intermediate values, $\xi < 1$, i.e. the expansion is not self-similar. The self-similarity is maximally violated in the vicinity of $A = 1$, although ξ departs significantly from 1 for a range $0.01 < A < 100$. The behavior at large A can be understood as follows. If the gas is at

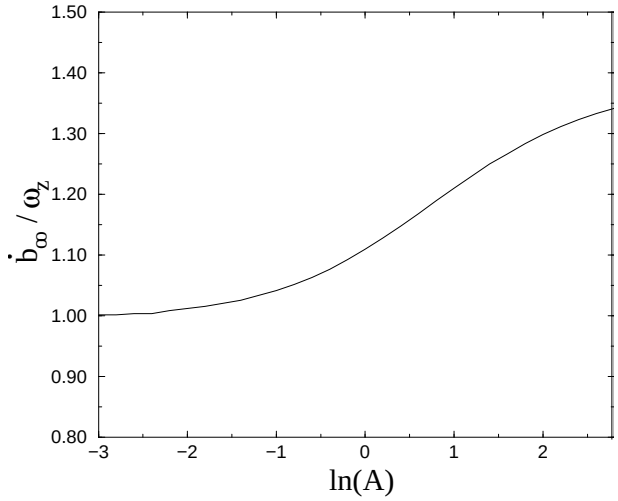

Figure 3.4: *Expansion velocity. Asymptotic value of* $\dot{b}$ *as a function of the parameter* A.

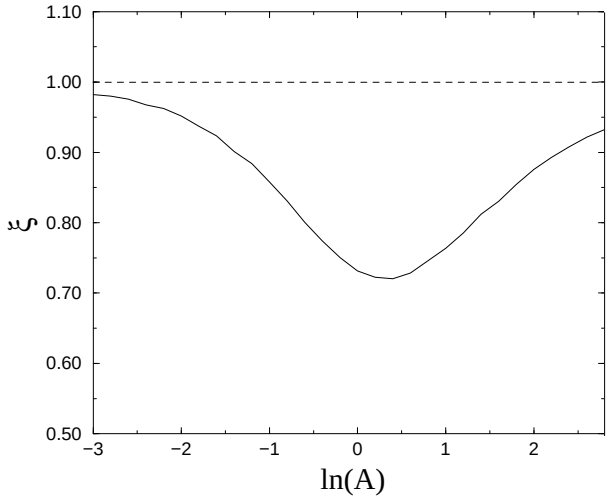

Figure 3.5: *Violation of the self-similarity. Value of* $\xi = s_\infty / s_0$ *as a function of the parameter* A. *The value* $\xi = 1$ *denotes self-similarity.*

$t = 0$ deeply in the MF regime, the change of the functional dependence of μ_{le} with the density occurs at very long expansion times, when the initial interaction energy of the gas has been fully transferred into kinetic energy. Therefore, for large values of A the self-similarity is recovered.

Chapter 4

Interacting atoms in a periodic potential

In this chapter we recall some general concepts about periodic potentials, as e.g. Bloch and Wannier functions, the effective mass, and a short explanation of the superfluid-insulator transition. The rest of the chapter is devoted to the analysis of a three-dimensional gas in a two-dimensional periodic potential where every site can be consider as a one dimensional system.

4.1 Optical lattices

Optical Lattices [42–46] can be generated optically with the help of a laser standing wave (see for example [114]). The basic idea is to shine counterpropagating lasers on a two-level atom. Far away from resonance, absorption is strongly suppressed and dissipative process can be neglected. Due to the spatial dependence of the laser intensity, the atoms experience a periodic force with period $d = \lambda/2$ where λ is the wave-length of the laser and the amplitude is proportional to the laser intensity. Since the force is

conservative, it can be written as a potential and included in the Hamiltonian as an external potential acting on the atoms:

$$\hat{H}_0 = -\frac{\hbar^2}{2m}\frac{\partial^2}{\partial x^2} + V_{\text{opt}}(x), \tag{4.1}$$

where V_{opt} is a periodic function with period d. The solution of this equation can be written as a Bloch-function [115]

$$\psi(x) = \exp\{ikx\}u_{n,k}(x), \tag{4.2}$$

where $u_{n,k}$ is a periodic function with the same periodicity of the potential, k is the quasi-momentum, and n is the band index. Working on a lattice it is more useful to deal with another basis called Wannier functions defined as

$$w_{n,j}(x) = \frac{1}{\sqrt{N}}\sum_k \psi_{n,k}(x)\exp(ikdj). \tag{4.3}$$

It is important to notice that we do not mix Bloch functions of different bands. Each Wannier functions is localized at a given lattice site, and fulfill that

$$w_{n,j}(x) = w_{n,0}(x - jd). \tag{4.4}$$

It is possible to omit the symbol of the site and keep just the band index since due the previous relation Wannier functions belonging to the same band are just the discrete translation of the same function. Let us consider a concrete case and write the many-body Hamiltonian for a bosonic system:

$$\hat{H} = -J\sum_{\langle i,j\rangle}\hat{b}_i^+\hat{b}_j + +\frac{U}{2}\sum_i \hat{b}_i^+\hat{b}_i^+\hat{b}_i\hat{b}_i - \mu\sum_i \hat{b}_i^+\hat{b}_i, \tag{4.5}$$

where $\hat{b}_i$ and $\hat{b}_i^+$ are bosonic operators. We have just considered hopping to neighboring sites and on-site interactions. This is justified in the tight-binding limit and for short-range interactions. The hopping coefficient reads

$$J = -\int d^3r w_1^*(\mathbf{r})H_0 w_1(\mathbf{r} + d\hat{\mathbf{x}}), \tag{4.6}$$

where $\hat{\mathbf{x}}$ is an element of the basis of the three-dimensional vectorial space, and the interaction coefficient reads

$$U = g \int d^3 r |w_1(\mathbf{r})|^4. \tag{4.7}$$

Let us describe in more detail the insulating-superfluid properties of the system. We can write a functional for the order parameter in order to obtain the phase diagram. A reasonable choice is

$$\psi = \langle \hat{b}_i \rangle \tag{4.8}$$

since in the superfluid phase the number of particles in each site is fluctuating and the order parameter is different than zero, while in the insulating phase, neglecting quantum fluctuations, it is zero. It is worthy to point out that this is not strictly true, since in fact even in the insulating phase one can have fluctuations of the number of particle and this fact is responsable of some correlation between sites [62]. The definition of this order parameter allows us to write a mean field approach

$$\sum_{\langle ij \rangle} \hat{b}_i^+ \hat{b}_j \approx z \sum_i \psi (\hat{b}_i + \hat{b}_i^+) + z \sum_i |\psi|^2, \tag{4.9}$$

where z is the coordination number (number of nearest neighboring sites) and the Hamiltonian can be rewritten as a sum of decoupled Hamiltonians

$$\hat{H} = \sum_i [-Jz\psi(\hat{b}_i^+ \hat{b}_i) - Jz|\psi|^2 + U\hat{b}_i^+ \hat{b}_i^+ \hat{b}_i \hat{b}_i]. \tag{4.10}$$

The first term can be treated in perturbation theory giving rise to a Ginzburg-Landau functional

$$H = A|\psi|^2 + B|\psi|^4, \tag{4.11}$$

where A and B depend on the parameter J, U and μ. To find the phase diagram one has to solve the equation $A = 0$ [116]. The insulating phase is incompressible and its excitations are gapped, while in the superfluid phase the spectrum is not gapped. The

presence or absence of this gap can be used to reveal the phase transition. By means of the Green function formalism, it is possible to obtain the border between the two phases precisely when the spectrum becomes gap-less. In the next section we discuss in detail how to calculate the phase diagram using this method.

We can retrieve a continuous limit making a course-graining procedure introducing the field $\hat{\Psi}(\mathbf{r}_i) \approx \hat{b}_i/d^{3/2}$. The Hamiltonian then reads

$$\hat{H} = \int d^3r \hat{\Psi}^+(\mathbf{r}) \left(-\frac{\hbar^2}{2m^*}\Delta - \mu^* + \frac{g^*}{2}\hat{\Psi}^+(\mathbf{r})\hat{\Psi}(\mathbf{r}) \right) \hat{\Psi}(\mathbf{r}), \tag{4.12}$$

where we have renormalized the mass, the chemical potential and the coupling constant. In this case the effective mass, the coupling constant and the chemical potential read

$$m^* = \frac{\hbar}{2Jd^2}; \qquad g^* = Ud^3; \qquad \mu^* = \mu + 2J. \tag{4.13}$$

Let us at this point discuss about the validity of the approximation introduced above. The continuous limit does not describe the insulating phase since only gap-less excitations are present, and does not take into account the occurrence of Bloch oscillations if the system is perturbed by a constant force (see appendix A.3). On the other side this method gives the correct sound velocity and the static properties. We show in the next section an application of this method.

4.2 2D lattice of 1D systems

We have seen in the previous section that it is possible to create periodic structures using light, this opens many possibilities regarding low-dimensional systems. In fact every site of a one-dimensional lattice can be seen as a two-dimensional system or in the case of a two-dimensional lattice, the sites can be considered one-dimensional. Some properties concerning the latter case are analyzed in this section.

4.2.1 Superfluid phase in a trap

In the following we consider a gas of N bosons in a cylindrically-symmetric harmonic trap, with axial (radial) frequency ω_z ($\omega_\perp$). We assume a superimposed periodic potential provided by an optical lattice of the form $V_l(x)+V_l(y) = V_0(\sin^2 qx+\sin^2 qy)$, where $q = 2\pi/\lambda$ is related to the laser wavelength λ, and V_0 is the lattice amplitude. The lattice has a periodicity $d = \pi/q = \lambda/2$. From a macroscopic point of view it is convenient to introduce the effective mass, m^*, to describe the effects of the lattice on the dynamics. The value of m^* can be obtained from $\partial^2 E_0/\partial k^2 = \hbar^2/m^*$, where $E_0(k)$ is the dispersion law corresponding to the lowest energy band. In tight-binding regime, m^* can be related with the tunneling rate J, as $m/m^* = \pi^2 J/E_R$, where $E_R = \hbar^2 q^2/2m$ is the recoil energy, $J = -\int w_i(x)(-\hbar^2\nabla_x^2/2m + V_l(x))w_{i+1}(x)dx$, and $\{w_i\}$ are the Wannier functions for the lowest band.

We first consider the case of a single isolated lattice site, which can be well approximated as a dilute gas of N_t bosons confined in a very elongated harmonic trap with radial and axial frequencies ω_l and ω_z ($\omega_l \gg \omega_z$). The transversal confinement is strong enough to fulfill that the interaction energy per particle is smaller than the zero-point energy $\hbar\omega_l$ of the transversal trap. In this way, the transversal dynamics is effectively "frozen" and the system can be considered 1D. The Hamiltonian describing the physics of the delta-interacting 1D gas is

$$\hat{H}_{1\mathrm{D}} = \hat{H}^0_{1\mathrm{D}} + \sum_{j=i}^{N_t} \frac{m\omega_z^2 z_i^2}{2}, \tag{4.14}$$

where

$$\hat{H}^0_{1\mathrm{D}} = -\frac{\hbar^2}{2m}\sum_{j=1}^{N_t}\frac{\partial^2}{\partial z_j^2} + g_{1\mathrm{D}}\sum_{i=1}^{N_t-1}\sum_{j=i+1}^{N_t}\delta\left(z_i - z_j\right) \tag{4.15}$$

is the Hamiltonian in absence of the harmonic trap, and $g_{1\mathrm{D}} = -2\hbar^2/ma_{1\mathrm{D}}$. As discussed in Chapter 3 the scattering problem under one-dimensional constraints was

analyzed in detail by Olshanii [21], and it is characterized by the 1D scattering length $a_{1\mathrm{D}} = (-a_l^2/2a)[1 - \mathcal{C}(a/a_l)]$, with a the 3D scattering length, $a_l = \sqrt{2\hbar/m\omega_l}$ the oscillator length in the radial direction, and $\mathcal{C} = 1.4603\ldots$. For the thermodynamic limit, a 1D gas at zero temperature with linear density ρ, is characterized by an energy per particle, which can be obtained from the previously discussed LL integral equations [25]. Assuming that the density variates sufficiently slowly, we can apply the local Lieb-Liniger (LLL) model, which as previously commented in chapter 3 consists in considering at each point z that the gas is at local equilibrium, and the local energy per particle is provided by the LL equations.

Although, strictly speaking, the LLL approach is only valid for 1D systems, for sufficiently low J, the processes involving transitions into nearest sites, should just result in a small correction to the 1D scattering of the order of J/μ, where μ is the chemical potential. Therefore, if $J/\mu \ll 1$, the actual local chemical potential can be well approximated by that obtained from the LLL approach. If the tunneling becomes very small ($J < J_c$), even for large values of N_t the system could enter into the MI regime. We analyze this possibility in Sec. 4.2.2. Summarizing, in what we called the quasi-Tonks regime, $(J_c/\mu) < J/\mu \ll 1$, the LLL chemical potential can be employed, and at the same time the tunneling cannot be neglected.

Assuming a sufficiently slow variation of the gas density, the dynamics can be well described by means of the corresponding macroscopic hydrodynamic equations [117]:

$$\frac{\partial \rho}{\partial t} + \nabla \cdot (\rho \mathbf{v}) = 0, \tag{4.16}$$

$$m^* \frac{\partial v_x}{\partial t} + \frac{\partial}{\partial x}(K + V + U) = 0, \tag{4.17}$$

$$m^* \frac{\partial v_y}{\partial t} + \frac{\partial}{\partial y}(K + V + U) = 0, \tag{4.18}$$

$$m \frac{\partial v_z}{\partial t} + \frac{\partial}{\partial z}(K + V + U) = 0, \tag{4.19}$$

where

$$K = \frac{m^*}{2}v_x^2 + \frac{m^*}{2}v_y^2 + \frac{m}{2}v_z^2, \tag{4.20}$$

$$V = \frac{m}{2}\omega_\perp^2(x^2+y^2) + \frac{m}{2}\omega_z^2 z^2, \tag{4.21}$$

$$U = \mu(\rho) = \mu_{1D}(d^2\rho), \tag{4.22}$$

where $\rho(x,y,z)$ is the macroscopic 3D density and $\mathbf{v} = (v_x, v_y, v_z)$ is the velocity field. Note that all the information about the lattice is contained in m^*, and in the local chemical potential $\mu(\rho)$. In Eq. (4.22) the local chemical potential of the 3D system is related to the 1D chemical potential, μ_{1D}, provided by the LLL approach. In order to obtain μ_{1D} the value of a_{1D} must be obtained for each site. The latter demands the knowledge of the effective oscillator length a_l associated with the on-site radial confinement. Since the latter can be very large, a Gaussian Ansatz can be assumed for the on-site radial wave function. In this way, we can calculate a_l by minimizing the radial energy

$$\frac{E(a_l)}{E_R} = \frac{1}{q^2 a_l^2} + \frac{V_0}{E_R}\left(1 - e^{-q^2 a_l^2}\right). \tag{4.23}$$

In Eq. (4.23) we have neglected the interaction energy, which for $V_0/E_R > 3$ does not provide any significant contribution. Once known the value of a_{1D}, we evaluate $\mu_{1D}(\rho)$ by numerically solving the corresponding LL integral equations.

By imposing the equilibrium conditions $\partial\rho/\partial t = v_i = 0$, we obtain the equation of state

$$\mu[\rho_0(x,y,z)] = \mu_T - V(x,y,z), \tag{4.24}$$

where ρ_0 is the equilibrium density, and μ_T is the chemical potential of the system. Inverting (4.24), one obtains the expression for ρ_0. Imposing the normalization to the

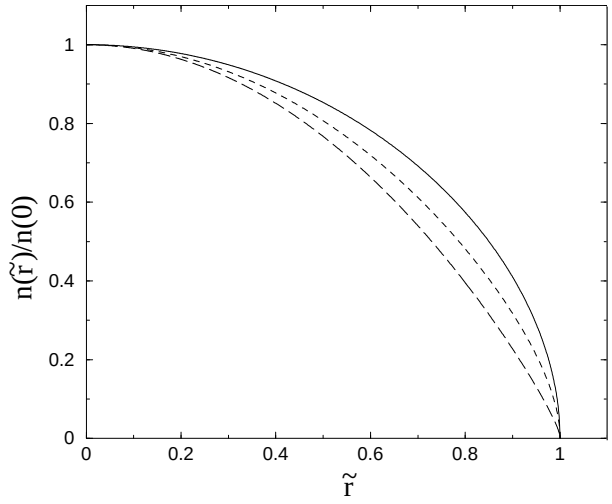

Figure 4.1: *Density profile as a function of the dimensionless radius* $\tilde{r}^2 = \sum_i (r_i/R_i)^2$ *(see text). The solid, doted and dashed lines correspond to* $\log A = -3,\ 0,\ 3$, *respectively. The resulting fit with a power law dependence* $(1-\tilde{r}^2)^s$ *provides* $s = 0.54,\ 0.72,\ 0.91$, *respectively, being an indicator of the transition from the MF regime to the strongly-interacting one.*

number of particles N we obtain:

$$A = \frac{|a_{1D}|^4 d^2 N}{a_x^2 a_\perp^4} = 4\pi\xi^3 \int_0^1 t^2 \tilde{\mu}_{1D}^{-1}[\xi^2(1-t^2)]dt, \tag{4.25}$$

where $\xi = 2\mu m|a_{1D}|^2/\hbar^2$. From Eq. (4.25) we observe that, similarly to the strict 1D case [33–35], the ground state of the system is completely characterized by a single parameter A. For $A \gg 1$ the mean-field (MF) regime is retrieved, whereas the TG is found for $A \ll 1$. In Eq. (4.25), $\tilde{\mu}_{1D}(x) = 2m|a_{1D}|^2\mu_{1D}(x)/\hbar^2$, is a function of the dimensionless density $\eta = |a_{1D}|d^2\rho$. Fig. 4.1 shows the density as a function of the dimensionless radius $\tilde{r}$, where $\tilde{r}^2 = \sum_i (r_i/R_i)^2$, with R_i the Thomas-Fermi radii. In order to compare the different cases, we re-scale the density with respect to the central one. Nevertheless, we stress that the values of R_i and the central density depend on the parameters, and in particular on the interaction regime. From the previous discussion,

it becomes clear that the 1D properties of the local chemical potential are transferred to the 3D stationary shape of the cloud. In particular, for small values of A, the transversal density profile is not an inverted parabola, as expected for the case of a BEC in a harmonic trap. We stress once more, that this remarkable effect is just possible in the presence of the 2D lattice, which guarantees, under the above discussed conditions, a LLL chemical potential. In the following we calculate the frequencies for the lowest excitations of a quasi-Tonks gas. In particular, we evaluate the breathing and quadrupole modes, by using the Ansatz $\rho = \rho_0 \, (r_i/b_i) \, / \prod_j b_j$, $v_i = (\dot{b}_i/b_i) r_i$, which constitutes an exact solution of the continuity equation (4.16). Multiplying the Euler equations by ρx_i and integrating, one obtains

$$\ddot{b_x} + \tilde{\omega}_\perp^2 b_x + \frac{\tilde{\omega}_\perp^2}{b_x} F(\prod_{j=x,y,z} b_j) = 0, \tag{4.26}$$

$$\ddot{b_y} + \tilde{\omega}_\perp^2 b_y + \frac{\tilde{\omega}_\perp^2}{b_y} F(\prod_{j=x,y,z} b_j) = 0, \tag{4.27}$$

$$\ddot{b_z} + \omega_z^2 b_z + \frac{\omega_z^2}{b_z} F(\prod_{j=x,y,z} b_j) = 0, \tag{4.28}$$

where we have employed the effective frequencies $\tilde{\omega}_\perp^2 = \omega_\perp^2 m/m^*$, and defined the function

$$F(\zeta) = \frac{1}{m\omega_i^2 N \langle x_i^2 \rangle_0} \int \rho_0 x_i \frac{\partial}{\partial x_i} \mu(\zeta^{-1} n_0) d^3 r. \tag{4.29}$$

Using the previously calculated equilibrium solution, one obtains that $F(\zeta)$ is independent of the particular choice of the coordinate i, and that $F(1) = -1$. Note that the function F only depends on A, which, as previously discussed, completely characterizes the static properties of the system. Linearizing around the equilibrium solution $b_i = 1$, one obtains the frequencies of the breathing mode (ω_B), the $M = 0$ quadrupole mode (ω_{Q1}) and the $M = \pm 2$ quadrupole one (ω_{Q2}):

$$\omega_B^2 = \frac{1}{2}\{\tilde{\omega}_\perp^2(2+2f) + \omega_z^2(2+f)$$

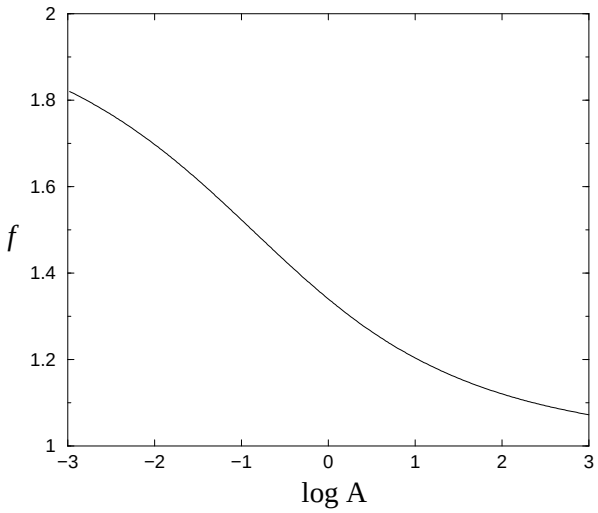

Figure 4.2: *Parameter f as a function of* $\log A$ *(see text).*

$$+\sqrt{[\tilde{\omega}_\perp^2(2+2f)+\omega_z^2(2+f)]^2-8\tilde{\omega}_\perp^2\omega_z^2(2+3f)}\} \tag{4.30}$$

$$\omega_{Q1}^2 = \frac{1}{2}\{(\tilde{\omega}_\perp^2(2+2f)+\omega_z^2(2+f) -\sqrt{[\tilde{\omega}_\perp^2(2+2f)+\omega_z^2(2+f)]^2-8\tilde{\omega}_\perp^2\omega_z^2(2+3f)}\} \tag{4.31}$$

$$\omega_{Q2}^2 = 2\tilde{\omega}_\perp^2 \tag{4.32}$$

In the expression for the frequencies we employ the parameter $f = \frac{\partial F(\zeta)}{\partial \zeta}|_{\zeta=1}$, which is an universal function of the parameter A. We show this dependence in Fig. 4.2. The parameter f ranges from 2, at the TG limit, to 1, for the MF regime. In this two limiting cases the function F can be obtained analytically, being $F = \zeta^{-2}$ (TG) and $F = \zeta^{-1}$ (MF).

The quasi Tonks regime is not only achievable for realistic conditions, but, actually, it is expected to be the case for typical parameters in ongoing experiments, as those of Fig. 4.3, which shows the dependence of the frequencies (4.30-4.32) on the lattice amplitude V_0/E_R. We stress that the system enters the MI regime for large values of V_0/E_R (around 40 for the case of Fig. 4.3). If this is the case, as discussed above, our

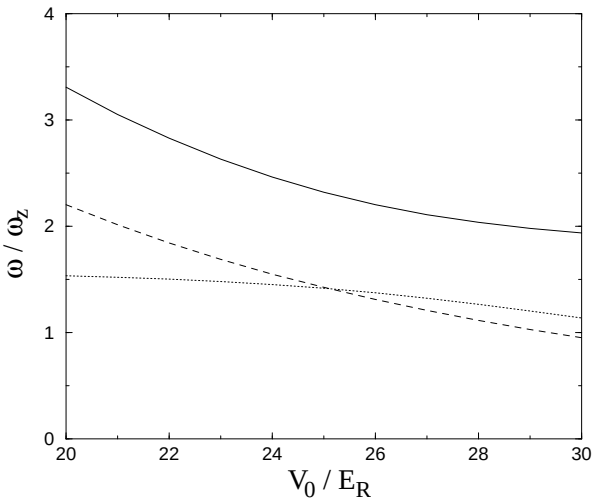

Figure 4.3: *Frequencies of the breathing mode (solid), quadrupole* 1 *(dotted) and quadrupole* 2 *(dashed) as a function of* V_0/E_R*, for the particular case of* ^{87}Rb *atoms,* $N = 2 \times 10^5$*,* $\omega_z = 2\pi \times 4Hz$*,* $\omega_\perp = 2\pi \times 40Hz$*, and* $d = 0.5\mu m$*.*

macroscopic hydrodynamic approach fails, and the system becomes a set of independent 1D gases. On the other hand, for decreasing values of V_0/E_R the system abandons the quasi-Tonks regime (which for the case of Fig. 4.3 occurs at $V_0/E_R \simeq 15$), and the condition $J/\mu \simeq 1$ is reached. This constitutes an additional intermediate cross-dimensional regime, in which the gas is 3D, but the local chemical potential is not that expected for a 3D Bose gas. For this regime, contrary to the case of the quasi-Tonks gas, the local chemical potential cannot be approximated by the LLL chemical potential. As a consequence of that, the challenging problem of describing the $J/\mu \simeq 1$ regime demands a completely different approach. In this sense, especially interesting could be to employ the analogies to the problem of coupled Luttinger liquids [118–120].

The existence of the quasi Tonks regime can be easily revealed in experiments, by either observing the size and the form of the stationary density profile, or monitoring the collective excitations. For increasing values of V_0/E_R, the frequency of the breath-

ing mode approaches that of the lowest compressional mode in 1D gases [34], whereas the quadrupolar frequencies tend to zero. For intermediate values of the lattice potential, the lowest excitations are significantly different than in 1D, for the same value of the dimensionless density η. In particular, more than one excitation mode is expected. We stress that the modes (4.30-4.32) also differ significantly from the expected results for a BEC in a lattice [117]. The latter are recovered from our formalism for large values of A (MF regime). We must point, however, that the local correlation properties are preserved in the quasi Tonks regime. In this sense, if the parameter A becomes sufficiently small the lifetime of the gas can be very significantly enlarged, due to the reduction of the two- and three-body losses [35].

4.2.2 Insulating phase

In the following we consider the situation in which the system is in a Mott-insulator phase on the lattice plane. In other words, contrary to the previously discussed Quasi-Tonks case, we consider here the case $J < J_c$. The value of J_c is also discussed in this section.

In the following we consider a Bose gas at zero temperature in a 2D optical lattice, such that every lattice site can be considered as an axially homogeneous 1D tube of finite size L, with $N = \rho L$ being the number of particles per tube, and ρ the 1D density. As previously discussed, the tunneling between neighboring tubes is characterized by the hopping t, which depends on a particular lattice potential and atomic species employed. We label tubes by the index j and denote by x the coordinate along the tubes.

The action describing the coupled tubes has the form:

$$S = \sum_j S_j - J \sum_{<ij>} \int_{-\infty}^{\infty} d\tau \int_{-L/2}^{L/2} dx \ \left(\psi_i^* \psi_j + \psi_j^* \psi_i\right), \tag{4.33}$$

where $\psi_j(x,\tau), \psi_j^*(x,\tau)$ are complex bosonic fields associated with the J-th tube, the symbol $< ij >$ denotes nearest neighbors, and S_j is the action describing the physics along the j-th tube:

$$S_j = \int_{-\infty}^{\infty} d\tau \int_{-L/2}^{L/2} dx \psi_j^* \left(-\frac{\hbar^2}{2m}\frac{\partial^2}{\partial x^2} + \frac{\partial}{\partial \tau} - \mu + g|\psi|^2 \right) \psi_j. \tag{4.34}$$

In the absence of tunneling, there are no correlations between different tubes, and the one-body Green function is diagonal:

$$\begin{aligned} G_{ij}(x_1 - x_2, \tau_1 - \tau_2) &= \langle \psi_i(x_1,\tau_1) \bar{\psi}_j(x_2,\tau_2) \rangle \\ &= \delta_{ij} G_0(x_1 - x_2, \tau_1 - \tau_2). \end{aligned} \tag{4.35}$$

The presence of tunneling between neighboring tubes, provided by the second term on the rhs of Eq. (4.33), modifies the momentum distribution. As previously commented, above a critical tunneling amplitude t_c the system undergoes a cross-over from the MI to an anisotropic 3D SF phase [61]. This cross-over and the MI phase can be analyzed within the random phase approximation (RPA) [121], successfully used in the studies of coupled spin chains [122–124]. Decoupling the tunneling term by using the Hubbard-Stratonovich transformation and keeping only the leading quadratic terms, yields the RPA Green function in the momentum-frequency representation:

$$G(\vec{q}, k, \omega) = \frac{G_0(k,\omega)}{1 - T(\vec{q}) G_0(k,\omega)}, \tag{4.36}$$

with $\vec{q} = (q_y, q_z)$ being the quasi-momentum in the lattice plane, $T(\vec{q}) = 2J(\cos q_y d + \cos q_z d)$, d the lattice constant, and $G_0(k,\omega)$ the Fourier transform of the Green function (4.35) (hereinafter we put $\hbar = 1$):

$$G_0(k,\omega) = \int_{-\infty}^{\infty} d\tau \int_{-L/2}^{L/2} dx \, e^{-ikx + i\omega\tau} G_0(x,\tau). \tag{4.37}$$

The long-wavelength behavior of the Green function $G_0(x,\tau)$ can be found using Luttinger liquid theory [27]. At zero temperature, employing a conformal transformation (see chapter 3) in order to take into account the finite size L of the tubes [121], we obtain:

$$G_0(x,\tau) = \rho \left(\frac{\pi^2/N^2}{\sinh\left(\pi\zeta/L\right)\sinh\left(\pi\bar{\zeta}/L\right)} \right)^{\nu}, \tag{4.38}$$

where $\zeta = v_s\tau + ix$, and v_s is the sound velocity. The interactions enter Eq.(4.38) through the factor $\nu = 1/4K$ related to the interaction-dependent Luttinger parameter K. The Fourier transform of Eq. (4.38) yields

$$G_0(k,\omega) = \frac{1}{\rho v_s} \left(\frac{N}{2\pi}\right)^{2-2\nu} I\left(\frac{kL}{2\pi}, \frac{\omega L}{2\pi v_s}\right), \tag{4.39}$$

where the quantity $I(p,\Omega)$ is expressed through the hypergeometric function ${}_3F_2$:

$$I(p,\Omega) = \frac{4\pi}{p!}\frac{\Gamma(\nu+p)}{\Gamma(\nu)} Re\left[\frac{{}_3F_2\left(\nu, \nu+p, \frac{\nu+p-i\Omega}{2}; 1+p, 1+\frac{\nu+p-i\Omega}{2}; 1\right)}{\nu+p-i\Omega} \right], \tag{4.40}$$

with $p = kL/2\pi$ and $\Omega = \omega L/2\pi v_s$ being the dimensionless momentum and frequency. Integrating Eq. (4.39) over ω one obtains the momentum distribution $N_0(kL/2\pi) = \int d\omega G_0(k,\omega)/2\pi$ in the absence of tunneling:

$$\frac{N_0(p)}{N} = \left(\frac{N}{2\pi}\right)^{-2\nu} \frac{\Gamma(\nu+p)}{p!\Gamma(d)} {}_2F_1(\nu, \nu+p; 1+p; 1), \tag{4.41}$$

which behaves as $p^{2\nu-1}$ for $p \gtrsim 1$. The Luttinger liquid description employed here is valid for low momenta $k \ll \pi\rho$. Accordingly, the dimensionless axial momentum $p = kL/2\pi$, which is an integer number, should satisfy the inequality $p \ll N$. The momentum distribution (4.41) represents the fraction of particles in the state with momentum p and is normalized as $\sum_p N_0(p) = N$.

The critical tunneling J_c for the MI to SF cross-over is obtained as the value of J for which the denominator of Eq. (4.36) vanishes for zero momenta k and $\vec{q}$ and zero

frequency ω. We thus have

$$\frac{J_c}{\mu} = \frac{\rho v_s}{4\mu} \left(\frac{N}{2\pi}\right)^{2\nu-2} \frac{1}{I(0,0)}. \tag{4.42}$$

Note that with J_c from Eq. (4.42), the Green function G in Eq. (4.36) becomes a universal function of the dimensionless quantities J/J_c, p, qd and Ω. For the TG regime of 1D bosons in the tubes, the Luttinger parameter is $K = 1$ and $\nu = 1/4$. Then, as the chemical potential is $\mu = mv_s^2 = \pi^2\rho^2/2m$, from Eq.(4.42) we obtain $J_c/\mu \simeq 0.05N^{-3/2}$. For the weakly interacting regime, the Luttinger parameter in the 1D tubes is $K = \pi(\rho/mg)^{1/2} \gg 1$ and Eq.(4.40) gives $I(0,0) = 16\pi K \gg 1$. In this regime the chemical potential is $\mu = mv_s^2 = \rho g$, and Eq.(4.42) then yields $J_c/\mu \simeq (1/16)N^{-2}$ (as expected from the mean-field calculations for a 2D lattice of zero-dimensional sites [116]). These results are in qualitative agreement with the recent calculations of Ho et al. [61]. One clearly sees that strong correlations along the tubes drastically shift the boundaries of the MI phase.

The momentum distribution for the coupled 1D tubes in the MI phase, $N(\vec{q}, k)$, is obtained by integrating the Green function (4.36) over the frequency. Our calculations show that only the lowest axial mode for which the momentum $k = 0$, is significantly affected by the tunneling. The physical reason is that the $k = 0$ mode is approaching the instability on approach to the critical tunneling J_c, whereas $k \neq 0$ modes are still far from instability. This is reflected in the resonance character of the Green function (4.36) for $k = 0$ and $J \to J_c$. Our results in Fig. 4.4 show that the transverse distribution $N(\vec{q}, 0)$ corresponding to the $k = 0$ axial mode is non-flat for any interaction regime along the tubes. In contrast, for $k \neq 0$ the quantity $T(\vec{q})G_0(k, \omega)$ is always small. Therefore, expanding the rhs of Eq. (4.36) in powers of $T(\vec{q})$ up to linear order and integrating over ω we obtain an almost flat transverse momentum distribution for $k \neq 0$ modes: $N(\vec{q}, p)/N(0, p) = 1 - (Ad^2/4p^{2-\nu})(J/J_c)(2 - \sum_{i=y,z} \cos q_i a)$, where the

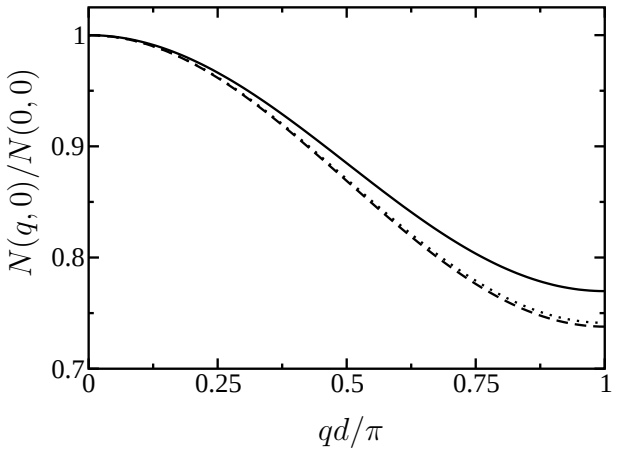

Figure 4.4: *Transverse momentum distribution for $k = 0$ at $J/J_c = 0.3$ for $K = 1$ (solid), $K = 4$ (dotted), and $K = 25$ (dashed). In the figure we have chosen $q_y = q_z = q$.*

coefficient A is of order unity and the second (q-dependent) term is always very small.

We now turn to the discussion of the transverse quasi-momentum distribution $N_\perp(\vec{q}) = \sum_k N(\vec{q}, k)$. The summation over the axial modes changes the picture drastically compared to the distribution for a given k. As only the $k = 0$ component is significantly affected by the tunneling, one can rewrite Eq. (4.36) in the form:

$$G(\vec{q}, k, \omega) \simeq G_0(k, \omega) + \frac{T(\vec{q})G_0^2(0, \omega)}{1 - T(\vec{q})G_0(0, \omega)}\delta_{k,0}. \tag{4.43}$$

In the second term on the rhs of Eq.(4.43) we may use the Green function $G_0(0, \omega)$ following from Eqs. (4.39) and (4.40). For $k = 0$ ($p = 0$), one can put the hypergeometric function ${}_3F_2 = 1$ in Eq.(4.40), which gives $I(0, \Omega) \simeq 4\pi\nu/(\nu^2 + \Omega^2)$. Omitted terms give a very small relative correction of the order of $\rho v_s^3 < 1/4^3$. Hence, using Eq.(4.42), for the Green function at $k = 0$ in the absence of tunneling we have $G_0(0, \omega) = \nu^2/4t_c(d\nu^2 + \Omega^2)$. Then, integrating Eq.(4.43) over Ω, summing over the axial modes k, and imposing the normalization condition $N = \sum_k \int d\omega G_0(k, \omega)/2\pi$

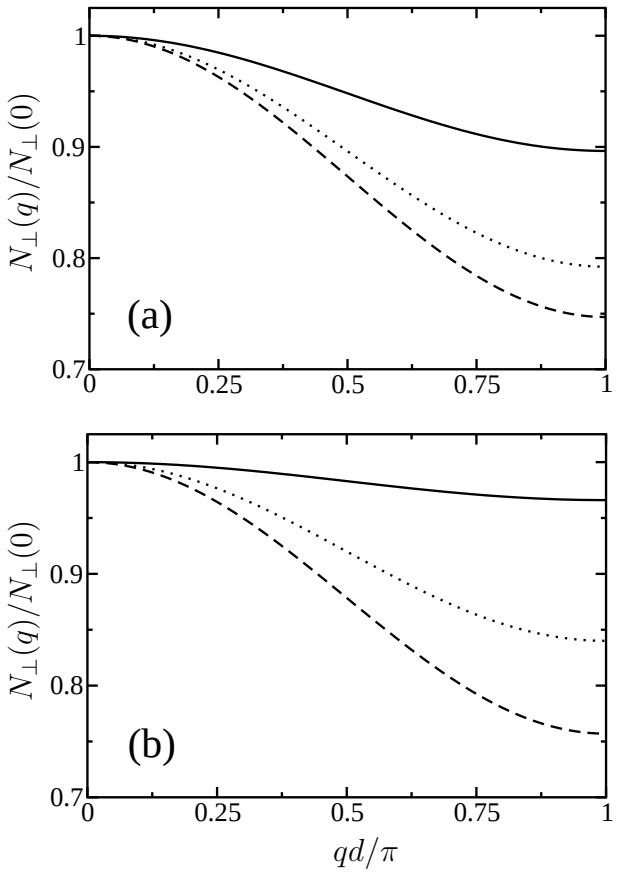

Figure 4.5: *Transverse momentum distribution for $J/J_c = 0.3$, at $K = 1$ (solid), $K = 4$ (dotted), and $K = 25$ (dashed), for $N = 50$ (a) and $N = 500$ (b). In the figures we have chosen $q_y = q_z = q$.*

for the first term on the rhs, we obtain the transverse momentum distribution

$$\frac{N_\perp(\vec{q})}{N} = 1 + \left(\frac{2\pi}{N}\right)^{2d} \left[\left(1 - \frac{t}{2t_c} \sum_{i=y,z} \cos q_i d \right)^{-1/2} - 1 \right], \tag{4.44}$$

normalized by the condition $(d/2\pi)^2 \int d^2q N_\perp(\vec{q}) = N$.

In Fig. 4.5 we depict the results of Eq. (4.44) for different values of N and the Luttinger parameter K. Due to the prefactor in the second term on the rhs of Eq. (4.44) the transverse momentum distribution strongly depends on the interaction regime along the tubes.

For the weakly interacting regime ($\nu \ll 1$), the distribution $N_\perp(\vec{q})$ is not flat even deeply inside the MI phase. Similar results have been obtained by means of Quantum Monte Carlo calculations [62] for the case of lattices of zero-dimensional sites. In our case, only for rather low tunneling ($J/J_c \lesssim 0.1$) the quasi-momentum distribution becomes flat, and switching off the lattice potential should lead to a blurred picture as that observed by Greiner et al. [24]. Non-flat distributions in the MI phase as those of Fig. 4.5 will manifest themselves through the appearance of interference peaks in the same type of experiment (see appendix A.1 and A.2).

On approach to the TG regime, the quasi-momentum distribution becomes progressively flatter. The main reason for this behavior is that when the system becomes more interacting, the $k = 0$ component is more depleted, contributing less to the total quasi-momentum distribution. Therefore, if the 1D tubes approach the strongly interacting TG regime, in experiments as those of Ref. [24] the interference pattern will be essentially smeared out. One may expect a partial destruction of the interference pattern even for moderate values of the Luttinger parameter (see, e.g., the case $K = 4$ in Fig. 4.5).

The random phase approximation used in our calculations, was shown to be a good approximation for a wide range of parameters of coupled one-dimensional Heisenberg spin chains [122]. Here we give yet another estimate for the applicability of RPA, relying on the Ginzburg criterion adapted to a quantum phase transition at zero temperature. We compare fluctuations of the order parameter in a volume determined by the correlation radius extracted from the Green function (4.36), with the scale on which the non-linear effects become important. The latter is obtained from the four-point correlation function of each tube. We have found that RPA is adequate for $(t_c - t)/t_c \gg B(\nu)$, where $B(\nu)$ has been obtained numerically from the four-

point correlation function. In the case of the Tonks-Girardeau regime along the tubes, we have $B \approx 0.1$, and it decreases significantly with decreasing ν and entering the Gross-Pitaevskii regime.

Chapter 5

Classical and Fermi gases

We have already discussed both classical and Fermi gases in Chapter 2, where we have introduced some general concepts. In this chapter, we analyze in more detail some dynamical aspects of a classical gas, a superfluid Fermi gas and a normal Fermi gas. We first introduce some useful techniques to deal with these systems.

5.1 Method of the averages and scaling ansatz

In this section we develop a method that allow us to calculate the dynamics of some observable without solving directly the Boltzmann equation. Multiplying the Boltzmann equation by an observable χ, and integrating on the phase space we obtain

$$\frac{d}{dt}\langle\chi\rangle - \langle\mathbf{v}_1\cdot\nabla_{\mathbf{r}}\chi\rangle - \langle\mathbf{F}\cdot\nabla_{\mathbf{p}_1}\chi\rangle = \langle\chi C[f]/f\rangle. \tag{5.1}$$

In principle Eq. (5.1) gives rise to a set of equations involving in principle many observables, as we discuss below in an example. The goal is to obtain a closed set of equations. In this way we reduce the problem to a set of ordinary differential equations that is much simpler to solve than the Boltzmann equation. This method has been used to calculate the shift of the collective frequencies due to collisions [125, 126].

The most difficult term to treat is the collisional integral, since it contains nonlinear terms. One way to treat this term is to make an appropriate Ansatz for the distribution function, and possibly rewrite it as a combination of other variables [125,126]. Due to symmetry properties of the transition amplitude T (see Chapter 2), if χ is a conserved quantity in a collision the collisional integral vanishes explicitely if $\chi = \alpha(\mathbf{r}) + \beta(\mathbf{r}) \cdot \mathbf{p} + \gamma(\mathbf{r})p^2$ [90]. As an example let us consider a gas confined in a spherical harmonic trap, i.e. under a force $\mathbf{F} = -m\omega_0^2\mathbf{r}$. It is easy to obtain the following set of equations for the averages of the observables:

$$\frac{d}{dt}\langle r^2\rangle - 2\langle \mathbf{v}\cdot\mathbf{r}\rangle = 0, \tag{5.2}$$

$$\frac{d}{dt}\langle \mathbf{v}\cdot\mathbf{r}\rangle - \langle v^2\rangle + \omega_0^2\langle r^2\rangle = 0, \tag{5.3}$$

$$\frac{d}{dt}\langle v^2\rangle + 2\omega_0^2\langle \mathbf{v}\cdot\mathbf{r}\rangle = 0. \tag{5.4}$$

Developing around the equilibrium solution we calculate the monopole frequency, $\omega_M = 2\omega_0$. To calculate the quadrupole frequencies we have to start with the following operators $\langle x^2 - y^2\rangle$, $\langle x^2 + y^2 - 2z^2\rangle$ and obtain a new closed set of equations [125]. In this case collisions play an important role and they are responsible of the damping of the oscillations [127]. The equations (5.2),(5.3),(5.4) can be used to calculate also the time evolution of the square radius when the external trapping is turned-off ($\omega_0 = 0$). Using the virial theorem ($\langle v^2\rangle = \omega_0^2\langle r^2\rangle$ at equilibrium) we obtain the following result:

$$\frac{\langle r^2\rangle(t)}{\langle r^2\rangle(0)} = 1 + \omega_0^2 t^2. \tag{5.5}$$

This is a simple but very important result. In fact any deviation from this law implies that the interactions play a role during the expansion. We show in the next section how the geometry of the trap, collisions and mean field interaction can affect the expansion and the lowest collective excitations.

The interaction between particles enter in the Boltzmann equation through the collisional term. A mean-field term must be included in the force in the Boltzmann equation if the temperature is sufficiently low or the gas is not too dilute [129]. This new equation receives the name of Vlasov equation [128].

$$\frac{\partial f}{\partial t} + \mathbf{v}_1 \cdot \nabla_{\mathbf{r}} f + (\mathbf{F}_{\text{ext}} + \mathbf{F}_{\text{mf}}) \cdot \nabla_{\mathbf{p_1}} f = C[f]. \tag{5.6}$$

The expression for the mean field $\mathbf{F}_{\text{mf}}(\mathbf{r})$ force can be assumed of the form $\mathbf{F}_{\text{mf}}(\mathbf{r}) = \nabla_{\mathbf{r}} \int d^3r' U(\mathbf{r}, \mathbf{r}')\rho(\mathbf{r}')$ where $U(\mathbf{r}, \mathbf{r})$ is the potential energy between two particles at position $\mathbf{r}$ and $\mathbf{r}'$. In the case of contact interactions $U = 2g\delta^3(\mathbf{r} - \mathbf{r}')$ so $\mathbf{F}_{\text{mf}}(\mathbf{r}) = 2g\nabla\rho(\mathbf{r})$. The basic idea of the scaling ansatz method is to use as an ansatz the equilibrium solution. The time dependence is introduced by means of some time dependent parameter. Let us make one example in order to clarify these points. We consider a trapped classical gas in collisionless regime and a mean field potential proportional to the density [129]. The equilibrium distribution fulfills the following equation

$$\sum_i \left(v_i \frac{\partial f_0}{\partial r_i} - \omega_i^2 r_i \frac{\partial f_0}{\partial v_i} - \frac{2g}{m} \frac{\partial \rho_0}{\partial r_i} \frac{\partial f_0}{\partial v_i} \right) = 0. \tag{5.7}$$

From equation (5.7) it is easy obtain the relation

$$\omega_i^2 \langle r_i \rangle - \langle v_i \rangle - \frac{2g}{mN} \int \rho_0^2 d^3r = 0, \tag{5.8}$$

that establish a relation among the kinetic energy, the potential energy and the mean field energy. The time dependence is introduced by means of scaling parameters

$$f(t, v_i, r_i) = f_0(V_i(t, r_i, v_i), R_i(t, r_i)), \tag{5.9}$$

where the new variables are defined as $V_i = b_i(t)v_i - \dot{b}_i(t)r_i$, and $R_i = r_i/b_i(t)$, and the parameters $b_i(t)$ are the scaling parameters. Substituting Eq. (5.9) into the Boltzmann

Eq. (5.6) we obtain

$$\sum_i \left[\frac{V_i}{b_i}\frac{\partial f_0}{\partial R_i} - b_i R_i(\ddot{b}_i + \omega_i^2 b_i)\frac{\partial f_0}{\partial V_i} - \frac{2g}{m\prod_j b_j}\frac{\partial \rho_0}{\partial R_i}\frac{\partial f_0}{\partial V_i} \right] \simeq 0. \tag{5.10}$$

Combining Eq. (5.7) with Eq. (5.11) we obtain the following expression

$$\sum_i \left[\left(\frac{V_i}{b_i^2} - \frac{V_i}{\prod_j b_j} \right) \frac{\partial f_0}{\partial R_i} - b_i R_i \left(\ddot{b}_i + \omega_i^2 b_i - \frac{\omega_i^2}{b_i \prod_j b_j} \right) \frac{\partial f_0}{\partial V_i} \right] \simeq 0. \tag{5.11}$$

Taking an average of $R_i V_i$ we obtain the following set of equations

$$\ddot{b}_i - \omega_i^2 b_i - \frac{\omega_i^2}{b_i} + \omega_i^2 \xi \left(\frac{1}{b_i^3} - \frac{1}{b_i \prod_j b_j} \right) = 0, \tag{5.12}$$

where $\xi = g\langle\rho_0\rangle/(g\langle\rho_0\rangle + T)$.

Summarizing, we have used the ground state properties without a detailed knowledge of the ground state. In fact the only parameter regarding the ground state properties is ξ. This method is used extensively in the rest of this chapter.

5.2 Dynamics of a classical gas with dissipative and mean-field effects

So far analytic calculations for the expansion of a classical gas have been limited to either the ballistic or to the hydrodynamic regime [65]. As a consequence, it is important to generalize such calculations to all intermediate collisional regimes. This is precisely the main purpose of this section. Our approach relies on an approximated solution to the Vlasov equation including collisions by means of a scaling ansatz, following the ideas introduced previously. This solution is used throughout this section to investigate two kinds of related problems: the lowest collective oscillation modes and the time-of-flight expansion when the confinement is released.

As previously discussed, the Boltzmann-Vlasov (BV) kinetic equation for the phase space distribution $f(t, \mathbf{r}, \mathbf{v})$ takes the form:

$$\frac{\partial f}{\partial t} + \mathbf{v} \cdot \frac{\partial f}{\partial \mathbf{r}} - \frac{1}{m} \frac{\partial (U_{\rm h} + U_{\rm mf})}{\partial \mathbf{r}} \cdot \frac{\partial f}{\partial \mathbf{v}} = I_{\rm coll}[f], \tag{5.13}$$

where $U_{\rm h}$ is the trapping potential chosen of harmonic form: $U_{\rm h}(\mathbf{r}) = \frac{m}{2} \sum_i \omega_i^2 r_i^2$. Interparticle interactions enter Eq. (5.33) in two different ways [130]. On the one hand, they modify the effective potential through the mean field term $U_{\rm mf}$ which affects the streaming part of the Boltzmann kinetic equation. The mean field potential $U_{\rm mf}$ is equal to $2g\rho$ for bosons and $g\rho$ for two fermion species[1], where the coupling constant $g = 4\pi\hbar^2 a/m$ is fixed by the s-wave scattering length a. The mean field term is linear in a and is non dissipative. On the other hand, two body interaction determines the collision integral $I_{\rm coll}[f]$ which is quadratic in the scattering length, and describes dissipative processes. Eq. (5.33) is valid in the semi-classical limit, namely when the thermal energy is large compared to the separation between the energy eigenvalues of the potential [90, 131].

We treat the collisional integral within the relaxation time approximation [90]. This model should suffice to capture the essential physics of the problem. We consequently write:

$$I_{\rm coll}[f] \approx -\frac{f - f_{\rm le}}{\tau}, \tag{5.14}$$

where τ is the relaxation time related to the average time between collisions, and $f_{\rm le}$ is the local equilibrium density in phase space. As a consequence, $f_{\rm le}$ has a spherical symmetry in velocity space, *i.e.* it depends on the velocity through $[\mathbf{v} - \mathbf{u}(\mathbf{r})]^2$ where $\mathbf{u}(\mathbf{r})$ is the local velocity field.

[1]For fermions, the density ρ as well as the distribution function f refers to a single species.

The dynamics of the gas will be described by the following scaling ansatz for the non equilibrium distribution function:

$$f(t, r_i, v_i) = \frac{1}{\prod_j (b_j \theta_j^{1/2})} f_0 \left(\frac{r_i}{b_i}, \frac{1}{\theta_i^{1/2}} \left(v_i - \frac{\dot{b}_i}{b_i} r_i \right) \right), \tag{5.15}$$

where f_0 is the equilibrium distribution function which satisfies the equation ($I_{\rm coll}[f_0] = 0$):

$$m\mathbf{v} \cdot \frac{\partial f_0}{\partial \mathbf{r}} = \frac{\partial U_{\rm h}}{\partial \mathbf{r}} \cdot \frac{\partial f_0}{\partial \mathbf{v}} + \frac{\partial U_{\rm mf}}{\partial \mathbf{r}} \cdot \frac{\partial f_0}{\partial \mathbf{v}}. \tag{5.16}$$

The dependence on time of f is contained in the dimensionless scaling parameters b_i and θ_i. The parameter b_i gives the dilatation along the i^{th} direction, while θ_i gives the effective temperature in the same direction. Such an ansatz generalizes the one used in [129]. We recall that in this method the shape of the cloud does not explicitly enter the equations.

Following Ref. [129], one can derive the set of equations for the scaling parameters b_i and θ_i (see Appendix A.4):

$$\ddot{b}_i + \omega_i^2 b_i - \omega_i^2 \frac{\theta_i}{b_i} + \omega_i^2 \xi \left(\frac{\theta_i}{b_i} - \frac{1}{b_i \prod_j b_j} \right) = 0 \tag{5.17}$$

$$\dot{\theta}_i + 2\frac{\dot{b}_i}{b_i}\theta_i = -\frac{1}{\tau}\Big[\theta_i - \bar{\theta}\Big], \tag{5.18}$$

where the dimensionless parameter $\xi = \langle U_{\rm mf}\rangle_0 / (\langle U_{\rm mf}\rangle_0 + 2m\langle v^2\rangle_0/3)$ accounts for the mean field interaction[2] and $\bar{\theta} = \sum_i \theta_i/3$ is the average temperature. For a classical gas $\langle v^2\rangle_0 = 3k_B T/m$. The parameter ξ is expected to be small for dilute gases ($\rho a^3 \ll 1$) since the ratio $U_{\rm mf}/k_B T$ scales as $(\rho a^3)^{1/3}(\rho \lambda_{db}^3)^{2/3}$, where λ_{db} is the de Broglie wavelength and ρ is the mean density [129]. Eq. (5.18) shows that the dissipation

[2]We define $\langle\chi\rangle_0$ as the average in position and velocity space of the function $\chi(\mathbf{r}, \mathbf{v})$ weighted by the equilibrium distribution function: $\langle\chi\rangle_0 = \int d^D r\, d^D v\, f_0(\mathbf{r}, \mathbf{v})\, \chi(\mathbf{r}, \mathbf{v}) / \int d^D r\, d^D v\, f_0(\mathbf{r}, \mathbf{v})$.

occurs when the temperature is not isotropic and the relaxation time τ has a finite value.

The collisionless regime is obtained by taking $\tau_0 = \infty$. In this limit, we have the simple relation $\theta_i = b_i^{-2}$ between the scaling parameters, and we recover the equations derived in [129]. In the opposite limit (hydrodynamic regime), local equilibrium is always ensured because of the high collision rate. As a consequence, we have $\theta_i = \bar{\theta} = \prod_j b_j^{-2/3}$ and the Eqs (5.17) and (5.18) can be recast in the form:

$$\ddot{b}_i + \omega_i^2 b_i - \frac{\omega_i^2}{b_i \prod_j b_j^{2/3}} + \omega_i^2 \xi \left(\frac{1}{b_i \prod_j b_j^{2/3}} - \frac{1}{b_i \prod_j b_j} \right) = 0. \tag{5.19}$$

For $\xi = 0$ (no mean field), we recover the equations first derived in [65]. Note that in both the collisionless and the hydrodynamic regimes, the collisional term does not contribute since there is no dissipation in these limits. We next focus our attention on the intermediate regimes where the collision term enters explicitly the equations of motion.

Let us first study the breathing mode in the case of spherical harmonic trapping with angular frequency ω_0. In this case, we find a solution with $b_i = b$ and $\theta_i = b^{-2}$. For such a solution the collision term identically vanishes in all intermediate collisional regimes. Our approach can be readily generalized to lower dimensions leading to the frequency $\omega_0(4+\xi(d-2))^{1/2}$ for the monopole mode [129], where d is the dimension of space. In two dimensions the mean field does not affect the frequency of the monopole. This comes out from the fact that in this case the ansatz is an exact solution of the BV equations, as already stressed in Ref. [132].

We now consider a sample of atoms confined in a three-dimensional cylindrically symmetric harmonic potential. We denote by $\lambda = \omega_z/\omega_\perp$ the ratio between the axial

and radial angular frequencies. Expanding Eqs. (5.17) and (5.18) around equilibrium ($b_i = \theta_i = 1$) we get a linear and closed set of equations which can be solved by looking for solutions of the type $e^{i\omega t}$. The associated determinant yields the dispersion law:

$$\Big(A[\omega] + \frac{1}{\tau_0}B[\omega]\Big)\Big(C[\omega] + \frac{1}{\tau_0}D[\omega]\Big) = 0, \tag{5.20}$$

where $A[\omega] = \omega^2(\omega^2 - \omega^2_{\rm cl+})(\omega^2 - \omega^2_{\rm cl-})$, $B[\omega] = \omega(\omega^2 - \omega^2_{\rm hd+})(\omega^2 - \omega^2_{\rm hd-})$, $C[\omega] = \omega(\omega^2 - \omega^2_{\rm cl})$ and $D[\omega] = (\omega^2 - \omega^2_{\rm hd})$ and τ_0 is the value of the relaxation time τ calculated at equilibrium and

$$\begin{aligned}
\omega^2_{\rm cl\pm} &= \frac{\omega^2_\perp}{2}\Big(4(1+\lambda^2) - \lambda^2\xi \\
&\quad \pm\sqrt{16 + \lambda^4(4-\xi)^2 + 8\lambda^2(\xi^2 - 4 + \xi)}\Big) \\
\omega^2_{\rm cl} &= \omega^2_\perp(4 - 2\xi) \\
\omega^2_{\rm hd\pm} &= \frac{\omega^2_\perp}{3}\Big(5 + 4\lambda^2 + \xi(1 + \lambda^2/2) \\
&\quad \pm\frac{1}{2}\sqrt{(10 + 8\lambda^2 + 2\xi + \lambda^2\xi)^2 - 72\lambda^2(4+\xi)}\Big) \\
\omega^2_{\rm hd} &= 2\omega^2_\perp.,
\end{aligned}$$

where ξ is the previously defined parameter accounting for the mean field effects, and (cl) and (hd) refer to the collisionless and hydrodynamics regimes respectively. The solution of Eq. (5.20) interpolates the frequencies of the low lying modes for all collisional regimes ranging from the collisionless to the hydrodynamic. As the confinement is cylindrically symmetric around the z axis, we can label the modes by their angular azimuthal number M. The first factor of the l.h.s. of Eq. (5.20) gives the frequencies of the two $M = 0$ modes, while the second factor gives that of the quadrupole ($M = \pm 2$) mode. The roots of A and C have already been obtained in [129], and correspond to the frequencies of the low lying modes of a collisionless gas in presence of mean field. Eq. (5.20) for $\xi = 0$ has been derived in Ref. [125] and

the corresponding frequencies have been investigated experimentally [74]. For $\xi = 1$, corresponding to $\langle g\rho_0\rangle_0 \gg \langle v^2\rangle_0$, we find $\omega^2_{\mathrm{cl}\pm} = \omega^2_{\mathrm{hd}\pm}$, $\omega^2_{\mathrm{cl}} = \omega^2_{\mathrm{hd}}$, and the frequencies coincide with the ones predicted for a Bose-Einstein condensate in the Thomas-Fermi regime [4].

So far, we have not given the explicit link between the relaxation time entering Eq. (5.20) and the collision rate. Following Ref. [125], we can establish this link for a classical gas by means of a Gaussian ansatz for the equilibrium distribution function $f(\mathbf{r}, \mathbf{v}, t)$. One obtains $\tau_0 = 5/(4\gamma)$ where $\gamma = 2(2\pi)^{-1/2}\rho_{\max}\sigma v_{\mathrm{th}}$ is the classical collision rate where $v_{\mathrm{th}} = (k_B T/m)^{1/2}$ is the thermal velocity, $\rho_{\max}$ is the peak density and σ is the cross section which is assumed to be velocity independent. For bosons the link between the scattering length and the cross section is $\sigma = 8\pi a^2$ whereas for two fermions species one has $\sigma = 4\pi a^2$.

We now establish the set of equations that describe the time-of-flight expansion. In the collisionless regime where the mean free path is very large with respect to the size of the trapped cloud and in the absence of mean field contribution, we readily obtain the exact equations $\ddot{b}_i = \omega_i^2/b_i^3$ which admit the solutions $b_i(t) = (1 + \omega_i^2 t^2)^{1/2}$, leading to isotropic density and velocity distributions after long time expansion.

When the effect of collisions is important the physics of the expansion changes dramatically. As an example, the radial directions of a cigar-shaped cloud expand faster than the longitudinal one finally resulting in an anisotropic velocity distribution. So far, an analytic approach has been proposed only in the full hydrodynamic regime [65]. However, this approach assumes that the hydrodynamic equations are always valid during the expansion. In general, this cannot be the case since the density decreases during the expansion reducing the effect of collisions. Alternatively, the expansion of an interacting Bose above T_c gas has been investigated by means of a

Monte Carlo simulation [79].

In our approach, we provide an interpolation between the two opposite collisionless and hydrodynamic regimes using the scaling formalism. The decrease of the collision rate during the expansion yields a non constant relaxation time $\tau(b_i, \theta_i)$ that depends explicitly on the scaling parameters and reflects the changes of the density and the temperature during the expansion. As a result, the expansion is described by the following set of 6 non-linear equations

$$\begin{aligned} \ddot{b}_i - \omega_i^2 \frac{\theta_i}{b_i} + \omega_i^2 \xi \left(\frac{\theta_i}{b_i} - \frac{1}{b_i \prod_j b_j} \right) = 0 \\ \dot{\theta}_i + 2\frac{\dot{b}_i}{b_i}\theta_i = -\frac{1}{\tau(b_i, \theta_i)} \left(\theta_i - \frac{1}{3} \sum_j \theta_j \right). \end{aligned} \tag{5.21}$$

The dependence of the relaxation time τ on the scaling parameters is obtained by noticing that the collision rate γ scales as $\rho T^{1/2}$. Using the scaling transformation $\rho \to \rho_0 (\prod_j b_j)^{-1}$ and $T \to T_0 \bar{\theta}$, where ρ_0 and T_0 are the initial density and temperature respectively, we deduce

$$\tau(b_i, \theta_i) = \tau_0 \Big(\prod_j b_j \Big) \Big(\frac{1}{3} \sum_k \theta_k \Big)^{-1/2} \tag{5.22}$$

where τ_0 is the average time of collision at equilibrium. Since both the results (5.20) for the dispersion of the linear oscillations and Eqs. (5.21) and (5.22) for the expansion have been derived starting from the same scaling equations (5.17) and (5.18) the relaxation time τ_0 entering the two processes is the same. As a consequence, the combined investigation of the expansion and of the quadrupole oscillations can provide a useful check of the consistency of the approach and, possibly, useful constraints on the value of the cross section.

The time evolution of the aspect ratio $R_\perp(t)/R_z(t) = \lambda b_\perp(t)/b_z(t)$ in the absence of mean field is depicted on Fig. 5.1 for different values of the product $\omega_\perp \tau_0$ and for

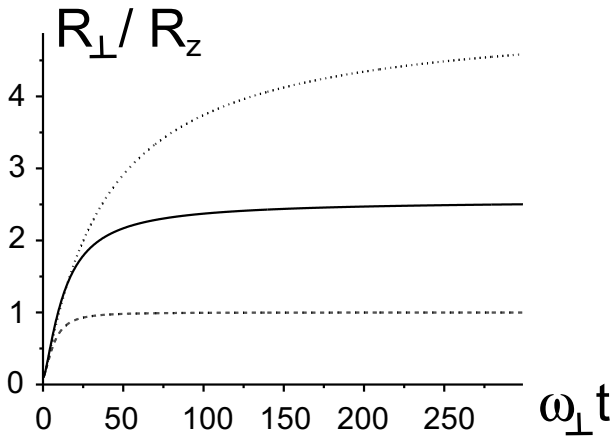

Figure 5.1: *Aspect ratio as a function of the normalized time $\omega_\perp t$ for different collisional regimes (initial aspect ratio $\lambda = 0.1$): collisionless (dashed line, $\tau_0 \longrightarrow \infty$), intermediate collisional regime (solid line, $\omega_\perp \tau_0 = 0.1$), hydrodynamic regime (dotted line, $\tau_0 \longrightarrow 0$).*

an initial aspect ratio $\lambda = 0.1$. In the collisionless regime ($\tau_0 = \infty$), the aspect ratio tends asymptotically to unity reflecting the isotropy of the initial velocity distribution. For other collisional regimes, the asymptotic aspect ratio is larger than one as a consequence of collisions during the expansion. We find a continuous transition from the collisionless to the hydrodynamic prediction as we decrease τ_0 from infinity to zero. We then conclude that in general the expansion cannot be described with either the hydrodynamic or the collisionless prediction [133], but requires a full solution of our equations (5.21). Similar conditions have been already encountered experimentally for classical or almost classical gases [76]. We also notice that it is very important to take into account the time dependence of the relaxation time, accounted for by the scaling law (5.22). For example by simply using $\tau = \tau_0$ during the whole expansion, the curve $\omega_\perp \tau = 0.1$ of Fig. 5.1 (solid line) would be shifted upward and the resulting prediction would result much closer to the hydrodynamic curve (dotted line). The

effect of quantum statistics on the calculation of the relaxation time will be treated is section 5.3. For a Bose gas at temperature above T_c the problem has been investigated in [134] where it has been shown that statistical effects do not play a significant role. In contrast, the relaxation time in a harmonically trapped dilute Fermi gases has been shown to be strongly affected by Pauli blocking at low temperature [82]. The effects of collisions in a strongly interacting Fermi gas, including the unitarity limit, have been recently addressed in [135].

5.3 Fermi gases

In the previous section we have shown how the interactions affect the collective excitations and the expansion of a classical gas. In this section we develop a similar analysis for a Fermi gas. We start comparing the expansion and the lowest collective modes of a superfluid Fermi gas with those of a normal Fermi gas at very low temperature, in order to show the effect of superfluidity. Then we discuss a geometrical effect on the expansion of normal Fermi gas, showing that, due to collisional effects, an increasing of entropy occurs.

5.3.1 Superfluid and normal gas

In this part of the thesis we study the problem of the expansion of an ultracold sample of fermions initially trapped in an anisotropic harmonic trap. We show that also in the case of fermions the expansion of the gas provides valuable information about the state of the system and the role of interactions. We consider a gas of atoms interacting with attractive forces. This is a natural requirement for the realization of Cooper-pairs and hence for the achievement of the superfluid phase [77]. Such interactions are naturally

present in some fermionic species like ^{6}Li and can otherwise be obtained by changing the scattering length profiting of the presence of a Feshbach resonance.

The description of the expansion of a cold fermionic gas in the normal and superfluid phase requires different theoretical approaches. For the normal phase we use the formalism of the Landau-Vlasov equations, while in the superfluid phase we study the expansion using the hydrodynamic theory of superfluids.

We consider the case of two different fermionic states, hereafter called 1 and 2, initially confined in a harmonic trap. We assume that the two species are present in the same amount and feel the same trapping potential, so that the densities of the two species are equal at equilibrium as well as during the expansion: $\rho_1(\mathbf{r},t) = \rho_2(\mathbf{r},t) = \rho(\mathbf{r},t)/2$. The trapping potential will be chosen of harmonic type

$$V_{ho} = \frac{1}{2}m(\omega_\perp^2 x^2 + \omega_\perp^2 y^2 + \omega_z^2 z^2), \tag{5.23}$$

describing a cilyndrically simmetric trap with deformation $\lambda = \omega_z/\omega_\perp$. The interaction between the two fermionic species is fixed by the coupling constant $g = 4\pi\hbar^2 a/m$, where a is the s-wave scattering length.

In this section we employ the equation of state

$$\mu_{\ell e}(\rho) = \frac{\hbar^2}{2m}(3\pi^2\rho)^{2/3} + \frac{1}{2}gn \tag{5.24}$$

to describe the uniform phase of the gas, where the first term is the kinetic energy evaluated at zero temperature, and the second one is the interaction energy evaluated in the mean field approximation. Equation (5.24) neglects the effects of correlations which become important for large values of the scattering length and affect in a different way the equation of state of the normal and superfluid phase. The formalism developed in this section can be easily generalized to include a more accurate description of the equation of state. It is however worth pointing out that, even using the

same equation of state for the normal and superfluid phases, the expansion of the gas behaves quite differently in the two cases being described by different kinetic equations. In the presence of the external potential (5.23), the equilibrium condition in the local density approximation is determined by the equation

$$\mu_{\rm le}(\rho) + V_{\rm ho}(\mathbf{r}) = \mu \tag{5.25}$$

where μ is the chemical potential of the sample fixed by the normalization condition.

The relevant parameter characterizing the interaction in the fermionic system is the ratio

$$\chi = \frac{E_{int}}{E_{ho}} \tag{5.26}$$

between the interaction energy

$$E_{int} = \frac{g}{4}\int \rho^2(\mathbf{r}) d^3r \tag{5.27}$$

and the oscillator energy

$$E_{ho} \;\; = \;\; \int V_{ho}(\mathbf{r})\rho(\mathbf{r}) d^3r. \tag{5.28}$$

In the perturbative regime the integrals (5.27,5.28) can be evaluated using the non interacting density profile which, in Thomas-Fermi approximation (5.25), takes the simple form

$$\rho(\mathbf{r}) = \frac{1}{3\pi^2}\left(\frac{2m}{\hbar^2}\right)^{3/2}\left[\mu - V_{ho}(\mathbf{r})\right]^{3/2}. \tag{5.29}$$

After integration of (5.27) and (5.28) one finds [82]

$$\frac{E_{int}}{E_{ho}} = 0.5\frac{N^{1/6}a}{a_{ho}} = 0.3ak_F, \tag{5.30}$$

where $k_F = (3\pi^2\rho(0))^{1/3}$ is the Fermi momentum evaluated at the central value of the density. In order to go beyond the perturbative regime, one determines numerically

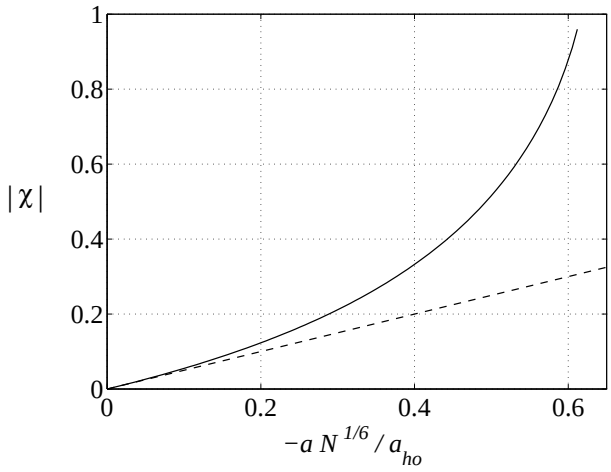

Figure 5.2: *Ratio $\chi = E_{int}/E_{ho}$ as a function of the universal parameter $aN^{1/6}/a_{ho}$ calculated with the mean field functional (5.31) up to the collapse point $aN^{1/6}/a_{ho} = -0.61$ (full line); the dashed line is the linear prediction (5.30).*

the ground state density by minimizing the energy of the system

$$E = \frac{3(3\pi^2)^{2/3}}{5}\frac{\hbar^2}{2m}\int \rho^{5/3}(\mathbf{r})d^3r + + \int V_{ho}(\mathbf{r})\rho(\mathbf{r})d^3r + \frac{g}{4}\int \rho^2(\mathbf{r})d^3r. \quad (5.31)$$

One easily finds that the equilibrium value of the ratio E_{int}/E_{ho} depends on the dimensionless combination $aN^{1/6}/a_{ho}$ also in the non perturbative regime [77], as reported in Fig.5.2. Using (5.31) one predicts that the compressibility of the gas becomes negative in the center of the trap if $|a|N^{1/6}/a_{ho} > 0.61$. For large values of $|a|$ the resulting predictions should be however taken with care since the functional (5.31) ignores correlation effects beyond mean field.

Let us now discuss the expansion of a fermionic sample trapped in an elongated harmonic trap ($\lambda < 1$). We describe first the expansion of the normal fluid and afterwards the one of the superfluid. In the ideal case, using the semiclassical description, one finds that the ratio of the square radii evolves according to the classical law

$$\frac{\langle r_\perp^2 \rangle}{\langle z^2 \rangle} = \frac{1+\omega_\perp^2 t^2}{1+\omega_z^2 t^2}\frac{\omega_z^2}{\omega_\perp^2}, \tag{5.32}$$

The ratio (5.32) approaches unity for large times, reflecting the isotropy of the momentum distribution. This result ignores the effects of collisions which are however expected to play a minor role at low temperature, due to Pauli blocking, unless the scattering length is very large or for large deformation of the trap (see next section).

In order to take into account the effects of the interactions, we consider the mean field description based on the Landau-Vlasov equation

$$\frac{\partial f}{\partial t} + \mathbf{v}\cdot\frac{\partial f}{\partial \mathbf{r}} - \frac{\partial V_{ho}}{\partial \mathbf{r}}\cdot\frac{\partial f}{\partial \mathbf{v}} - \frac{1}{2}\frac{g}{m}\frac{\partial n}{\partial \mathbf{r}}\cdot\frac{\partial f}{\partial \mathbf{v}} = 0, \tag{5.33}$$

where as in the previous sections $f(\mathbf{r},\mathbf{v},t)$ is the distribution function, and $n = \int f d^3v$ is the atomic density. Eq.(5.33) describes the dynamics of a normal weakly interacting gas in the collisionless regime.

Following the ideas of the previous sections, an approximate solution of Eq.(5.33), is obtained by making a scaling ansatz for the distribution function

$$f(\mathbf{r},\mathbf{v},t) = f_0(\tilde{\mathbf{r}}(t),\tilde{\mathbf{v}}(t)), \tag{5.34}$$

where f_0 is the equilibrium distribution, $\tilde{r}_i(t) = r_i/b_i$ and $\tilde{v}_i(t) = b_i v_i - \dot{b}_i r_i$. Under the scaling assumption the velocity field $\mathbf{u}(\mathbf{r},t) = \int \mathbf{v} f d^3v/n$ takes the simple form $u_i = \dot{b}_i r_i/b_i$. This ansatz has been recently used by Guéry-Odelin [129] to investigate the effect of the interaction on the collective oscillation of a classical gas in the collisionless regime.

The equations for the scaling parameters b_i can be obtained by multiplying (5.33) by $\tilde{r}_i$ and $\tilde{v}_i$ and integrating in phase space. Making use of the equilibrium properties

of the distribution function, after some straightforward algebra one finds

$$\ddot{b}_i + \omega_i^2 b_i - \frac{\omega_i^2}{b_i^3} + \frac{3}{2}\chi\omega_i^2\left(\frac{1}{b_i^3} - \frac{1}{b_i\prod_j b_j}\right) = 0, \tag{5.35}$$

where χ is the ratio (5.26) evaluated at equilibrium. The second term in Eq. (5.35) describes the restoring force of the external oscillator potential, the third one originates from the kinetic energy, whereas the last term, linear in χ, accounts for the effects of the mean field interaction.

An immediate application of Eq.(5.35) concerns the study of the oscillations of the gas. By linearizing the equations around equilibrium ($b_i = 1$) one finds, in the presence of isotropic harmonic trapping ($\omega_\perp = \omega_z = \omega_0$), the result:

$$\omega_M = 2\omega_0\sqrt{1+3\chi/8}, \;\; \omega_Q = 2\omega_0\sqrt{1-3\chi/4}, \tag{5.36}$$

for the frequencies of the monopole and quadrupole oscillations which coincide with the results already derived in [136] using a sum-rule approach.

The equations describing the expansion are obtained by suddenly removing the second term of Eq.(5.35), originating from the trapping potential. In the study of the expansion we are interested in the case of anisotropic trapping. In particular we consider the case of cigar shaped traps. For high deformations ($\lambda = \omega_z/\omega_\perp \ll 1$) Eq.(5.35) yields the asymptotic result

$$b_z^2 \;\rightarrow\; \omega_z^2(1-\frac{3}{2}\chi)t^2, \tag{5.37}$$

$$b_\perp^2 \;\rightarrow\; \omega_\perp^2 t^2, \tag{5.38}$$

showing that the aspect ratio

$$\frac{R_\perp(t)}{R_z(t)} \rightarrow \frac{1}{\sqrt{1-3\chi/2}} \tag{5.39}$$

approaches a value smaller than 1 if the interaction is attractive ($\chi < 0$). In Eq.(5.39), $R_\perp$ and R_z are the radii where the atomic density vanishes (Thomas-Fermi radii).

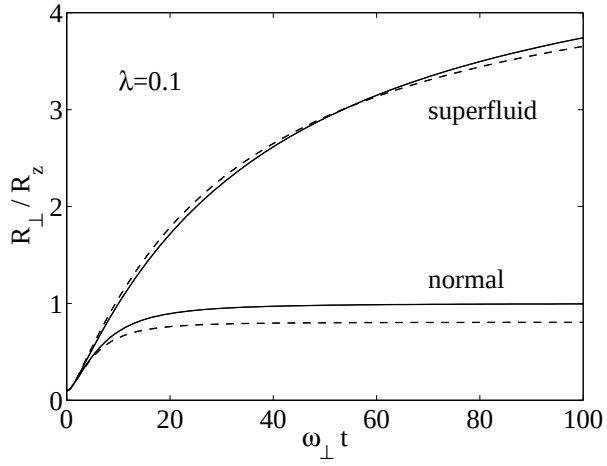

Figure 5.3: *Aspect ratio as a function of time for the expansion of the normal (lower curves) and superfluid phase (upper curves) for* $\lambda = 0.1$ *and two different values of the parameter* χ*:* $\chi = 0$ *(full line) and* $\chi = -0.4$ *(dashed line).*

The results of the numeric integration of the equations of motion (5.35) are reported in Fig.5.3 and 5.4 as a function of time for the choices $\chi = 0$ and $\chi = -0.4$.

We address now the problem of the expansion of a superfluid Fermi gas. As already anticipated we make use of the hydrodynamic equations of superfluids. Those equations have been already used to describe the collective oscillations of a superfluid trapped Fermi gas [137] including its rotational behavior [138,139]. The hydrodynamic equations are applicable if the healing length is much smaller than the size of the sample, which implies that the energy gap should be larger than the oscillator energies $\hbar\omega_z$, $\hbar\omega_\perp$. This non trivial condition implies that the whole system behaves like superfluid. Furthermore the hydrodynamic equations are applicable up to excitation energies of the order of the energy gap. In the problem of the expansion it is crucial that the system remains superfluid in the first instants when the hydrodynamic forces provide the relevant acceleration to the expanding atoms. One expects that this condition is

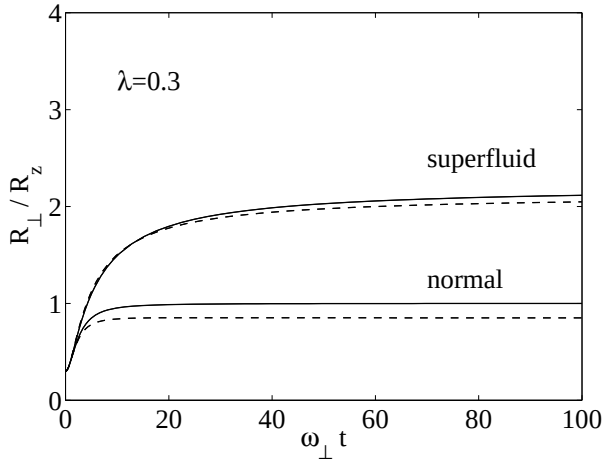

Figure 5.4: *Aspect ratio as a function of time for the expansion of the normal (lower curves) and superfluid phase (upper curves) for* $\lambda = 0.3$ *and different values of the parameters* χ*:* $\chi = 0$ *(full line) and* $\chi = -0.4$ *(dashed line).*

satisfied if the initial temperature is small enough. The hydrodynamic description is based on the equation of continuity

$$\frac{\partial}{\partial t}\rho + \nabla(\rho \mathbf{u}) = 0, \tag{5.40}$$

and on the Euler equation

$$m\frac{\partial}{\partial t}\mathbf{u} + \nabla\left(\mu_{\rm le}(\rho) + V_{ho}(\mathbf{r}) + \frac{1}{2}mu^2\right) = 0, \tag{5.41}$$

where $\mu_{\rm le}(\rho)$ is the chemical potential of a uniform gas calculated at the density ρ and $\mathbf{u}$ is the velocity field. If the equation of state is a power law ($\mu_{\rm le} \propto \rho^\gamma$) these equations admit the simple scaling solution

$$\rho(r_i, t) = \frac{1}{\prod_j b_j}\rho_0\left(\frac{r_i}{b_i}\right), \tag{5.42}$$

$$u_i(r_i, t) = \frac{\dot{b}_i}{b_i}r_i, \tag{5.43}$$

and the Thomas-Fermi radii evolve according to the law $R_i(t) = R_i(0)b_i(t)$. In this case, it is immediate to show that, during the expansion, the scaling parameters obey

the coupled differential equations

$$\ddot{b}_i = \frac{\omega_i^2}{(b_x b_y b_z)^\gamma b_i}. \tag{5.44}$$

which reduce to

$$\ddot{b}_z = \frac{\omega_z^2}{b_\perp^{2\gamma}}, \quad \text{and} \quad \ddot{b}_\perp = \frac{\omega_\perp^2}{b_\perp^{(2\gamma+1)}}. \tag{5.45}$$

for highly elongated configurations ($\lambda \ll 1$). For $\gamma = 1$ (corresponding to a Bose-Einstein condensed gas) the equation for the radial motion is integrable analytically and one finds the result $b_\perp(t) = (1 + \omega_\perp^2 t^2)^{1/2}$ [64].

To describe the expansion of a superfluid Fermi gas we use the same equation of state (5.24) as for the normal phase. The case of a very dilute gas is also described by a power law with $\gamma = 2/3$ (first term in (5.24)). For $\lambda = 0.1$ and 0.3 the solution is given by the full upper line in Fig.5.3 and 5.4 respectively which show that the deformation of the trap is inverted in time and the aspect ratio $R_\perp/R_z$ reaches asymptotically a value significantly larger than 1 [3]. Superfluidity has hence the effect of distributing the release energy in a strongly asymmetric way along the axial and radial directions. It is worth noticing that the same scaling equations (5.44), with $\gamma = 2/3$, are obtained for a classic gas in the collisional regime [65].

In the more general case (5.24), a useful approximation to the solution of the hydrodynamic equations, based on the scaling ansatz (5.42,5.43), is obtained by multiplying the Euler's equation (5.41) by $r_i \rho(\mathbf{r})$ and integrating over the spatial coordinates. Using the equation of state (5.24), one finally obtains the following set of differential equations

$$\ddot{b}_i + \omega_i^2 b_i - \frac{\omega_i^2}{b_i} \frac{1}{(\prod_i b_i)^{2/3}} +$$

[3] For highly elongated traps ($\lambda \ll 1$), the asymptotic value of the aspect ratio is given by $0.38/\lambda$, G.V. Shlyapnikov private communication

$$+\frac{3}{2}\chi\frac{\omega_i^2}{b_i}\left(\frac{1}{(\prod_i b_i)^{2/3}}-\frac{1}{\prod_i b_i}\right)=0, \tag{5.46}$$

with χ defined by Eq.(5.26). Equations (5.46) differ from the analogous equations (5.35) holding in the normal phase. By linearizing Eqs.(5.46) around $b_i = 1$ one gets, in the case of a spherical trap, the result $\omega_Q = \sqrt{2}\omega_0$ for the quadrupole frequency [137], which, contrary to (5.36), is independent of the interaction term in χ.

5.3.2 Effects of strong trap anisotropy

In this section, we complete our analysis by calculating explicitly the dynamics of the expansion of a dilute, degenerate normal Fermi gas, taking into account the role of collisions. The main purpose is to provide quantitative predictions for the aspect ratio and the thermal broadening of the density distribution, as a function of the relevant parameters like the ratio of the trap frequencies, the scattering length and the number of atoms.

The system we consider in this section is a dilute two component Fermi gas. At low temperatures the collisions between two atoms of the same species are suppressed due to Pauli blocking, and only atoms of different species can collide. We assume that the two species have the same mass and density, and hence the same distribution function in phase-space. The starting point is once more the Boltzmann equation

$$\frac{\partial f}{\partial t}+\mathbf{v}_1\cdot\nabla_{\mathbf{r}}f-\frac{1}{m}\nabla U_{\rm ext}\cdot\nabla_{\mathbf{v}_1}f=C[f], \tag{5.47}$$

where for each component $f(\mathbf{r},\mathbf{v}_1,t)$ is the distribution function in phase-space and $U_{\rm ext}(\mathbf{r}) = (m/2)(\omega_\perp^2(x^2+y^2)+\omega_z^2 z^2)$ is the external trapping potential. We note that the potential is cylindrically symmetric, which is the form favored by experiments. Moreover, in (5.47) we have neglected the mean field interaction term [129] which, however, has a minor effect on the expansion of a dilute Fermi gas as shown in Sec. 5.3.1

[70]. The collisional integral in the case of a dilute Fermi system reads

$$C[f] = \frac{\sigma m^3}{4\pi h^3} \int d^3v_2\, d^2\Omega\, |\mathbf{v}_1 - \mathbf{v}_2| [(1 - f(\mathbf{v}_1))(1 - f(\mathbf{v}_2)) f(\mathbf{v}_1') f(\mathbf{v}_2') \\ - f(\mathbf{v}_1) f(\mathbf{v}_2)(1 - f(\mathbf{v}_1'))(1 - f(\mathbf{v}_2'))], \qquad (5.48)$$

where in the low-energy limit, $\sigma = 4\pi a^2$, with a the s-wave scattering length. The scattering length is assumed to be smaller than the average distance between atoms.

The dynamics can be studied analytically using the previously discussed method of the averages [129, 140], which in this case involve calculating moments of the form $\langle r_i^2 \rangle$, $\langle r_i v_i \rangle$ and $\langle (v_i - u_i)^2 \rangle$, where $u_i(\mathbf{r})$ represents the velocity fields within the gas. If χ is a conserved quantity during a collision then the collisional term disappears. This is true for the moments $\langle r_i^2 \rangle$ and $\langle r_i v_i \rangle$ as well as for the quantity $\sum_i \langle (v_i - u_i)^2 \rangle$. This method has been used to study collective excitations in [82].

To explicitly include the collisional term in the calculations, it is convenient to introduce the following parameterization for the distribution function

$$f(\mathbf{r}, \mathbf{v}, t) = \left[\exp\left(\frac{E(\mathbf{r}, \mathbf{v}, t) - \mu}{T} \right) + 1 \right]^{-1}, \qquad (5.49)$$

with

$$E(\mathbf{r}, \mathbf{v}, t) = \frac{m}{2} \sum_i \left[\frac{\omega_i^2 r_i^2}{b_i^2} + \frac{(v_i - u_i)^2}{K_i} \right], \qquad (5.50)$$

where $u_i = \beta_i r_i$, and β_i, b_i, K_i, μ and T are time dependent parameters, with $i \in \{x, y, z\}$. The ansatz (5.49,5.50) contains more free parameters than necessary, so that we can, without any loss of generality, set $\prod_i b_i = (\prod_i K_i)^{-1/2}$. This fixes a unique definition of the effective temperature T[4]. The chemical potential, μ, is then obtained from the normalization condition, $(T/\hbar\bar{\omega})^3 f_3(\mathrm{e}^{\mu/T}) = N/2$, where N is the total number of atoms in *both* components, $\bar{\omega}^3 = \prod_i \omega_i$, and $f_s(z) = \sum_n (-1)^{n+1} z^n / n^s$. From

[4]In practice, the $T = 0$ approximation is compatible with the assumption that the gas is non superfluid, the critical temperature for the BCS transition being exponentially small in a dilute gas.

Eqs.(5.49,5.50) one can evaluate the entropy per particle of the gas, $S = (4\rho - \mu)/T$, where $\rho = T f_4(\mathrm{e}^{\mu/T})/f_3(\mathrm{e}^{\mu/T})$. This result, taken together with the normalization condition, shows that there is a one-to-one correspondence between the entropy and the temperature T, and consequently changes in T taking place during the expansion are associated with a change of entropy.

The ansatz (5.49,5.50) includes the initial equilibrium configuration predicted by Fermi statistics, and accounts for rescaling effects in coordinate as well as in momentum space. It allows, in particular, for anisotropic effects in momentum space which are crucial for describing correctly the mechanism of the expansion. The parameterization can describe both the collisionless and the hydrodynamic expansion as well as other intermediate regimes. Furthermore it accounts for possible changes in the effective temperature of the system during the expansion.

The next step is to evaluate the moments $\langle\chi\rangle$ in terms of the scaling parameters, which gives $\langle r_i^2\rangle = b_i^2\rho/m\omega_i^2$. Other moments can be expressed in terms of this quantity, so that $\langle r_i v_i\rangle = \beta_i\langle r_i^2\rangle$, $\langle(v_i - u_i)^2\rangle = \omega_i^2 K_i\langle r_i^2\rangle/b_i^2$, and $\langle u_i^2\rangle = \beta_i^2\langle r_i^2\rangle$. The moment equations then become

$$\beta_i = \frac{\dot{b}_i}{b_i} + \frac{\dot{\rho}}{2\rho}, \tag{5.51}$$

$$\dot{\beta}_i + \beta_i^2 - \frac{\omega_i^2}{b_i^2}K_i + \omega_i^2 = 0, \tag{5.52}$$

$$\frac{\dot{K}_i}{K_i} - 2\frac{\dot{b}_i}{b_i} + 4\beta_i = \frac{\langle(v_i - u_i)^2 C/f\rangle}{\langle(v_i - u_i)^2\rangle}, \tag{5.53}$$

where the final term in (5.52) arises from the confining potential. We set this term to zero in studying the expansion of the gas, while rescaling time in units of $\omega_\perp$, the original radial trap frequency. In addition, it is convenient to rewrite (5.53) as equations for the anisotropy in momentum space, $s = (K_z/K_\perp)^{1/2}$, and the entropy, S

$$\frac{\dot{s}}{s} = \frac{\dot{b}_\perp}{b_\perp} - \frac{\dot{b}_z}{b_z} - \frac{(2+s^2)}{4s^2}K^2\xi J(s,\tau), \tag{5.54}$$

$$\frac{T}{\rho}\dot{S} + \frac{(1-s^2)}{2s^2}K^2\xi J(s,\tau) = 0. \tag{5.55}$$

where we have defined

$$\frac{1}{\omega_\perp}\frac{\langle (v_\perp - u_\perp)^2 C/f\rangle}{\langle (v_\perp - u_\perp)^2\rangle} = K^2\xi J\left(s,\tau\right), \tag{5.56}$$

with $J(s,\tau)$ given by

$$\begin{aligned} J(s,\tau) &= \frac{3^{1/3}}{4\pi^6}\tau^2\frac{s^{5/3}}{f_4(\mathrm{e}^{\mu/T})}\int d^3R\, d^3V_1\, d^3V_2\, d^2\Omega\, V'\Delta V_z^2 \\ &\quad \times f(\mathbf{V}_1)f(\mathbf{V}_2)(1-f(\mathbf{V}_1'))(1-f(\mathbf{V}_2')). \end{aligned} \tag{5.57}$$

Here $V' = \sqrt{(V_{1x}-V_{2x})^2 + (V_{1y}-V_{2y})^2 + s^2(V_{1z}-V_{2z})^2}$, and we have rescaled variables so that $f(\mathbf{V}) = [\exp(R^2+V^2-\mu/T)+1]^{-1}$. The function J depends on both s and the reduced temperature $\tau = T/T_F$, where $T_F = (3N)^{1/3}\hbar\bar{\omega}$ is the Fermi temperature. In Eqs. (5.54-5.56) we have introduced the relevant dimensionless interaction parameter

$$\xi = (\lambda N)^{1/3}(k_F a)^2, \tag{5.58}$$

where k_F is the initial Fermi wave-vector at the center of the trap, and $\lambda = \omega_z/\omega_\perp$ is the trap anisotropy. Further, we have introduced the geometric average $K = (K_\perp^2 K_z)^{1/3} = (b_\perp^2 b_z)^{-2/3}$.

Eq. (5.55) explicitly shows that the entropy (and hence the temperature) of the gas will remain constant during the expansion ($\dot{S}=0$) either in the absence of collisions ($J=0$) or when the distribution in momentum space is isotropic ($s=1$)[5] . The latter situation arises when starting from a spherical trap, $\lambda = 1$, or when collisions are sufficiently frequent so that the gas is in the hydrodynamic regime. In regimes intermediate

[5]Alternatively, one can fix the value of T to the initial value and obtain an equivalent set of equations, as in the work of Pedri *et al.* [140]. The choice made in the present work is particularly convenient if the expansion starts from a $T=0$ configuration.

between the collisionless and hydrodynamic limits, deformations in momentum space produce an increase of entropy and temperature. The equations (5.51-5.57) can also be used to study small oscillations around equilibrium, where the momentum distribution is isotropic ($s = 1$). This procedure reproduces exactly the results of [82], in particular the collisional term takes the form $\langle (v_i - u_i)^2 C/f \rangle / \langle (v_i - u_i)^2 \rangle = (s-1)/\tilde{\tau}$, with $1/(\omega_\perp \tilde{\tau}) = \mathcal{C} K^2 \xi F_Q(T/T_F)$ and $\mathcal{C} = 8/(5 \cdot 3^{5/3})$. Here $\tilde{\tau}$ is the typical relaxation time for the shape oscillations and F_Q is given in [82]. Note that $1/\tilde{\tau} \propto T^2$ at small temperatures, so that the collisional contribution disappears when $T = 0$. This is the result of Pauli blocking of collisions for a spherical momentum distribution. However, during expansion large deformations in momentum space can lead to collisions that scatter atoms outside of the Fermi surface, and the function J differs from zero, even at zero temperature, as pointed out in [83].

We assume that the gas is initially in equilibrium at low temperature, and that the effective temperature contained in the ansatz (5.49) remains small during the expansion. One can then expand the Fermi functions $f_s(z)$ using low-T Sommerfeld expansions, so that the normalization condition gives $\mu \simeq T_F(1 - \pi^2\tau^2/3)$, $\rho \simeq T_F(1 + 2\pi^2\tau^2/3)/4$ and $S = \pi^2\tau$. Substituting these expressions into (5.51,5.52,5.54,5.55) yields a new set of equations that can be solved numerically to study the time evolution of the gas. To simplify matters we also approximate the function $J(s,\tau)$ with its zero temperature value

$$\begin{aligned} J(s,0) &= \frac{2 \cdot 3^{4/3} s^{5/3}}{\pi^6} \int d^3R\, d^3V_1\, d^3V_2\, d^2\Omega\, V' \Delta V_z^2 \\ &\quad \times \theta_0(\mathbf{V}_1)\theta_0(\mathbf{V}_2)(1 - \theta_0(\mathbf{V}_1'))(1 - \theta_0(\mathbf{V}_2')), \end{aligned} \tag{5.59}$$

where we have rescaled the coordinates again such that $\theta_0(\mathbf{V}) = \Theta(1 - V^2 - R^2)$, where Θ is the Heaviside step function. The integral for $J(s)$ can be evaluated numerically

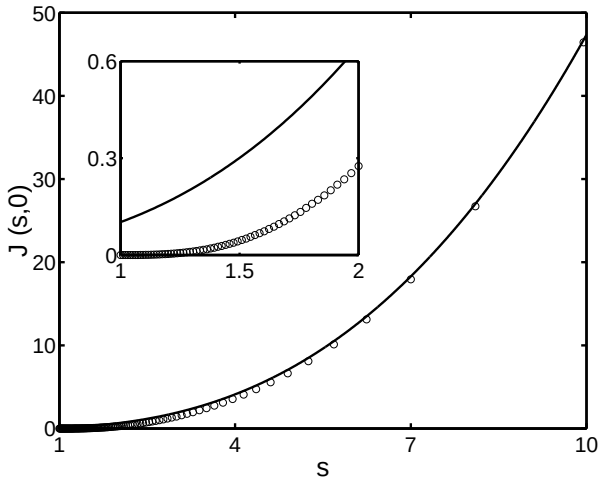

Figure 5.5: $J(s,0)$ *as a function of* s *for a range between* 1 *and* 10*, and (inset) between* 1 *and* 2*. The solid line shows the analytical form* $J(s) = 2s^{8/3}/(3^{5/3}\pi)$ *for the limit* $s \to \infty$*.*

using a standard Monte Carlo technique, and is plotted in Fig. 5.5. Also plotted is the result $J(s) = 2s^{8/3}/(3^{5/3}\pi)$ holding for large s, where the integral can be evaluated analytically by noting that virtually all collisions in this limit will scatter atoms outside of the Fermi surface (i.e. $(1-\theta_0(\mathbf{V}_1'))(1-\theta_0(\mathbf{V}_2')) \simeq 1$). We discuss the validity of this zero-temperature approximation later.

We now use these equations to study the expansion for different choices of the trap anisotropies, $\lambda < 1$, starting from a $T = 0$ configuration[6]. We plot the aspect ratio of the cloud $\sqrt{\langle r_\perp^2\rangle/\langle z^2\rangle} = \lambda b_\perp/b_z$ as a function of time for $\xi = 1$ and $\xi = 20$ and compare to the expected collisionless and hydrodynamic behavior in Fig. 5.6. We notice that the effects of collisions are far less pronounced for $\lambda = 0.3$, where the results are barely distinguishable from the collisionless behavior. However, for $\lambda = 0.03$ the expansion lies intermediate between the two limits if one chooses $\xi = 20$. This is to be expected since the deformation in momentum space reached in this case is much larger. In

[6]Note that Eq. (5.55) can also be obtained by starting strictly from the Boltzmann H-theorem.

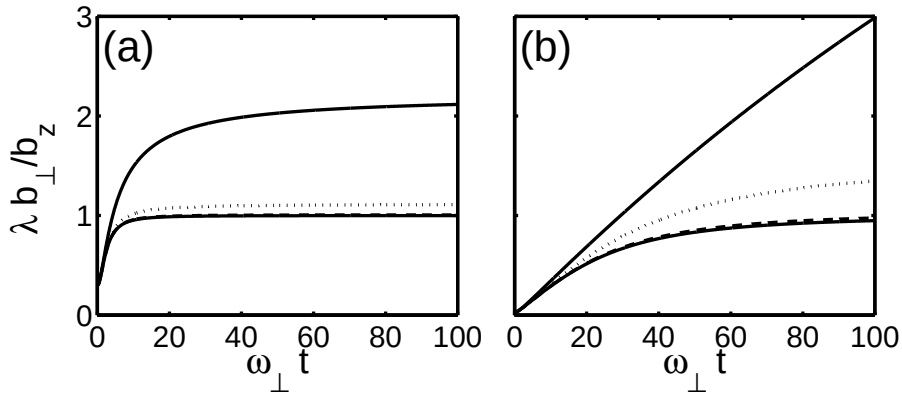

Figure 5.6: *Aspect ratio against time for the free expansion of a zero-temperature Fermi gas from a trap with (a)* $\lambda = 0.3$ *and (b)* $\lambda = 0.03$*. The upper and lower solid lines on each plot represents the behavior in the hydrodynamic and collisionless regimes respectively, with the other lines displaying results of solving the equations (5.51-5.57) for* $\xi = 1$ *(dashed) and* $\xi = 20$ *(dotted).*

particular, in the collisionless case one would expect $s \to 1/\lambda$ at long times, and this fixes the maximum s possible. Since J takes large values only for large s, then the collisional term is potentially more effective for smaller λ. An interesting consequence of the momentum space deformation is that atoms scattering outside the Fermi surface will tend to smooth out the distribution function. This aspect appears in Eq. (5.55) as an increase in the temperature, even if we start from an initial $T = 0$ configuration. Fig. 5.7(a) shows the temperature calculated at $\omega_\perp t = 100$ for different values of λ. Again, one sees a much larger effect for $\lambda \ll 1$. The function tends to zero for both $\xi \to 0$ and $\xi \to \infty$, representing the crossover from collisionless to hydrodynamic behavior in a similar manner to damping times in collective oscillations [82,125]. Since (5.55) is an equation for τ^2 one finds that starting from a non-zero temperature, τ_0, gives a final temperature of approximately $\tau = \sqrt{\tau_0^2 + (\delta\tau)^2}$, where $\delta\tau$ is the change for an initially zero temperature gas obtained from Fig. 5.7(a). Hence the temperature

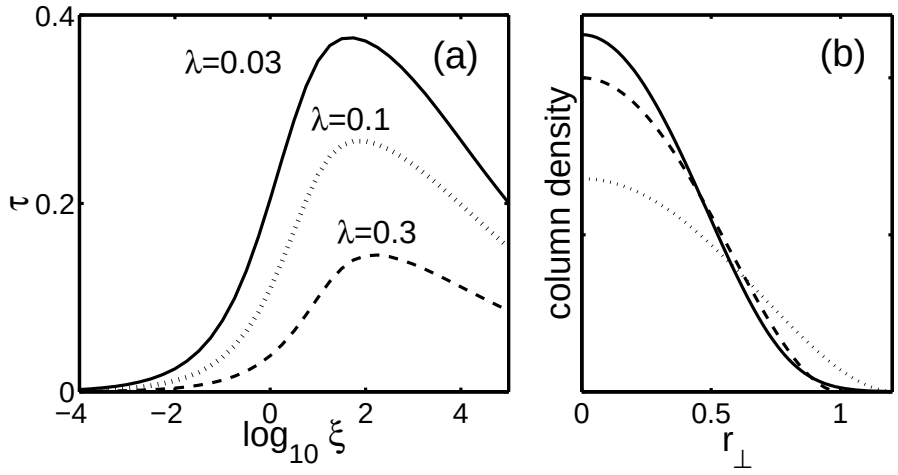

Figure 5.7: *(a) Temperature at $\omega_\perp t = 100$, $\tau = T/T_F$, as a function of ξ, for different values of λ. The gas prior to expansion is at zero temperature.(b) Column density (see text) as a function of radial distance at $\omega_\perp t = 100$, for $\lambda = 0.03$ and $\xi = 1$ (solid line), compared to the result of expansion in the collisionless (dashed) and hydrodynamic (dotted) limits. Both axes are in arbitrary units.*

increase produced by collisions will become smaller as one raises the initial temperature of the gas.

The change in temperature during the expansion, as well as the fact that experiments will be initially at a non-zero temperature, will lead to corrections to the zero-temperature collisional term (5.59). We can estimate the effects at finite temperatures by approximating $J(s,\tau)$ (5.57) with the sum of the zero-T result to that derived for finite-T but small deformations, so that $J(s,\tau) = J(s,0) + \mathcal{C}(s-1)F_Q(\tau)$, with the function $F_Q(\tau)$ given in [82]. We find that the inclusion of the temperature dependence in J has little impact on the results, even allowing for an initial temperature of $\tau = 0.2$.

Since for a dilute gases ($k_F|a| \ll 1$) the value of ξ for realistic parameters will be, at most, of the order of 1, we conclude that collisional effects on the aspect ratio of the

expanding gas are negligible (see Fig. 5.6). This is consistent with experimental results in dilute degenerate gases (see for example [73,142]). In contrast, we find that the effect of collisions on the thermal broadening can be significant at low temperatures even if $\xi \simeq 1$, especially for highly deformed traps. As an example in Fig. 5.7(b) we show the column density $\rho(r_\perp) = (m/h)^3 \int dz d\mathbf{v} f(\mathbf{r}, \mathbf{v}, t)$, calculated at $\omega_\perp t = 100$, $\lambda = 0.03$ and $\xi = 1$, starting from an initial zero temperature configuration. Around 80% of the increase in T (and the consequent broadening of the density profile) takes place over the first $\omega_\perp t = 20$ of the expansion. The comparison with the prediction of ballistic expansion (dashed line) explicitly reveals the importance of collisions. Experimentally one could observe this difference by cooling down a two component Fermi gas to very low temperatures. Ballistic expansion could be achieved either by first removing one of the two components, or by suddenly tuning the scattering length to zero at the start of the expansion.

In order to also observe large effects in the aspect ratio one should increase the value of ξ, and hence of $k_F|a|$, by, for example working close to a Feshbach resonance. In this case, however, the formalism of the Boltzmann equation is not strictly applicable. A rough estimate of the collisional effects can be obtained by replacing a^2 with the unitarity limited expression $a^2/(1 + K(k_F a)^2)$, where k_F is the initial Fermi momentum and K accounts for the decrease of the density during the expansion. In the unitarity limit $k_F|a| \to \infty$ equation (5.56) is then modified by replacing K^2 with K and setting $\xi = (\lambda N)^{1/3}$. These changes result in a sizable increase of the anisotropy effects. Apart from the fact that the parameter ξ can easily take large values, the replacement of K^2 with K makes the collisional term effective for longer times during the expansion. One should however note that in the unitarity limit the gas is expected to be superfluid at low temperatures and its dynamics should be consequently described

by the hydrodynamic equations of superfluids.

Chapter 6

Conclusion

In this thesis we have studied some dynamical aspects of different systems recently realized with ultracold atomic gases. In this last chapter we summarize our results.

In Chapter 3 we have extended the analysis of Ref. [41] on the expansion dynamics of a one-dimensional Bose gas in a guide. We have shown that the expansion violates under certain conditions the self-similarity, and in this sense differs significantly from the expansion dynamics of a BEC. We have shown that the problem can be solved by employing the hydrodynamic approach, and the local Lieb-Liniger model. We have developed a variational approach based on a Lagrangian formalism to study the expansion for any regime of parameters. We have identified the possible physical situations at which self-similarity is violated. The particular properties of the expansion of a gas in the strongly-interacting regime could therefore be employed to discern between mean-field and strongly-interacting regimes. In addition, the asymptotic behavior of the expanded cloud could be employed to discriminate between different initial interaction regimes of the system.

In Chapter 4 we have considered what we call the quasi-Tonks regime, in which a gas confined in a 2D optical lattice, can present significant tunneling, and at the same

time maintain the local chemical potential obtained for each site using the LLL model. In this cross-dimensional regime, a 3D cloud acquires 1D properties. In particular, we have shown that both the ground-state properties and the excitation spectrum are significantly different than the expected results for a harmonically confined BEC. We have also focused our attention on the momentum distribution in the Mott-Insulator phase. We have shown that the strong correlations along the 1D tubes significantly modify the quasi-momentum distribution in the lattice plane. We have found that in the MI regime only the lowest momentum along the tubes is affected by the inter-site hopping, and hence only this component contributes to the formation of interference fringes. Consequently, the larger the interactions are (larger depletion) the less pronounced is the visibility of the interference fringes. In particular, for the Tonks-Girardeau regime in the tubes, the quasi-momentum distribution becomes progressively flatter, leading to an observable blurring of the interference pattern after expansion. This effect can be observed in current time of flight experiments, and can be used to reveal a clear signature of the strong correlations along the sites.

In Chapter 5 we have studied classical and Fermi gases. By means of a scaling ansatz, we investigated an approximated solution of the Boltzmann-Vlasov equation for a classical gas. Within this framework, we derived the frequencies and the damping of the collective oscillations of a harmonically trapped gas and we investigate its expansion after release of the trap. The method is well suited to studying the collisional effects taking place in the system and in particular to discuss the crossover between the hydrodynamic and the collisionless regimes. An explicit link between the relaxation times relevant for the damping of the collective oscillations and for the expansion is established. We have shown that the expansion of a superfluid Fermi gas, governed by the equations of hydrodynamics, differs in a crucial way from the one of a normal gas

in the collisionless regime. From a theoretical point of view several questions remain to be investigated: among them, the effect of large scattering lengths [141] on the equation of state and the role of collisions which, under certain conditions, might give rise to a hydrodynamic regime, and hence to anisotropic expansion, also in the normal phase. Finally one should develop the formalism at finite temperature where both the normal and superfluid components are present. The resulting bimodal structure in the expanding cloud is expected to be affected by the transfer of atoms from the superfluid to the normal component during the first stage of the expansion. We have also shown that collisions can be effective in a dilute normal Fermi gas even at zero temperature, as a consequence of large deformations of the distribution function in momentum space after expansion from a very elongated trap. They can give rise to a sizeable entropy increase and hence thermal broadening of the density distribution, which should be visible by imaging the atomic cloud. In contrast a $T = 0$ superfluid should expand anisotropically, without any entropy increase due to the absence of collisions.

Appendix A

Brief summary of calculations

In this appendix we provide more details about some expression employed in this thesis.

A.1 Measurement of the momentum distribution of a quantum system

In this section we show how it is possible to measure the momentum distribution by free expansion. The momentum distribution is directly related to the one-body density-matrix, so it is possible to obtain important information about the correlations of the system. For this reason it is very important to have access to the momentum distribution.

Let us first define the quantities we employ. The momentum distribution of a system is defined as

$$\tilde{\rho}(\mathbf{p}) = \frac{\mathbf{1}}{(\mathbf{2}\pi\hbar)^{\mathbf{3}}} \int \mathbf{d^3 r d^3 r'} \langle \mathbf{\Psi}^+(\mathbf{r}) \mathbf{\Psi}(\mathbf{r'}) \rangle \exp[-\mathbf{i p} \cdot (\mathbf{r} - \mathbf{r'})/\hbar]. \tag{A.1}$$

In the case of an infinite and homogeneous system it is better to define the momentum

distribution for unit of volume. The density is the diagonal part of the one-body density-matrix

$$\rho(\mathbf{r}) = \langle \mathbf{\Psi}^+(\mathbf{r})\mathbf{\Psi}(\mathbf{r})\rangle. \tag{A.2}$$

For the case of a non-interacting it is possible to relate the one-body density-matrix at different time using the single-particle propagator for the particular case considered:

$$\langle \Psi^+(t,\mathbf{r}_1)\Psi(t,\mathbf{r}_2)\rangle = \int d^3r_1' d^3r_2' K^*(t,\mathbf{r}_1,t',\mathbf{r}_1')K(t,\mathbf{r}_2,t',\mathbf{r}_2')\langle \Psi^+(t',\mathbf{r}_1')\Psi(t',\mathbf{r}_2')\rangle. \tag{A.3}$$

In particular we want to calculate the dynamics of the density:

$$\rho(t,\mathbf{r}) = \int d^3r_1' d^3r_2' K^*(t,\mathbf{r},t',\mathbf{r}_1')K(t,\mathbf{r},t',\mathbf{r}_2')\langle \Psi^+(t',\mathbf{r}_1')\Psi(t',\mathbf{r}_2')\rangle. \tag{A.4}$$

Let us consider the case of the free propagator (without any external potential). In this case the product of the propagators in Eq. (A.4) becomes

$$K^*(t,\mathbf{r},t',\mathbf{r}_1')K(t,\mathbf{r},t',\mathbf{r}_2') \simeq \left(\frac{m}{2\pi\hbar(t-t')}\right)^3 \exp\left[-\frac{im}{\hbar(t-t')}\mathbf{r}\cdot(\mathbf{r}_1'-\mathbf{r}_2').\right] \tag{A.5}$$

The previous equation is valid for large times $t - t' \gg mL^2/2\hbar$, where L is the size of the system. This resembles a Fourier transform, and hence we obtain a relation between the density at time t and the momentum distribution at the time t'

$$\rho(t,\mathbf{r}) \simeq \frac{m}{t-t'}\tilde{\rho}(t', m\mathbf{r}/|t-t'|). \tag{A.6}$$

This is not extremely surprising, but we have always to keep in mind that it is possible to use this method only when the expansion can be considered free, which is not the case in many experiments. For example in the first experiment of time of flight measurement [1] the interactions played a major role. In this experiments it actually happens the opposite of what we are discussing here, i.e. the initial kinetic energy can be neglected.

The free expansion technique has been used in experiments of atoms in a lattice [56, 143], since in this case it is possible to treat the expansion as free, due to the presence of the lattice. In such experiments the highest scale of energy is the kinetic energy of a single site, which is larger than the interaction energy, and hence we are allowed to use the free propagator. A similar analysis can be done using the propagator of the harmonic oscillator, in this case the time required is $t - t' \simeq \pi/2\omega$, where ω is the frequency of the harmonic oscillator.

A.2 Relation between quasi-momentum and momentum distribution

In this section, we derive the relation between the momentum and the quasi-momentum distribution.

$$\tilde{\rho}(\mathbf{p}) = \frac{1}{(2\pi)\hbar)^3}\int d^3r d^3r' \langle \Psi^+(\mathbf{r})\Psi(\mathbf{r}')\rangle \exp[-i\mathbf{p}\cdot(\mathbf{r}-\mathbf{r}')/\hbar] \tag{A.7}$$

$$= \frac{1}{(2\pi)\hbar)^3}\int d^3r d^3r' \sum_{jj'} \phi_j^*(\mathbf{r})\phi_j(\mathbf{r}')\langle a_j^+ a_{j'}\rangle \exp[-i\mathbf{p}\cdot(\mathbf{r}-\mathbf{r}')/\hbar] \tag{A.8}$$

$$= \left|\tilde{\phi}_0(\mathbf{p})\right|^2 \sum_{jj'} \langle a_j^+ a_{j'}\rangle \exp[-i\mathbf{p}\cdot(\mathbf{r}_j-\mathbf{r}_{j'})/\hbar] \tag{A.9}$$

$$= \left|\tilde{\phi}_0(\mathbf{p})\right|^2 \langle a_{\mathbf{p}}^+ a_{\mathbf{p}}\rangle \tag{A.10}$$

$$= \left|\tilde{\phi}_0(\mathbf{p})\right|^2 \tilde{\rho}_{qm}(\mathbf{p}), \tag{A.11}$$

where a_j^+ and a_j are creation and annihilation operators of Wannier functions, $a_{\mathbf{p}}^+$ and $a_{\mathbf{p}}$ are creation and annihilation operators of Bloch functions. In the previous equation, we have written the field in the Wannier basis, employed the translational property of the Wannier function $\phi_j(\mathbf{r}) = \phi_0(\mathbf{r}-\mathbf{r}_j)$, performed the Fourier transformation, and finally used the relation between Bloch and Wannier basis $a_{\mathbf{p}} = \sum_j a_j \exp[-i\mathbf{p}\cdot\mathbf{r}_j]$, where $\mathbf{p}$ is the quasi-momentum

A.3 Bloch Oscillations

Let us consider a non interacting system on a lattice in the first band. The Hamiltonian in this case reads

$$H_0 = -\sum_{n,l} J_l[\hat{a}^+_{n+l}\hat{a}_n + \hat{a}^+_{n-l}\hat{a}_n], \tag{A.12}$$

where we have considered the hopping to any site and not just to nearest neighboring sites. The Hamiltonian can be easily diagonalized by means of

$$\hat{b}_\theta = \sum_n e^{in\theta}\hat{a}_n, \tag{A.13}$$

and the energy reads

$$\varepsilon(\theta) = -2\sum_l J_l \cos(l\theta). \tag{A.14}$$

Let us introduce a constant force as a perturbation

$$H_1 = \mathcal{F}\sum_n n\hat{a}^+_n\hat{a}_n, \tag{A.15}$$

and let us calculate the time evolution of $\hat{b}_\theta$

$$i\hbar\frac{d}{dt}\hat{b}_\theta = \varepsilon(\theta)\hat{b}_\theta + i\mathcal{F}\frac{\partial}{\partial\theta}\hat{b}_\theta. \tag{A.16}$$

The first term of the r.h.s. can be absorbed in a phase factor doing the transformation $\hat{b}_\theta \to \exp[-i\varepsilon(\theta)t/\hbar]\hat{b}_\theta$. Assuming the index θ time dependent, we obtain the following result

$$\hbar\frac{d\theta}{dt} = \mathcal{F}. \tag{A.17}$$

The solution reads

$$\theta(t) = \theta_0 + \frac{\mathcal{F}}{\hbar}t, \tag{A.18}$$

meaning that if we perturb the system with a constant force, the system, in a time average, does not move.

A.4 Scaling equations (5.17),(5.18)

We make the following ansatz for the non equilibrium distribution function: $f(\mathbf{r},\mathbf{v},t) = \Gamma f_0(\mathbf{R}(t),\mathbf{V}(t))$ with $R_i = r_i/b_i$, $V_i = (v_i - \dot{b}_i r_i/b_i)\theta_i^{-1/2}$ and $\Gamma = \Pi_j b_j^{-1}\theta_j^{-1/2}$. The dependence on time is contained through the parameters b_i and θ_i. Following [129], we substitute this ansatz into Eq. (5.16) and use the equation for the equilibrium distribution f_0. We find

$$\begin{aligned}
&\dot{\Gamma} f_0 + \Gamma \sum_i \Big\{ V_i \frac{\partial f_0}{\partial R_i}\Big(\frac{\theta_i^{1/2}}{b_i} - \frac{1}{b_i \theta_i^{1/2}}\frac{1}{\Pi_j b_j}\Big) \\
&-\frac{\partial f_0}{\partial V_i}\Big[\frac{R_i}{\theta_i^{1/2}}\Big(\ddot{b}_i + \omega_i^2 b_i - \frac{\omega_i^2}{b_i}\frac{1}{\Pi_j b_j}\Big) \\
&+V_i\Big(\frac{1}{2}\frac{\dot{\theta}_i}{\theta_i} + \frac{\dot{b}_i}{b_i}\Big)\Big]\Big\} = I_{\rm coll}. \qquad \text{(A.19)}
\end{aligned}$$

Integrating in phase space, we calculate the average moment of $R_i V_i$. This leads to Eq. (5.17). Note that this equation is not affected by the collision integral since the quantity $R_i V_i$ is conserved by the collisions.

To derive Eq. (5.18), we consider instead the average moment of V_i^2. This yields:

$$\frac{\dot{\theta}_i}{\theta_i} + 2\frac{\dot{b}_i}{b_i} = \frac{m}{N\Gamma k_B T_0}\int V_i^2 I_{\rm coll} d^3R d^3V, \qquad \text{(A.20)}$$

where T_0 is the equilibrium temperature. Differently from (5.17), Eq. (A.20) depends explicitly on the collision integral . In order to calculate the r.h.s of Eq. (A.20), we use the relaxation time approximation: $I = -(f - f_{\rm le})/\tau_0$. The first term gives: $\int V_i^2 f d^3R d^3V = N\Gamma k_B T_0/m$. To obtain a relation among the θ scaling parameters one uses the identity $\langle v^2\rangle = \langle v^2\rangle_{\rm le}$, from which we deduce $\bar{\theta} = \sum_i \theta_i/3$. The contibution to the integral due to the second term is obtained by noticing that, at local equilibrium, $\theta_i^{\rm le} = \bar{\theta}$: $\int V_i^2 f_{\rm le} d^3R d^3V = \bar{\Gamma}\int V_i^2 f_0(\bar{\mathbf{R}},\bar{\mathbf{V}}) d^3R d^3V = N\Gamma\bar{\theta}k_B T_0/(m\theta_i)$. Hence Eq. (A.20) can be recast in the form (5.18).

Bibliography

[1] M. H. Anderson, J. R. Ensher, M. R. Matthews, C. E. Wieman and E. A. Cornell, Science **269**, 198 (1995).

[2] K.B. Davis, M. O. Mewes, M. R. Andrews, N. J. van Druten, D. S. Durfee, D. M. Kurn and W. Ketterle, Phys. Rev. Lett. **75**, 3969 (1995).

[3] C. C. Bradley, C. A. Sackett, and R. G. Hulet , Phys. Rev. Lett. **78**, 985 (1997).

[4] S. Stringari, Phys. Rev. Lett. **77**, 2360 (1996).

[5] D. S. Jin, J. R. Ensher, M. R. Matthews, C. E. Wieman, and E. A. Cornell Phys. Rev. Lett. **77**, 420 (1996).

[6] M.-O. Mewes, M. R. Andrews, N. J. van Druten, D. M. Kurn, D. S. Durfee, C. G. Townsend, and W. Ketterle Phys. Rev. Lett. **77**, 988 (1996).

[7] A. Görlitz, J. M. Vogels, A. E. Leanhardt, C. Raman, T. L. Gustavson, J. R. Abo-Shaeer, A. P. Chikkatur, S. Gupta, S. Inouye, T. Rosenband, and W. Ketterle, Phys. Rev. Lett. **87**, 130402 (2001).

[8] A. I. Safonov, S. A. Vasilyev, I. S. Yasnikov, I. I. Lukashevich, and S. Jaakkola, Phys. Rev. Lett. **81**, 4545 (1998).

[9] W. Hänsel, P. Hommelhoff, T. W. Hänsch, J. Reichel, Nature **413**, 498 (2001).

[10] S. Burger, F. S. Cataliotti, C. Fort, P. Maddaloni, F. Minardi and M. Inguscio, Europhys. Lett. **57**, 1 (2002).

[11] F. Schreck, L. Khaykovich, K. L. Corwin, G. Ferrari, T. Bourdel, J. Cubizolles, and C. Salomon, Phys. Rev. Lett. **87**, 080403 (2001).

[12] M. Greiner, I. Bloch, O. Mandel, T. W. Hänsch, and T. Esslinger, Phys. Rev. Lett. **87**, 160405 (2001).

[13] D. S. Petrov, G. V. Shlyapnikov, and J. T. M. Walraven, Phys. Rev. Lett. **85**, 3745 (2000).

[14] Yu. Kagan, V. A. Kashurnikov, A. V. Krasavin, N. V. Prokof'ev, and B.V. Svistunov, Phys. Rev. A **61**, 43608 (2000).

[15] D. S. Petrov, M. Holzmann, and G. V. Shlyapnikov, Phys. Rev. Lett. **84**, 2551 (2000).

[16] D. S. Petrov, G. V. Shlyapnikov, and J. T. M. Walraven, Phys. Rev. Lett. **87**, 050404 (2001).

[17] S. Dettmer, D. Hellweg, P. Ryytty, J. J. Arlt, W. Ertmer, and K. Sengstock, Phys. Rev. Lett. **87**, 160406 (2001).

[18] I. Shvarchuck, Ch. Buggle, D. S. Petrov, K. Dieckmann, M. Zielonkowski, M. Kemmann, T. G. Tiecke, W. von Klitzing, G. V. Shlyapnikov, and J. T. M. Walraven, Phys. Rev. Lett. **89**, 270404 (2002).

[19] F. Gerbier, J. H. Thywissen, S. Richard, M. Hugbart, P. Bouyer, and A. Aspect Phys. Rev. A **67**, 051602 (2003).

[20] M. Girardeau, J. Math. Phys. **1**, 516 (1960).

[21] M. Olshanii, Phys. Rev. Lett. **81**, 938 (1998).

[22] S. L. Cornish, N. R. Claussen, J. L. Roberts, E. A. Cornell, and C. E. Wieman, Phys. Rev. Lett. **85**, 1795 (2000).

[23] J. Stenger, S. Inouye, M. R. Andrews, H.-J. Miesner, D. M. Stamper-Kurn, and W. Ketterle, Phys. Rev. Lett. **82**, 2422 (1999).

[24] M. Greiner, O. Mandel, T. Esslinger, T. W. Hänsch, Immanuel Bloch, Nature **415**, 39 (2002).

[25] E. H. Lieb and W. Liniger, Phys. Rev. **130**, 1605 (1963).

[26] C. N. Yang and C. P. Yang, J. of Math. Phys. **10**, 1115 (1969).

[27] F. D. M. Haldane, Phys. Rev. Lett. **47**, 1840 (1981).

[28] T. Giamarchi, *Quantum Physics in One Dimension*, Oxford University Press (2003).

[29] M. D. Girardeau and E. M. Wright, Phys. Rev. Lett. **87**, 210401 (2001).

[30] M. D. Girardeau and E. M. Wright, Phys. Rev. Lett. **84**, 5691 (2000).

[31] M. D. Girardeau and E. M. Wright Phys. Rev. Lett. **87**, 050403 (2001).

[32] M. D. Girardeau, E. M. Wright, and J. M. Triscari, Phys. Rev. A **63**, 033601 (2001).

[33] V. Dunjko, V. Lorent, and M. Olshanii, Phys. Rev. Lett. **86**, 5413 (2001).

[34] C. Menotti and S. Stringari, Phys. Rev. A **66**, 043610 (2002).

[35] D. M. Gangardt and G. V. Shlyapnikov, Phys. Rev. Lett. **90**, 010401 (2003).

[36] D. M. Gangardt and G. V. Shlyapnikov, New J. Phys. **5**, 79 (2003).

[37] M. Olshanii and V. Dunjko, Phys. Rev. Lett. **91**, 090401 (2003).

[38] G.E. Astrakharchik, and S. Giorgini, Phys. Rev. A **68**, 031602 (2003).

[39] K. V. Kheruntsyan, D. M. Gangardt, P. D. Drummond, and G. V. Shlyapnikov, Phys. Rev. Lett. **91**, 040403 (2003).

[40] B. Paredes, A. Widera, V. Murg, O. Mandel, S. Fölling, I. Cirac, G. V. Shlyapnikov, T. W. Hänsch, I. Bloch Nature **429**, 277 (2004).

[41] P. Öhberg and L. Santos, Phys. Rev. Lett. **89**, 240402 (2002).

[42] B. P. Anderson and M. Kasevich, Science **282**, 1686 (1998).

[43] O. Mörsch, J. H. Müller, M. Cristiani, D. Ciampini, and E. Arimondo, Phys. Rev. Lett. **87**, 140402 (2001).

[44] W. K. Hensinger, H. Häffner, A. Browaeys, N. R. Heckenberg, K. Helmerson, C. McKenzie, G. J. Milburn, W. D. Phillips, S. L. Rolston, H. Rubinsztein-Dunlop, B. Upcroft, Nature **412**, 52 (2001).

[45] F. S. Cataliotti, S. Burger, C. Fort, P. Maddaloni, F. Minardi, A. Trombettoni, A. Smerzi, and M. Inguscio, Science, **293** 843 (2001).

[46] C. Orzel, A. K. Tuchman, M. L. Fenselau, M. Yasuda, and M. A. Kasevich, Science **291**, 2386 (2001).

[47] M. P. A. Fisher, P. B. Weichman, G. Grinstein, and D. S. Fisher Phys. Rev. B **40**, 546 (1989).

[48] D. Jaksch, C. Bruder, J. I. Cirac, C. W. Gardiner, and P. Zoller, Phys. Rev. Lett. **81**, 3108 (1998).

[49] S. Cowell, H. Heiselberg, I. E. Mazets, J. Morales, V. R. Pandharipande, and C. J. Pethick, Phys. Rev. Lett. **88**, 210403 (2002).

[50] B. Paredes, P. Fedichev, J. I. Cirac, and P. Zoller, Phys. Rev. Lett. **87**, 010402 (2001).

[51] N. K. Wilkin and J. M. F. Gunn, Phys. Rev. Lett. **84**, 6 (2000).

[52] A. Recati, P. O. Fedichev, W. Zwerger, and P. Zoller, Phys. Rev. Lett. **90**, 020401 (2003).

[53] H. Moritz, T. Stöferle, M. Köhl, and T. Esslinger, Phys. Rev. Lett. **91**, 250402 (2003).

[54] T. Stferle, H. Moritz, C. Schori, M. Köhl, and Tilman Esslinger, Phys. Rev. Lett. **92**, 130403 (2004).

[55] B. Laburthe Tolra, K. M. O'Hara, J. H. Huckans, W. D. Phillips, S. L. Rolston, and J. V. Porto, Phys. Rev. Lett. **92**, 190401 (2004).

[56] B. Paredes, A. Widera, V. Murg, O. Mandel, S. Fölling, I. Cirac, G. V. Shlyapnikov, T. W. Hänsch, I. Bloch, Nature **429**, 277 (2004).

[57] T. Kinoshita, T. Wenger, and D. S. Weiss Science **20**, 1125 (2004).

[58] S. Biermann, A. Georges, A. Lichtenstein, and T. Giamarchi, Phys. Rev. Lett. **87**, 276405 (2001).

[59] K. B. Efetov and A. I. Larkin, Sov. Phys. JETP **42**, 390 (1975).

[60] P. Pedri and L. Santos, Phys. Rev. Lett. **91**, 110401 (2003).

[61] A. F. Ho, M. A. Cazalilla, and T. Giamarchi, Phys. Rev. Lett. **92**, 130405 (2004).

[62] V. A. Kashurnikov, N. V. Prokof'ev, and B. V. Svistunov Phys. Rev. A **66**, 031601 (2002).

[63] S. Wessel, F. Alet, M. Troyer, and G. G. Batrouni, cond-mat/0404552.

[64] Y. Castin, and R. Dum, Phys. Rev. Lett. **77**, 5315 (1996).

[65] Yu. Kagan, E. L. Surkov, and G. V. Shlyapnikov, Phys. Rev. A **55**, R18 (1997).

[66] V. M. Pérez-García, H. Michinel, J. I. Cirac, M. Lewenstein, and P. Zoller, Phys. Rev. Lett. **77**, 5320 (1996).

[67] K. G. Singh and D. S. Rokhsar, Phys. Rev. Lett. **77**, 1667 (1996).

[68] D. M. Stamper-Kurn, M.R. Andrews, A.P. Chikkatur, S. Inouye, H.-J. Miessner, J. Stenger and W. Ketterle, Phys. Rev. Lett. **80**, 2027 (1998).

[69] U. Ernst, J. Schuster, F. Schreck, A. Marte, A. Kuhn and G. Rempe, Appl. Phys. B **67**, 719 (1998).

[70] Menotti C., Pedri P. and Stringari S. Phys. Rev. Lett **89** 250402 (2002).

[71] K. M. O'Hara, S. L. Hemmer, M. E. Gehm, S. R. Granade, and J. Thomas, Science **298**, 2179 (2002).

[72] J. Cubizolles, T. Bourdel, S. J. J. M. F. Kokkelmans, G. V. Shlyapnikov, and C. Salomon Phys. Rev. Lett. **91**, 240401 (2003).

[73] C. A. Regal and D. S. Jin Phys. Rev. Lett. **90**, 230404 (2003).

[74] D. M. Stamper-Kurn, H.-J. Miesner, S. Inouye, M. R. Andrews, and W. Ketterle, Phys. Rev. Lett. **81**, 500 (1998).

[75] M. Leduc, J. Leonard, F. P. dos Santos, E. Jahier, S. Schwartz, C.M. Cohen-Tannoudji, Acta Physica Polonica B **33**, 2213 (2002).

[76] Private communications from J. Walraven (Amolf, Amsterdam), Zoran Hadzibabic (MIT, Cambridge), Fabrice Gerbier (IOTA, Orsay).

[77] H. T. C. Stoof, M. Houbiers, C. A. Sackett, and R.G. Hulet, Phys. Rev. Lett. **76**, 10 (1996).

[78] M. Houbiers and H. T. C. Stoof, Phys. Rev. A **54**, 5055 (1996).

[79] H. Wu and E. Arimondo, Europhys. Lett. **43**, 141 (1998).

[80] I. Shvarchuck, Ch. Buggle, D. S. Petrov, M. Kemmann, W. von Klitzing, G. V. Shlyapnikov, and J. T. M. Walraven Phys. Rev. A **68** 063603 (2003).

[81] F. Gerbier, J. H. Thywissen, S. Richard, M. Hugbart, P. Bouyer, and A. Aspect Phys. Rev. Lett **92** 030405 (2004).

[82] L. Vichi, J. Low. Temp. Phys. **121**, 177 (2000).

[83] S. Gupta, Z. Hadzibabic, J. R. Anglin, and W. Ketterle Phys. Rev. Lett **92** 100401 (2004).

[84] P. Pieri, G.C. Strinati Phys. Rev. B **61**, 15370 (2000).

[85] D.S. Petrov, C. Salomon, G.V. Shlyapnikov Phys. Rev. Lett. **93**, 090404 (2004).

[86] S. Stringari Europhys. Lett. **65**, 749 (2004).

[87] J. Kinast, S.L. Hemmer, M.E. Gehm, A. Turlapov, J.E. Thomas Phys. Rev. Lett. **92**, 150402 (2004).

[88] Bartenstein M, Altmeyer A, Riedl S, Jochim S, Chin C, Denschlag JH, Grimm R Phys. Rev. Lett. **92**, 203201 (2004).

[89] C. A. Regal, M. Greiner, and D. S. Jin Phys. Rev. Lett. **92**, 040403 (2004).

[90] K. Huang, *Statistical Mechanics*, J. Wiley, New York (1987).

[91] F. Dalfovo, S. Giorgini, L.P. Pitaevskii and S. Stringari, Rev. Mod. Phys. **71**, 463 (1999).

[92] L.P. Pitaevskii, S. Stringari, *Bose-Einstein Condensation*, Oxford University Press (2003).

[93] P. Noziéres, D. Pines, *The theory of quantum liquids* Addison-Wesley, New York (1989).

[94] E. M. Lifshic, L.P. Pitaevskij, *Statistical physics part II*, Pergamon press, Oxford (1980).

[95] J. J. Sakurai. *Modern quantum mecanics* Addison-Wesley, New York (1994)

[96] J. R. Taylor *Scattering theory* John Wiley & Sons, New York (1972).

[97] N. Bogoliubov, J. Phys. (Moscow) **11**, 23 (1947).

[98] A.L. Fetter, Ann. Phys. (N.Y.) **70**, 67

[99] E. P. Gross, Nuovo Cimento **20**, 454 (1961).

[100] L. P. Pitaevskii, Sov. Phys. JETP **13**, 451 (1961).

[101] E. P. Gross, J. Math. Phys. (N.Y.) **4**, 195 (1963).

[102] A.L. Fetter and J.D. Walecka *Quantum Theory of Many-Particle Systems* McGRAW-HILL N.Y. (1971).

[103] M. Cozzini, L. P. Pitaevskii, and S. Stringari Phys. Rev. Lett. **92**, 220401 (2004).

[104] A. Hauerbach *Interacting Electrons and Quantum Magnetism*, Springer (1994).

[105] L.P. Gorkov and T.K. Melik-Barkhudarov Sov. Phys. JEPT **13**, 1018 (1961).

[106] N. Nagaosa, Stefan Heusler, Naoto Nagaosa *Quantum Field Theory in Condensed Matter Physics* Springer (1995).

[107] P. Jordan and E.Wigner, Z. Phys. **47**, 631 (1928).

[108] P. Pedri, L. Santos, P. Öhberg, and S. Stringari, Phys. Rev. A. **68**, 043601 (2003).

[109] V.E. Korepin, N.M. Bogoliubov, and A.G. Izergin, *Quantum Inverse Scattering Method and Correlation Functions* (Cambridge University Press, Cambridge, (1993).

[110] P. Di Francesco, P. Mathieu, David Sénéchal, *Conformal Field Theory*, Spinger New York (1997).

[111] M. Rigol *Numerically exact studies of ultracold atoms on optical lattics* PhD thesis Stuttgart (2004)

[112] E. B. Kolomeisky, T. J. Newman, J. P. Straley, and Xi. Qi Phys. Rev. Lett. *85*, 1146 (2000).

[113] F. Dalfovo, C. Minniti, S. Stringari, L. Pitaevskii, Phys. Lett. A, **227**, 259 (1997).

[114] P. Meystre, M. Sargent III *Elements of Quantum Optics* 3rd Edition, Springer (1999).

[115] N.W. Ashcroft, N.D. Mermin, *Solid State Physics*, Thomson Learning (1976).

[116] D. van Oosten, P. van der Straten, and H. T. C. Stoof, Phys. Rev. A **63**, 053601 (2001).

[117] M. Krämer, L. Pitaevskii, and S. Stringari, Phys. Rev. Lett. **88**, 180404 (2002).

[118] M. Fabrizio, Phys. Rev. B **48**, 15838 (1993).

[119] A. M. Finkel'stein and A. I. Larkin, Phys. Rev. B **47**, 10461 (1993).

[120] H J. Schulz, Phys. Rev. B **53**, R2959 (1996).

[121] See e.g. A. M. Tsvelik, *"Quantum field theory in condensed matter physics"*, Cambridge University Press, (1995).

[122] H.J. Schulz, Phys. Rev. Lett. **77**, 2790 (1996).

[123] V.Yu. Irkhin and A.A. Katanin, Phys. Rev. B **61**, 6757 (1999).

[124] M. Bocquet, Phys. Rev. B **65**, 184415 (2002).

[125] D. Guèry-Odelin, F. Zambelli, J. Dalibard, and S. Stringari, Phys. Rev. A **60**, 4851 (1999).

[126] U. Al Khawaja, C.J. Pethick, H. Smith, J. Low Temp. Phys. **118**, 127 (2000).

[127] This effect has been measured with great precission at the group of Jook Walraven at Amsterdam University. C. Buggle, private communication.

[128] E.M. Lifshitz, L.P. Pitaevskii, *Physical Kinetics*, Oxford (1998).

[129] D. Guéry-Odelin, Phys. Rev. A **66**, 033613 (2002).

[130] E. Zaremba, T. Nikuni, A. Griffin J. Low Temp. Phys. **116**, 277 (1999).

[131] L.P. Kadanoff and G. Baym, *Quantum Statistical Mechanics* (W.A. Benjamin, New York, 1962).

[132] L. P. Pitaevskii and A. Rosch, Phys. Rev. A **55**, R853 (1997).

[133] I. Shvarchuck, Ch. Buggle, D. S. Petrov, M. Kemmann, W. von Klitzing, G. V. Shlyapnikov, and J. T. M. Walraven Phys. Rev. A **68**, 063603 (2003).

[134] G. M. Kavoulakis, C. J. Pethick, and H. Smith, Phys. Rev. A **61**, 053603 (2000).

[135] M. E. Gehm, S. L. Hemmer, K. M. O'Hara, and J. E. Thomas Phys. Rev. A **68**, 011603 (2003).

[136] L. Vichi and S. Stringari, Phys. Rev. A **60**, 4734 (1999)

[137] M. A. Baranov and D. S. Petrov, Phys. Rev. A **58**, R801 (1998).

[138] A. Minguzzi and M. P. Tosi, Phys. Rev. A **63**, 023609 (2001).

[139] F. Zambelli and S. Stringari, Phys. Rev. A **63**, 033602 (2001).

[140] Pedri P., Guéry-Odelin D. and Stringari S. Phys. Rev. A **68** 043608 (2003).

[141] M. L. Chiofalo, S. J. J. M. F.Kokkelmans, J. N. Milstein and M.J. Holland, Phys. Rev. Lett. **88**, 090402 (2002).

[142] B. DeMarco and D. S. Jin, Science **285** 1703 (1999).

[143] P. Pedri, L. Pitaevskii, S. Stringari, C. Fort, S. Burger, F. S. Cataliotti, P. Maddaloni, F. Minardi, and M. Inguscio, Phys. Rev. Lett. **87**, 220401 (2001)

Selbstständigkeitserklärung

Hiermit versichere ich, die vorliegende Doktorarbeit selbstständig und unter ausschließlicher Verwendung der angegebenen Hilfsmittel angefertigt zu haben.

Hannover, den 2. November 2004

Paolo Pedri